Generalized Temperature-Driven Insect Population Dynamics Model – a Mechanistic Approach

by

Dominique Delay

A thesis submitted in partial fulfillment

of the requirements for the degree of

Master of Science (M.Sc.) in Computational Sciences

The Faculty of Graduate Studies

Laurentian University

Sudbury, Ontario, Canada

THESIS DEFENCE COMMITTEE/COMITÉ DE SOUTENANCE DE THÈSE
Laurentian Université/Université Laurentienne
Office of Graduate Studies/Bureau des études supérieures

Title of Thesis
Titre de la thèse: Generalized Temperature-Driven Insect Population Dynamics Model – a Mechanistic Approach

Name of Candidate
Nom du candidat: Delay, Dominique

Degree
Diplôme: Master of Science

Department/Program
Département/Programme: Computational Sciences

Date of Defence
Date de la soutenance: January 18, 2023

APPROVED/APPROUVÉ

Thesis Examiners/Examinateurs de thèse:

Dr. Aaron Langille
(Supervisor/Directeur(trice) de thèse)

Dr. Ralf Meyer
(Committee member/Membre du comité)

Dr. Nathan Basiliko
(Committee member/Membre du comité)

Dr. Cortland Griswold
(External Examiner/Examinateur externe)

Approved for the Office of Graduate Studies
Approuvé pour le Bureau des études supérieures
Tammy Eger, PhD
Vice-President Research (Office of Graduate Studies)
Vice-rectrice à la recherche (Bureau des études supérieures)
Laurentian University / Université Laurentienne

ACCESSIBILITY CLAUSE AND PERMISSION TO USE

Abstract

Demand for computer models that simulate insect population dynamics is growing due to many factors including increased pressure on natural resources and climate change. Generalized models are a practical way to simulate multiple insect species with a single computer model, reducing the time spent developing species-specific models for each insect of interest. In this thesis, a generalized insect population dynamics model is presented. The model uses a mechanistic approach, leveraging data on underlying population drivers such as temperature-dependent vital rates to simulate changes in a population. The general model structure and code were adapted from the species-specific *Drosophila suzukii* model by Langille et al. (2016). The species-specific model was modified to account for a variety of insect species, minimise the number of required parameters, and use parameters that are available through literature, ensuring the general model's simplicity and ease of use. Through exploration and sensitivity tests, the model's elements were found to largely behave as expected from the real-life systems. The model was also validated for its intended use as a non-predictive, exploratory model through the comparison of published field or simulation population studies. The model successfully approximated published population studies when simulating insect species with simple life cycles, however, simulations of insect species with more complex life cycles, or social structures, were not as successful. Overall, despite some limitations, the general model presented in this thesis can simulate many insect species population dynamics and is ideal for study ideation, prototyping, and rapid exploration.

Keywords: generalized model; insect; mechanistic model; population dynamics; temperature dependent.

Acknowledgment

I would like to thank my supervisor, Dr. Aaron Langille, without whom this thesis project would not exist; for knowing when to give me guidance and when to give me the space I needed to make progress. You have been such a great inspiration and have had such a big impact on my time at Laurentian University.

I would also like to thank my committee members, Dr. Ralf Meyer and Dr. Nathan Basiliko, for providing me with feedback and an outside point of view on my thesis.

To Dr. Jonathan Newman, your insight on the field of ecology and computer modelling was indispensable. Thank you for giving me great advice on my model testing and validation results.

Finally, I would like to thank my family, for helping me through the process of writing this thesis. To my parents who have supported me during my graduate studies and nurtured a love of science and technology. To my sister, I couldn't have asked for a better, more encouraging, stay-at-home lab mate.

Table of Contents

Abstract ..... *ii*

Acknowledgment ..... *iii*

List of Tables ..... *vi*

List of Figures ..... *vi*

1. General Introduction - Background and Review *1*

1.1 Ecological Computer Simulation Models 1

1.2 Modelling Approaches 2

1.3 Insect Population Dynamics 4

1.4 Species-specific and General Multi-species Insect Population Dynamics Models 6

1.5 Thesis Objectives and Overview 8

2. Generalized Mechanistic Insect Population Dynamics Simulation Model *10*

2.1 Introduction 10

2.2 Model Generalization 10

2.3 Model Structure 11

2.4 Model Equations 13

2.4.1 Fecundity Rate 14

2.4.2 Development Rate 15

2.4.3 Mortality Rate 17

2.4.4 Reproductive Diapause 19

2.4.5 Overwintering 20

2.4.6 Mortality Event 23

2.4.7 Environmental Equations 24

2.4.8 Model State Equations 26

2.5 Model Differential Equation Solving Method 28

2.6 Technical Details and Model Implementation 29

3. Chapter 3 Model Exploration and Sensitivity Testing *32*

3.1 Introduction 32

3.2 Temperature Tests 33

3.2.1 Population Response to Constant Temperatures 33

3.2.2 Population Response to Cosine Temperature Profiles 34

3.3 Initial Population Tests 37

3.3.1 Effect of Starting Population Date and Size 37

3.3.2 Effect of Starting Population Life Stage 38

3.4 Overwintering Sub Model Tests 40

3.4.1 Effect of Overwintering Induction Date 40

3.5 Life Stage Tests 44

3.5.1 Model Handling of Pre-adult and Pre-egg Laying Life Stages 44
3.6 Mortality Event Sub Model Tests 46
3.6.1 Effect of Mortality Event Date and Mortality Event Percentage 47
3.6.2 Effect of Mortality Event Life Stage 49
4. General Model Validation 53
4.1 Introduction 53
4.2 Methods 54
4.3 Model Validation Test Results 57
4.3.1 *Drosophila suzukii* (Spotted Wing Fruit Fly) 57
4.3.2 *Halyomorpha halys* (Brown Marmorated Stink Bug) 65
4.3.3 *Dendroctonus ponderosae* (Mountain Pine Beetle) 73
4.3.4 *Contarinia nasturtii* (Swede Midge) 77
4.3.5 *Aphis gossypii* (Cotton Aphid) 82
5. Discussion and Conclusion 86
5.1 Generalized Mechanistic Insect Population Dynamics Model Discussion 86
5.2 Model Exploration and Sensitivity Testing Discussion 88
5.3 General Model Validation Discussion 89
5.4 Final Thoughts and Future Work 93
6. Bibliography 97
7. Appendix A: List of General Model Parameters 106
8. Appendix B: Default Toy Species' Configuration Parameter File 109
9. Appendix C: Supplementary Figures 110
10. Appendix D: List of Sources Used to Parameterize the General Model for the Validation Tests 112
11. Appendix E: Model User's Guide 113
12. Appendix F: Model Vital Rate Fitting Algorithm 115
13. Appendix G: Model Graphical User Interface (GUI) Description and User's Guide 119

List of Tables

Table 1 List of cosine curve temperature profiles tempA, tempB, tempC and tempD, including their temperature characteristics and the approximate location that they represent. These temperature profiles are provided with the general model and used in the exploration and sensitivity model testing. 25

Table 2 Overwintering critical induction daylight hours used in each model run for the overwintering induction date tests (figure 3.6 & figure 3.7) along with the associated Julien days of overwintering induction. 41

Table 3 Stages included in simulated life cycles and adult female egg viability values. 45

Table 4 List of all general model parameters including the graphical user interface (GUI) section, the equation in which they appear, the value's type, the value's units, whether the parameter is required to run the model and a description of the parameter. Note that the names of the parameters listed below are the parameter names used in the user interface and are not written as they should appear in the species' parameter file. For the proper parameter file parameter names see appendix B. 106

List of Figures

Figure 2.1 Basic flow diagram of the general model's insect population dynamics that represents the relationship between insect life stages found in the model's state equations (based on the Langille et al. (2016) flow diagram). The number of instars (n) and adult stages (m) along with the inclusion of a pupal stage can be set depending on the insect species modelled. A stage's mortality rate (μ), development rate (*d*) and fecundity (*f*) depend on temperature (T). Subscripts for each of these symbols represent the associated life stage. θ represents the male to female ratio and *v* is the variation of egg viability per female stage. Black arrows represent a life stage development transitions, long dashed lines are possible life stage development transitions depending on the specie's life cycle, grey arrows represent mortality, dashed line arrows represent egg production, and three dots represents possible additional development life stages. 13

Figure 2.2 General model's temperature-dependent fecundity curve. A Gaussian curve bounded between the model parameter values of fTmin and fTmax, with the peak value of Fmax. 15

Figure 2.3 General model's temperature-dependent development curve. The curve follows the briere2 development equation, with a Gaussian rising curve and a descending parabolic curve, which intersect zero at the model parameter values *Tmin* and *Tmax*. 17

Figure 2.4 General model's temperature-dependent mortality rate curve. A parabolic curve with a vertex at mortality rate *minMort*, bounded between the model parameter values *TL* and *TU*, beyond which the mortality rate is equal to *maxMort*. 19

Figure 2.5 Cosine temperature curve profiles tempA, tempB, tempC and tempD, that represent approximate daily average temperatures for a year in a certain climatic zone. These temperature profiles are provided with the general model and used in the exploration and sensitivity model testing. 25

Figure 2.6 (a) Normalized daily female population produced by a one-year general model simulation run with default parameters (Appendix B) with different integration step sizes: 0.05, 0.1, 0.5 and 1 day. (b) Enhanced visualization of the boxed area in (a) (for Julian Days 230 to 280 and normalized female population 0.8 to 1), where the female populations have the greatest size difference between runs with different integration step sizes. 29

Figure 2.7 Simplified UML (Unified Modelling Language) diagram of the relationships between the model's object classes. Solid arrows represent association relationships and dashed line arrows represent dependency relationships. 30

Figure 3.1 Normalized cumulative female population on a log scale for various constant temperature simulations. The general model was run for 365 days with 50 F1 females introduced on Julian day 140. The negative population axis is due to the cumulative female population values being both normalized and log scaled and does not represent real population numbers... 34

Figure 3.2 Simulated life stage population curves for the toy insect under the cosine temperature profiles (a) tempA, (b) tempB, (c) tempC and (d) tempD (figure 2.5). The general model was run for one year with 50 F1 females introduced on Julian day 140. 35

Figure 3.3 (a) vital rates (development, mortality and fecundity) for the toy species at various constant temperatures. (b) temperatures over one year for the cosine temperature profiles tempA, tempB, tempC, and tempD (Note that the temperature and Julian day axes have been switched). The vital rate values for each Julian day under the cosine temperature profiles can be determined by linking these figures through their shared temperature axis. 36

Figure 3.4 Normalized cumulative female population on a log scale produced by general model simulations with various introduction dates and initial population sizes. Each simulation is run for 365 days with the default toy species, under the temperature profile tempB. The negative population axis is due to the cumulative female population values being both normalized and log scaled and does not represent real population numbers. 38

Figure 3.5 Adult female population curve for model simulations initialized with various initial population life stages (egg, instar, pupa and female1) on Julian day 140. The initial population was always composed of 50 females and the model was run with the temperature profile tempB. The spike and subsequent decrease in the females initial population life stage curve (lightest blue line) is caused by the introduction of 50 females on Julian day 140, which quickly decrease due to temperature conditions on the following dates causing high female mortality. 40

Figure 3.6 (a) Adult overwintering population (measured on Julian day 365) produced when the general model was run with various overwintering induction dates. (b) Life stage population curves for a simulation with the same model parameters as the simulations in (a) but with no

overwintering induction date. (b) can be used to visualize the (a) simulations' population size and life stage composition before the overwintering induction dates. For all model simulations in (a) and (b), overwintering was terminated on Julian day 122..... 42

Figure 3.7 (a) Juvenile (instar1) overwintering population (measured on Julian day 365) produced when the general model was run with various overwintering induction dates. (b) Life stage population curves for a simulation with the same model parameters as the simulations in (a) but with no overwintering induction date. (b) can be used to visualize the (a) simulations' population size and life stage composition before the overwintering induction dates. For all model simulations in (a) and (b), overwintering was terminated on Julian day 122. 43

Figure 3.8 (a), (b) and (c) Life stage population curves for model simulations with different life cycles but the same vital rates for each life stage. (a) used the basic toy species life cycle, (b) replaced the toy specie's pupal stage with a second instar stage and (c) replaced the toy specie's pupal stage with an additional adult female life stage with an egg viability of zero. Each simulation was run for one year with 50 introduced F1 females on Julian day 140, under the temperature conditions of tempB. (d) Combined life stage population on each Julian day for the simulated life cycles seen in (a), (b) and (c). Note that in (d), the combined life stage population (a) is not visible since the combined life stage population (b) is nearly perfectly superposed due to their near identical curves. 46

Figure 3.9 (a) Peak adult female population produced by general model simulations where mortality events were applied to the instar life stage on various days (Julian day 170 to 300 with 10 day intervals) and with various mortality event percentages (0%, 25%, 50%, 75% and 100%). Each simulation was initialized with an initial population of 50 F1 females on Julian day 140 and run for one year with the default toy parameters, under the temperature profile tempB. (b) Instar1 population curve for a one year simulation, using the same parameters and initial conditions as in (a) but with no mortality events applied. (b) can be used to determine the instar mortality event life stage's population size on the date of each mortality event in (a). For example, on the mortality event Julian day 220, the instar life stage has a population of 154 instars..... 49

Figure 3.10 (a) Peak and (b) cumulative adult female population produced by general model simulations where 50% mortality events were applied on various days (Julian day 170 to 300 with 10 day intervals) and to various life stages (egg, instar1, pupa, female). Each simulation was initialized with an initial population of 50 F1 females on Julian day 140 and run for one year with the default toy parameters, under the temperature profile tempB. (c) All life stage population curves for a one year simulation, using the same parameters and initial conditions as in (a) and (b) but with no mortality events applied. (c) can be used to determine a mortality event life stage's population size on the date of each mortality event in (a) and (b). For example, on the mortality event Julian day 240, the egg, instar1, pupa and female life stages have populations of 91, 101, 85 and 51 respectively. 52

Figure 4.1 Normalized *Drosophila suzukii* life stage population curves under the temperature profiles (a) tempA, (b) tempB, (c) tempC, and (d) tempD. Simulations were run for one year with an initial population of 50 F1 females on Julian day 120, using the Langille et al. (2016) model (left column) and the general model (right column). 58

Figure 4.2 Comparison of the Langille et al. (2016) and general model simulated *Drosophila suzukii* population from figure 4.1. (a) percent error of the general model's normalized peak *D. suzukii* population for each life stage simulated with each cosine temperature profile. (b) percent error of the general model's normalized cumulative *D. suzukii* population for each life stage simulated with each cosine temperature profile..... 59

Figure 4.3 Ratio between the Langille et al. (2016) model and the general model's average life stage cumulative *Drosophila suzukii* population when simulated under each cosine temperature profile (figure 4.1). Note that the tempC population's ratio is not visible but has the value of 0.00367..... 62

Figure 4.4 *Drosophila suzukii* life stage mortality rate, at various constant temperatures, used in (a) the species-specific Langille et al. (2016) model and (b) the general model. 62

Figure 4.5 Normalized daily number of *Drosophila suzukii* females simulated under the temperature conditions of Clark county, WA for the years 1993 to 2013 and the 20 year average temperature. An initial population of 100 females was introduced on the termination date of reproductive diapause. (a) results from the species-specific Langille et al. (2016) model and (b) results from the general model..... 64

Figure 4.6 Daily percent error between the species-specific Langille et al. (2016) and the general model's normalized *Drosophila suzukii* female populations under Clark county, WA temperatures for the years 1993 to 2013 and the 20 year average temperature (figure 4.5). 64

Figure 4.7 *Halyomorpha halys* life stage progression and population survival at constant temperatures (a) 20°C, (b) 23°C, (c) 27°C, (d) 30°C, (e) 33°C produced by the Govindan and Hutchison (2020) model (left column) and general model (right column)..... 67

Figure 4.8 Comparison of the proportion of *Halyomorpha halys* eggs to survive to adulthood in the Govindan and Hutchison (2020) model and the general model..... 68

Figure 4.9 Total cumulative number of eggs laid by a *Halyomorpha halys* population, composed of 23 females, under daily average temperatures in Switzerland, 2013, (a) observed by Haye et al. (2014) and (b) modelled by the general model. 69

Figure 4.10 Adult male and adult female *Halyomorpha halys* population survival under daily average temperatures in Switzerland, 2013, (a) observed by Haye et al. (2014) and (b) modelled by the general model. 70

Figure 4.11 *Halyomorpha halys* life stage proportion under daily average temperatures in Switzerland, 2013, (a) observed by Haye et al. (2014) and (b) modelled by the general model. Note that the life stage population proportions were measured on dates that are not equally distributed over the observed and simulated time period. 72

Figure 4.12 Absolute error between the Haye et al. (2014) and the general model's *Halyomorpha halys* life stage population proportion for each life stage (figure 4.11). 72

Figure 4.13 Normalized daily *Halyomorpha halys* combined life stage population size observed by Haye et al. (2014) and simulated by the general model. 73

Figure 4.14 *Dendroctonus ponderosae* population life stage density (ratio) between Julian day 222 and 590 under the phloem temperature of an infested lodgepole pine in Sawtooth National Recreation Area, ID, (a) produced by the Bentz et al. (1991) model and (b) the general model. 75

Figure 4.15 Historic (1970-1979) and recent (2000-2008) smoothed daily average temperature curves in Colorado for one year. 76

Figure 4.16 Normalized *Dendroctonus ponderosae* life stage population curves produced by the general model under (a) historic and (b) recent Colorado temperatures (figure 4.15). 77

Figure 4.17 Mean relative number of *Contarinia nasturtii* adults in the observed population and in the simulated MidgEmerge model population under the temperature conditions at the University of Guelph Elora Research Station between the months of May and September 2009. Figure from Liu (2019). 78

Figure 4.18 Normalized adult *Contarinia nasturtii* population simulated by the general model under the temperature conditions at the University of Guelph Elora Research Station in 2009. This figure's population is compared to figure 4.17's populations. 79

Figure 4.19 Normalized adult *Contarinia nasturtii* population simulated by the general model under the temperature conditions at the University of Guelph Elora Research Station in 2009, converted to a logarithmic scale to extract the population's approximate generation timing (May 8, July 3 and August 26). This figure's population is compared to figure 4.17's populations. 80

Figure 4.20 Normalized adult *Contarinia nasturtii* population produced by three separate general model simulations terminated on the peak female population date and initialized with the number of eggs produced by the previous simulation's peak female population. All general model runs used the temperature conditions at the University of Guelph Elora Research Station in 2009. This figure's population is compared to figure 4.17's populations. 81

Figure 4.21 Normalized three year average (1992, 1993 and 1994) *Aphis gossypii* and predator species (75.4% *Harmonia dimidiata*) populations observed by Parajulee et al. (1997) at the Texas Agricultural Experiment Station in Munday, TX. 83

Figure 4.22 Normalized *Aphis gossypii* population simulated by the general model under the three-year average (1992, 1993 and 1994) mean daily temperatures in Abilene, TX. The general model was initialized with 100 eggs on May 20th. This figure's population is compared to figure 4.21's populations. Note that the *Aphis gossypii* population continues to grow exponentially outside of the range of the figure and peaks on October 29th with the normalized peak value of 1. 85

Figure 8.1 Content of the Toy specie's configuration parameters file including all model parameters. 109

Figure 9.1 Supplementary Life stage toy species population curves for one year general model simulation with an initial population of 50 F1 adult females introduced on Julian day 140. A 100% mortality event was applied to the instar life stage on (a) Julian day 210, (b) Julian day 220, and (c) Julian day 230. 110

Figure 9.2 Supplementary (a) Peak and (b) cumulative adult female population produced by general model simulations where 50% mortality events were applied on various days (Julian day 170 to 300 with 10 day intervals) and to various life stages (egg, instar1, pupa, female). Each simulation is run for 365 days with the toy species parameters and under the temperature conditions of tempB. The model was initialized with an initial population of 50 instars on Julian day 140. 111

Figure 9.3 Supplementary (a) Peak and (b) cumulative instar population produced by general model simulations where mortality events were applied on various days (Julian day 170 to 300 with 10 day intervals) and to various life stages (egg, instar1, pupa, female). Each simulation is run for 365 days with the toy species parameters and under the temperature conditions of tempB. The model was initialized with an initial population of 50 F1 females on Julian day 140. 111

Figure 12.1 Example constant temperature vital rate file used as input in the curve fitting algorithm. The file contains values for the development rate of the life stages: egg, instar1, instar2, instar3, and pupa at various constant temperatures..... 115

Figure 13.1 Flow diagram of the connection between the UI, the general model and the fitting algorithm. Arrows represent the user interface executing external programs. Dashed arrows are optional execution of a program and solid arrows are mandatory execution of a program..... 121

Figure 13.2 Storyboard of the general model graphical user interface being run for the spotted wing fruit fly. 122

1. General Introduction - Background and Review

1.1 Ecological Computer Simulation Models

Computer simulation models have become a vital tool in ecology, used to simulate a number of complex ecological systems and processes including forests growth (Bugmann 1994), animal movements (Johnson et al. 1992), and animal population dynamics and phenology (Petrice et al. 2021). Developing an ecological computer model can be a practical way to determine a system's potential response to certain conditions, events or scenarios, especially for systems that may be difficult to study empirically such as those on extremely small or large spatial, temporal or population scales (Adler and Lauenroth 2003; Peck 2004). Models may also be chosen over field studies for logistical, ethical, political, or financial reasons (Jackson et al. 2000; Peck 2004). They may be used, even when a field study is possible, to isolate a specific ecological process or to improve the understanding of a process to guide further empirical studies (Langille 2017). Ecological models can be created for several purposes including:

- developing theories and hypotheses about a system or its elements
- testing theories and hypotheses
- drawing generalizations about a system's most important properties
- understanding how a system functions including the consequences of changes to a system's mechanisms
- explaining the cause of changes to a system's mechanisms
- predicting qualitatively or quantitatively the future state of a system
- supporting decisions by illustrating alternative future states of a system to decision makers
- communicating or presenting information to an audience

- teaching students analytical techniques that can later be applied to more relevant or complex models
- organizing a system's existing knowledge
- identifying a system's knowledge gaps
- designing experiments (Duarte et al. 2003; Baumgärtner et al. 2008)

Irrespective of the specific purpose, the demand for computer models is growing in ecology due to a variety of factors including increased pressure on natural resources and climate change. Changes to the Earth's systems and a reduction in its biodiversity, particularly in the 21st century, is increasing demand for predictive data, which can often be provided by models (Duarte et al. 2003).

Increases in computational power, over the past few decades, have resulted in more complex computational models. However, complex models are not necessarily preferable (Grimm 1994; Scheffer and Beets 1994). As a model approaches the complexity of the real ecological system by incorporating more of its components, it can become more difficult to develop, calibrate and validate. In most cases, a model should focus on the system's components that have the greatest influence on the observed patterns, excluding any unnecessary parameters. In other words, an ideal model maximizes result accuracy while minimizing the number of parameters, and in turn overall model complexity (Lagergren et al. 2018).

1.2 Modelling Approaches

When developing a computer model, several approaches can be employed such as statistical, machine learning, and mechanistic. Statistical models make predictions based on a statistical description of a system using data correlation and historical data trends to project a

system's future behavior (Maino et al. 2016). Machine learning models employ machine learning techniques to build predictive models, using large data sets to "train" the model until accurate predictions are produced (Baker et al. 2018). While, mechanistic models are based on explicit knowledge of the system's known mechanisms and processes (Hilborn and Mangel 1997), using those underlying processes and interactions to reasonably replicate the real-world counterpart's functionality. A particular modelling approach, or combination of multiple modelling approaches, may be more effective depending on the model's goal and use cases due to each approaches' inherent benefits.

A statistical model's main advantage is its ability to bypass the need for in-depth knowledge, yielding predictions without causality (Baker et al. 2018) and its relatively small data requirements. Given the appropriate modelling objectives and relatively few data points, this modelling approach can often produce effective predictive results. However, if the collected data is not representative of the entire studied system, the statistical model may not hold beyond the range of the observed data (Maino et al. 2016). This is a common pitfall when trying to oversimplify a statistical model; if the data's range is overly small, trends used to create the model may change outside the measured bounds, resulting in the model yielding inaccurate predictions when it is applied to different spatial or temporal ranges (Duarte et al. 2003).

Machine learning models can produce rapid, scalable, efficient predictions (Baker et al. 2018) but, similar to statistical models, sacrifice a system's theoretical understanding that can be obtained with a mechanistic model (Hartig and Dormann 2013). Any results obtained with a machine learning model are based on the training data sets; the users must ensure that data sets are sufficiently large to insure model accuracy (Baker et al. 2018).

Mechanistic models are designed for many purposes but their primary advantage, when compared to other modelling approaches, is their ability to illustrate the active elements and processes in a given system (Duarte et al. 2003). They can be used to identify the most influential factors in obtaining the modelled results, making them useful in exploration. Since mechanistic models are based on a process-level understanding of a system, however, they often require more specific empirical data than statistical models (Penning De Vries 1983). The model developer must often possess detailed descriptions of the system components and their interactions in order to reproduce the system's functionality (Maino et al. 2016).

Each of the modelling approaches described above can be used alone or in combination to model insect population dynamics. This thesis takes a mechanistic modelling approach based on the model goals of providing a deeper understanding of system mechanisms which can be applied to various ends. Modelling insect population dynamics with a mechanistic approach can improve insect species understanding (Abbott and Dwyer 2007, 2008; Kehoe et al. 2022), inform pest species mitigation and management strategies (Vinatier et al. 2011; Gilioli et al. 2016; Poggi et al. 2021), give insight into species' potential success under a changing climate or a new region (Estay et al. 2009; Hartley et al. 2010; Maino et al. 2016), and provide a way to explore various "what-if" insect population scenarios.

1.3 Insect Population Dynamics

Insects occupy nearly every ecosystem in the world. At an estimated 5.5 million known species globally (Stork 2018), they make up more than 60% of global animal diversity (Kim 2009). Insects are vital to ecosystem function, playing a role in pollination, decomposition, improving soil fertility and structure, nutrient cycling, seed dispersal, and pest control, as well as being a

major food source for many taxa and helping to maintain an ecosystem's balance (Huis 2014). Their broad roles result in insects having a considerable impact on humans. They influence ecology, agriculture, human health, and natural resources (Scudder 2017). Changes in insect populations can have serious, often disruptive, effects. Spikes in populations of pest species can devastate forests and decrease crop yields. It is estimated that insect pests are responsible for a 14% loss of crops, worldwide, the value of which is estimated to be $680 billion per year (Pimentel 2009). Studying and understanding insect population dynamics and phenology, including the changes in a population's age, size and distribution over time, can help inform pest mitigation and management strategies along with supporting general insect research.

Insect population dynamics are influenced by many factors including both abiotic (temperature, humidity, and light) and biotic (host species, biodiversity, crowding, and diet) stresses (Khaliq et al. 2014). However, temperature and humidity are the principal drivers of most insect abundance and distribution (Bale 2002; Stange and Ayres 2010) since they directly affect an insect's activity levels, growth, developmental rate, reproduction and mortality, along with indirectly affecting external influences such as abundance and distribution of host plants, predators, prey and parasitoids (Boggs and Inouye 2012; Jaworski and Hilszczański 2013).

A species' population dynamics can also be affected by life cycle characteristics and progression. Insect life cycles can be classified by metamorphosis types; ametabolous (no metamorphosis), with three life stages: egg, immature stages and adult; hemimetabolous (incomplete metamorphosis), with three life stages: egg, nymph and adult and holometabolous (complete metamorphosis) with four life stages: egg, larva, pupa and adult (Belles 2011). There can be some variation in these life cycles; for example, many aphid species produce live young throughout the year, only laying eggs as a hardy overwintering life stage (Dixon 1977).

Overwintering also affects the life cycles of species residing in temperate and cold climates. Insects generally have two main overwintering strategies; freeze tolerance and freeze avoidance (Bale and Hayward 2010). Overwintering success can also be linked to diapause which increases cold hardiness. Diapause is induced in insects when a minimum or maximum temperature and daylength is reached where conditions are not suitable for survival (Tauber et al. 1986; Bale and Hayward 2010). Insects stay in diapause, where their metabolism slows and their development stops, until conditions become favorable (Tauber et al. 1986; Denlinger 2002; Hahn and Denlinger 2011). Diapause usually occurs at a single life stage which varies depending on the species (Bale and Hayward 2010), however, a few insect species transition between life stages during diapause. Extreme cold temperatures or fluctuating winter temperatures can decrease overwintering survival (Ladányi and Horváth 2010) especially if insects leave and re-enter diapause several times in one winter (Bale and Hayward 2010).

Diapause is not singularly an overwintering or extreme environmental conditions survival strategy, it is also employed in the adult life stage of certain insects to synchronize life cycles with optimal conditions for growth and offspring survival (Tatar and Yin 2001). Reproductive diapause is also induced by environmental cues but is not characterised by insect inactivity, rather the cessation of reproductive functions (Pener et al. 1972; Herman 1981; Pener 1992).

1.4 Species-specific and General Multi-species Insect Population Dynamics Models

Insects are notoriously difficult to study empirically due to their spatial and temporal scales, diverse behaviors and often complex life history. Simulation models are commonly used to better understand observed and theoretical changes in insect populations and have been shown to be an effective study method (Kendall et al. 2005; Matis et al. 2008; Estay et al. 2009; Balenghien

et al. 2010). Temperature-driven models are commonly developed to study changes in specific insect species populations (Régnière et al. 2012b; Jia et al. 2016; Cuddington et al. 2018; Pertierra et al. 2020).

Many current insect population dynamics models are species-specific. These models are designed to simulate a specific insect species' population dynamics, and use hard coded values or modelled processes specific to the species making them only suitable for a single species. Although species-specific models can potentially produce more accurate predictive results for the target species, a new model must be developed for each species of interest. A general insect model, on the other hand, can be used to simulate multiple insect species with a single model. A user can then repeatedly run simulations with the model without requiring any additional model creation. General models therefore reduce the time spent developing multiple models and can increase accessibility to a wider audience.

There are some established multi-species (i.e., general) insect computer models that are viable options to simulate and study insect population dynamics including: CLIMEX (Sutherst 1985; Kriticos et al. 2015), DYMEX (Maywald et al. 2007), Maxent (Phillips et al. 2006; Phillips and Dudík 2008), BioSim (Régnière 1996; Régnière et al. 2014), and ILCYM (Sporleder et al. 2009). These general models have successfully been used to studied population dynamics and potential species distribution (Sutherst et al. 2000; Logan et al. 2003; Tanga et al. 2018), including the combined use of Maxent and CLIMEX to simulate the western cherry fruit fly, *Rhagoletis indifferens',* potential risk of establishment in North America (Kumar et al. 2014). The general models listed above, excluding Maxent, take a mechanistic modelling approach, utilizing species-specific characteristics data to simulate population dynamics for each of the species' life stages. The model equations, species parameter data, and climate data, differ between the different general

models. Each model uses temperature data, but some (such as BioSim) also have the option to used other climate information to determine potential distributions. General models (such as CLIMEX & DYMEX) may also include additional considerations for diapause and competition between species.

While established general insect computer models can effectively simulate multiple insect species, they are often very complex, requiring a large number of input species parameters to run a simulation; they can be costly, are usually not open-source, and often don't focus on ease of use.

1.5 Thesis Objectives and Overview

The overall objective of this thesis is to create and validate a generalized insect population dynamics model, contributing to the range of multi-species insect modelling tool options. This model is intended for rapid, easy and accessible insect population dynamics exploration, using simple insect life cycle mechanisms that can be obtained through published laboratory research. Results produced by this model are approximations of insect life cycles in response to intrinsic and extrinsic factors, providing a quick exploratory modelling option for ideation, study planning and species population response exploration to various "what-if" scenarios. This generalized model doesn't attempt to produce forecasting results like many of the multi-species insect models and should not be viewed as a predictive model.

The general model's mechanistic and life stage populations simulation approach can offer a deeper understanding of insect populations and their response to intrinsic and extrinsic factors. This modelling approach allows model parameters that represent population dynamics driving biological and environmental mechanisms to be examined and modified directly along with providing additional information about the population's life stage development and the specific

timing of life stage peak populations. The information obtained from this mechanistic, split life stage insect population dynamics model can be leveraged to various ends, including giving crucial insight into a species survival under a changing climate or in a new environment, and identifying effective methods to control pest populations and reduce their impact on crops and natural resources.

This thesis is split into three content chapters that lend themselves to achieving the thesis' goals. In Chapter 2, the structure of the generalized mechanistic insect population dynamics model is presented, the underlying model equations are displayed, and the changes made to generalize the *D. suzukii* species-specific base model by Langille et al. (2016) are discussed. In Chapter 3, the updated model's elements are explored through sensitivity testing to ensure that the results are in line with existing knowledge of insect population dynamics. In Chapter 4, the generalized model is tested and validated for its intended purpose as a non-predictive model and the extent of the model's use as a multi-species model is further tested through the comparison of published insect species population studies. Chapter 5 summarizes and discusses the thesis' work, and presents some possible general model applications along with suggesting future work.

2. Generalized Mechanistic Insect Population Dynamics Simulation Model

2.1 Introduction

Given the lack of simple tools for rapid and easy insect population dynamics simulations, a generalized model was created and will be presented in this chapter. The chapter objectives are to (1) create a generalized temperature-driven insect population dynamics model that can account for a number of insect species, and (2) minimize the number of species parameters that are required as model input, improving model simplicity and ease of use.

2.2 Model Generalization

The proposed model is based on, and shares code with, the species-specific *Drosophila suzukii* mechanistic model by Langille et al. (2016). The original *D. suzukii* model was expanded from a single, species-specific, population dynamics model into a general, multi-species model. To achieve this generalization, modifications were made to the original model, changing life stage flow to allow for a varying number of juvenile life stages and the optional inclusion or exclusion of a pupal stage. These modifications were all made to the model's state equations, the differential equations that drive population dynamics.

The model's vital rate equations (development, mortality and fecundity) were also changed, firstly to include all species-specific parameter values as user input rather than pre-set constants, secondly to simplify the equations to require fewer parameters, and thirdly to function for a variety of insect species. Each of the vital rate equations maintain the *D. suzukii* model's temperature dependent curve shapes but use a simplified version of the curve equation in order to reduce the number of parameters.

In the original model, adult female development was represented as a single development value, “development max”, where females would develop at the same rate independent of temperature. This was modified in the general model to better match insect development data collected in laboratory research where it was found that adult life stage development is dependent on temperature. The Langille et al. (2016) model also didn’t have a way to limit the adult life stage’s longevity. In the generalized version, the temperature-dependent development rate was adapted to be used as a longevity rate for the male life stage and the final female life stage. This function is well-suited to this purpose due to longevity’s temperature dependent nature, following a similarly shaped longevity vs temperature curve as that of development vs temperature.

The final major aspect of generalizing the model was reducing the number of required species-specific input parameters. The original Langille et al. (2016) model took upwards of 185 parameters to model *D. suzukii*, which was reduced to 128 parameters (excluding optional sub models) in the general model. This parameter reduction was essential for the general model to achieve its goal of being easier to use, simpler, and more accessible. The general model’s accessibility is further improved by its use of parameter values that are available through literature. This avoids replicating or conducting expensive and time-consuming laboratory experiments.

Overall, model generalization was realized while maintaining the general model’s ability to simulate *D. suzukii* by iteratively modifying aspects of the model and comparing the general model’s results to those produced by the species-specific model.

2.3 Model Structure

The proposed general model simulates insect population dynamics using linear differential equations approximated using Euler’s method. Each of these state equations are specific to an

insect's single life stage and progress the population through time. Each simulated population is split into developmental stages, based on the insect species' life cycle, including an egg stage, one to *n* juvenile instar stages, a possible pupal stage, and male and female adult stages. The adult female life stage can be further divided into sub-stages each with their own egg viability rate. This can be used to represent age-based changes in insect egg production including pre- and post-female oviposition life stages, and female age-specific egg viability (or senescence) as seen in Langille et al. (2016). Adult males are generally ignored, as they are not the drivers of population and are assumed to have adequate numbers to produce fertile eggs. The model's population progression can be seen in figure 2.1's flow diagram.

The model uses a mechanistic approach, leveraging data on underlying population drivers such as fecundity, egg viability, development rate and intrinsic and extrinsic mortality to produce changes in a population. The model uses a limited set of parameters that were deemed to be the most impactful on insect population dynamics. Limiting the amount of data required to run the model is crucial since available data may be limited for some insect species due to inadequate research or data collection. This minimization of input parameters was considered for each of the model's equations. The number of model parameters required to run the model depends on the insect species' number of life stages, with the fewest possible parameters being 50 (for a species with an egg stage, no pupal stage, a single juvenile instar and an adult male and female stage), a relatively small number of parameters for a mechanistic model. A full list of required species-specific parameters can be seen in appendix A.

The principal environmental population driver in this model is temperature, having been found to be the most influential environmental factor in each life stage's driving mechanisms (fecundity, development, and mortality) (Liu and Tsai 2000; Bommireddy et al. 2004; Parajulee

2007; Ragland and Kingsolver 2008; Jandricic et al. 2010). The model uses daily average temperature data to simulate a species' response to temperature. This temperature data can be readily obtained from a number of sources, including, but not limited to, any location's daily average temperatures, projected climate change temperature data, fabricated smooth cosine curve temperature data or constant daily temperatures.

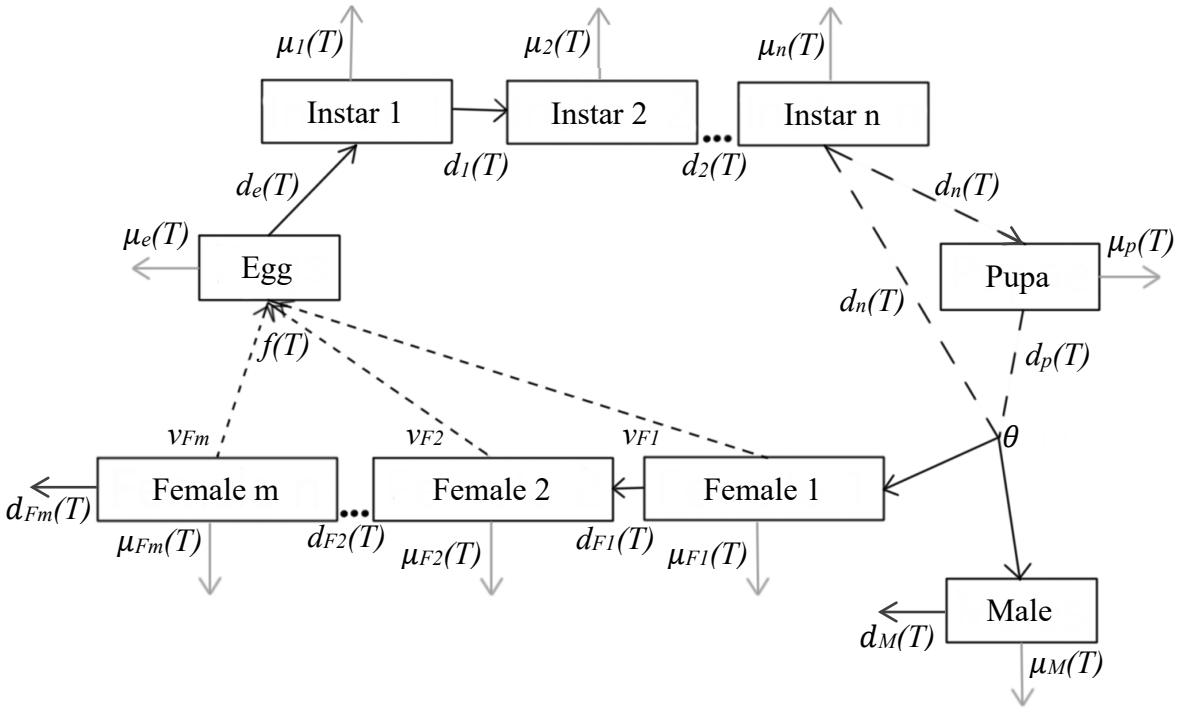

Figure 2.1 Basic flow diagram of the general model's insect population dynamics that represents the relationship between insect life stages found in the model's state equations (based on the Langille et al. (2016) flow diagram). The number of instars (n) and adult stages (m) along with the inclusion of a pupal stage can be set depending on the insect species modelled. A stage's mortality rate (μ), development rate (*d*) and fecundity (*f*) depend on temperature (T). Subscripts for each of these symbols represent the associated life stage. θ represents the male to female ratio and *v* is the variation of egg viability per female stage. Black arrows represent a life stage development transitions, long dashed lines are possible life stage development transitions depending on the specie's life cycle, grey arrows represent mortality, dashed line arrows represent egg production, and three dots represents possible additional development life stages.

2.4 Model Equations

In this section, the equations used to modify the population at each developmental life stage will be explored. These equations include fecundity rate, development rate, mortality rate,

overwintering, reproductive diapause, mortality events, environmental equations, and the model's state equations that progress the population from one life stage to the next.

2.4.1 Fecundity Rate

Insect fecundity is dependent on temperature, with laboratory studies showing that the maximum number of eggs are laid at a species optimal fecundity temperature and the number of eggs laid reduces as temperatures diverge from the optimum (figure 2.2). The generalized model's temperature dependent fecundity rate is modelled as a Gaussian-like curve bounded between the fixed intervals of 3 standard deviations of the mean. These bounds represent the maximum and minimum temperatures beyond which fecundity is observed to be zero.

The temperature-dependent fecundity curve's bounded Gaussian shape was taken from the base Langille et al. (2016) model but the base model's fecundity equation, with parameters specific to *D. suzukii,* was replaced with the simple Gaussian curve function seen below.

$$f(x) = a\, e^{-\frac{1}{2}\left(\frac{x-b}{c}\right)^2} \tag{1}$$

Here *f(x)* is the Gaussian curve function, a is the height of the curve, b is the center of the peek and c is the standard deviation of the curve, determining its width. a, b and c are all real constants.

The model's full temperature dependent fecundity rate equation is as follows:

$$f(T) = \begin{cases} a\, e^{-\frac{1}{2}\left(\frac{T-b}{c}\right)^2} & if\ (\mathrm{T} \leq\ \mathrm{fTmax\ and\ T} \geq\ \mathrm{fTmin}) \\ 0 & otherwise \end{cases} \tag{2}$$

where

$$a = fmax \tag{3}$$

$$b = \frac{fTmax - fTmin}{2} + fTmin \tag{4}$$

$$c = \frac{fTmax - b}{3} \tag{5}$$

where *f(T)* is the per capita eggs laid per day at temperature *T* and the real constants *a*, *b* and *c* are calculated using three easily visualized species fecundity parameters. Fmax is the greatest fecundity at the optimal temperature (number of eggs laid by an adult female per day, when temperatures are optimal). *fTmax* and *fTmin* are the maximum and minimum temperature for fecundity to be non-zero. Each of these values are species dependent and can be measured in a laboratory setting and input by the user.

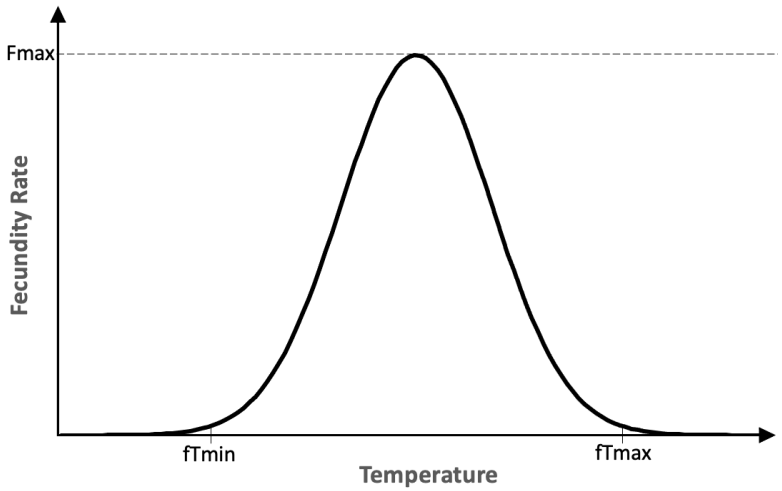

Figure 2.2 General model's temperature-dependent fecundity curve. A Gaussian curve bounded between the model parameter values of *fTmin* and *fTmax*, with the peak value of *Fmax*.

2.4.2 Development Rate

The model utilizes the same development rate equation for all insect life stages but can represent three different biological processes: immature development, mature development, and longevity – all of which are temperature dependent. For immature life stages (eggs, instars and pupas) this equation is used to represent the development rate to the next life stage. For mature life stages, it is the rate at which female sub-stages transition to the next egg viability sub-stage. While for adult males and final sub-stage females the equation acts as the stage's longevity.

In the base Langille et al. (2016) model, a modified version of the Brière et al. (1999) equation 1 (briere1) temperature-dependent development rate equation was used, whereas this generalized insect model uses Brière et al. (1999) equation 2 (briere2) seen below which replaces briere1's constant value of 2 with the dimensionless shape variable *m*.

$$d_i(T) = a_i\, T\, (T - Tmin)(Tmax - T)^{\frac{1}{m}} \quad (6)$$

where d_i is the temperature-dependent development or longevity rate (1/days) for stage *i*. a_i is a dimensionless shape parameter for stage *i*. This shape parameter can be obtained through the fitting of the development rate equation with measured constant temperature development data. *T* is the current air temperature (°C), *Tmin* is the lower development temperature threshold (°C) and *Tmax* is the upper temperature threshold (°C). The value of the max and min development temperatures depend on the species and can be determined through laboratory studies or estimated based on existing species' knowledge. *m* is a dimensionless constant, that effects the shape of the curve including the position of the optimum temperature, set to equal 3 in this general model.

The briere2 development equation was chosen over other existing models because of its simplicity and minimal parameter requirements, making it well-suited for a general insect model with the goal of reducing input parameters. The briere2 equation's parameters were further reduced by giving the dimensionless shape parameter *m* the constant value of 3, chosen based on the curve shape's goodness of fit to many insect species' temperature-dependent development rate data.

Like several temperature-dependent development rate equations (Logan et al. 1976; Taylor 1981; Lactin et al. 1995), this equation follows an asymmetric curve with a linear ascension (Gaussian) as temperatures rise, peaking at the optimal development temperature and descending in a parabolic curve (figure 2.3).

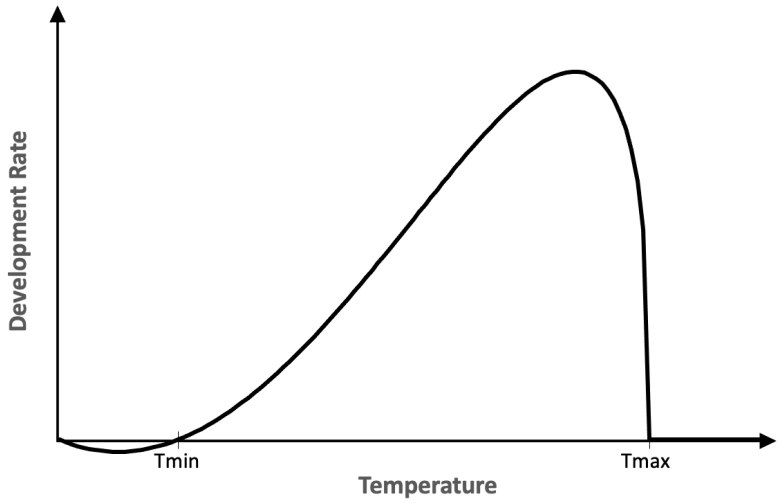

Figure 2.3 General model's temperature-dependent development curve. The curve follows the briere2 development equation, with a Gaussian rising curve and a descending parabolic curve, which intersect zero at the model parameter values *Tmin* and *Tmax*.

2.4.3 Mortality Rate

Temperature-dependent mortality is applied to each developmental life stage (egg to adult) and represents the effect of daily temperatures on the insects' survival. The mortality function follows a parabolic curve that becomes linear with a null slope once outside of the bounds of TL and TU (figure 2.4). This function is based on the temperature-dependent mortality equation seen in Langille et al. (2016), however, the driving polynomial equation was reduced from a third-degree to a second-degree polynomial. A second-degree polynomial or parabola equation was found to produce a good fit with temperature-dependent mortality data collected in laboratory studies and has been used as the best fit for insect mortality data as seen in a study of Temperature Dependent Growth and Mortality of the Turnip Moth (*Agrotis segetum*) in (Esbjerg and Sigsgaard, 2019).

The model incorporates the second-degree polynomial equation:

$$p(x) = a\,x^2 + b\,x + c \tag{7}$$

where *a*, *b* and *c* are real constants in the model's complete mortality rate equation as seen below.

$$\mu_i(T) = \begin{cases} a_i\,T^2 + b_i\,T + c_i \;if\; (\mathrm{T} \leq \mathrm{TU\ and\ T} \geq \mathrm{TL}) \\ maxMort \quad otherwise \end{cases} \tag{8}$$

where

$$a_i = \frac{TU(maxMort - minMort) + TL(minMort - maxMort)}{denom} \tag{9}$$

$$b_i = \frac{TU^2\,(minMort - maxMort) + TL^2\,(maxMort - minMort)}{denom} \tag{10}$$

$$c_i = \frac{\begin{matrix} TU*Topt*(TU - Topt)*maxMort + Topt*TL*(Topt - TL)*maxMort + \\ TL*TU*(TL - TU)*minMort \end{matrix}}{denom} \tag{11}$$

where

$$Topt = \frac{(TU - TL)}{2} + TL \tag{12}$$

$$denom = (TL - TU)(TL - Topt)(TU - Topt) \tag{13}$$

where $\mu_i(T)$ is the daily per capita temperature-dependent mortality for an insect species at life stage *i*. *T* is the current air temperature (°C). The constants a_i, b_i and c_i are calculated using measurable insect species and mortality temperature parameters. *TL* and *TU* are the lower and upper mortality temperature thresholds (°C) beyond which mortality is at its maximum, *maxMort*. *minMort* is the lowest possible daily mortality rate which occurs at the optimal temperature *Topt*. *TL*, *TU*, *minMort* and *maxMort* are the only stage-specific parameters input by the user and can be determined through laboratory studies.

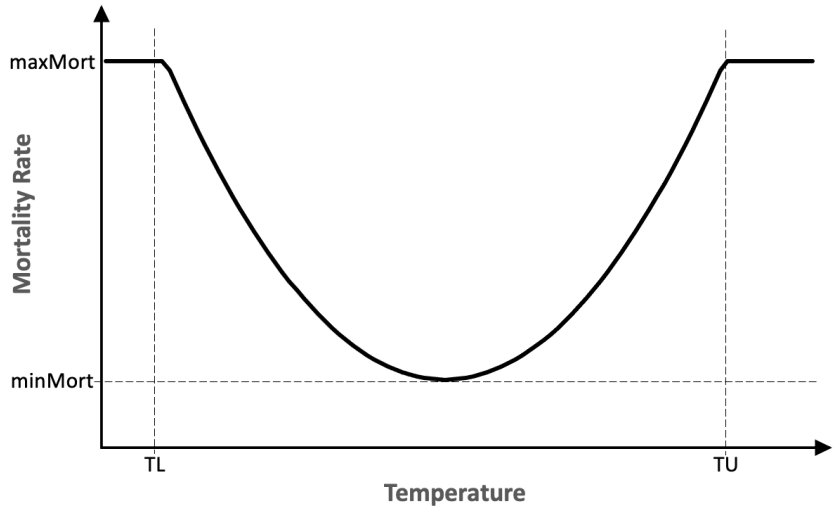

Figure 2.4 General model's temperature-dependent mortality rate curve. A parabolic curve with a vertex at mortality rate *minMort*, bounded between the model parameter values *TL* and *TU*, beyond which the mortality rate is equal to *maxMort*.

2.4.4 Reproductive Diapause

The reproductive diapause sub model present in the original *D. suzukii* model by Langille et al. (2016) was generalized to account for a greater number of fecundity diapause termination curves. The general model's reproductive diapause sub model maintains the same computational control switches s1 and s2 used to enable and disable diapause in Langille et al. (2016) along with maintaining the reproductive diapause's effect on fecundity. However, the equation that provides the proportion of females currently in reproductive diapause based on photoperiod in hours, was generalized to potentially account for various insects species, which could terminate diapause with different critical photoperiod and do so more or less rapidly than *D. suzukii* (equation 14). A logistic function was chosen due to its good fit to both the original Langille et al. (2016) diapause curve and the reproductive diapause termination proportion curve for *Aphalara itadori* seen in Grevstad et al. (2022). The general model's equation that represents the proportion of adult females

currently in reproductive diapause, can be seen below. The equation was based on the logistic function, but, was modified to always have a maximum value of 1.

$$pDia(h) = \frac{1}{1+e^{-diaRate(h-dLh_{halfDia})}} \quad (14)$$

where *pDia* is the proportion of reproductive diapause females, *diaRate* is the rate that reproductive diapause is terminated or induced, h is the current number of daylight hours and $dLh_{halfDia}$ is the number of daylight hours for half of the female population to be in reproductive diapause.

2.4.5 Overwintering

A rudimentary overwintering sub model, independent from the Langille et al. (2016) base model, was implemented to allow multi-year simulations of insect species in temperate climates. Simplifications were made to this sub model in order to account for more varied overwintering strategies and to reduce the number of required user input parameters. The sub model can function as a variety of overwintering strategies such as freeze avoidance, freeze tolerance, diapause, quiescence, and migration. The sub model was created based on the biological mechanisms that drive overwintering, explored in section 1.3. The overwintering sub model is designed to have a single overwintering life stage which is regulated by three variables: currentOWCondition, OWstate and OWflag whose function in the model is described below.

currentOWCondition represents the current temperature and daylength conditions. It is set to 1 if conditions are suitable for overwintering termination (when current temperature and daylight hours are less than the species overwintering critical induction temperature and induction daylight hours) and set to 0 if conditions are suitable for overwintering induction (when the current temperature and daylight hours are greater than the overwintering critical termination temperature

and termination daylight hours). Since overwintering induction and termination can have different critical values, it is possible for temperature and daylight hours to have values such that the species should both be inducing overwintering and terminating overwintering. In this case currentOWCondition is set to 2. See equation 15.

The Boolean value, overwintering state or OWstate, indicates whether the insect species' overwintering life stage population is (0), or is not (1), currently overwintering. When the life stage is overwintering, development and mortality are paused. If the modelled species overwinters in its adult life stage, fecundity is also paused. The overwintering life stage development, mortality and, in adults, fecundity rate is set to 0 by using the OWstate value as a multiplier on development, mortality and egg viability. Overwintering state is set to overwinter based on the currentOWCondition value. While the population is in an overwintering state, any new insects that develop into the overwintering life stage will also pause their development, mortality and potentially fecundity.

Without any additional control variables, when temperature and daylength conditions are suited to both overwintering induction and overwintering termination for a series of days, the overwintering sub model would oscillate between a state of overwintering and not overwintering. The variable OWflag, a switch that has no biological meaning, was used to ensure that if conditions are suitable for both overwintering induction and termination (currentOWCondition == 2), OWstate will only be switched on the first timestep under these conditions and will then remain in the same state until the currentOWCondition value changes. Overall, this means that when conditions become favorable to both induction and termination, the sub model switches its overwintering state, and maintains that state until conditions are only favorable for either induction or termination. See pseudo code below.

The overwintering model is driven by the equations and pseudo code below.

$$currentOWCondition = \begin{cases} \text{if } (temp \leq IcritT \text{ and } hours \leq IcritH) \text{ and} & 2 \\ \quad (temp \geq TcritT \text{ and } hours \geq TcritH) & \\ \text{else if } (temp \leq IcritT \text{ and } hours \leq IcritH) & 0 \\ \text{else if } (temp \geq TcritT \text{ and } hours \geq TcritH) & 1 \end{cases} \quad (15)$$

where *currentOWCondition* is a value that indicates if conditions are suitable to be overwintering, not overwintering or both. *temp* is the current temperature, *hours* is the current number of daylight hours, *IcritT* is the overwintering critical induction temp, *IcritH* is the overwintering induction daylight hours, *TcritT* is the overwintering critical termination temp and *TcritH* is the overwintering termination daylight hours.

Pseudo code for overwintering sub model; run for each model time step:

```
//set the Owstate based on currentOWCondition and previous Owflag
if (Owflag == 1 && currentOWCondition == 2){
      Owflag = 1
      Owstate = 0
}
else if (Owflag == 0 && currentOWCondition == 2){
      Owflag = 0
      Owstate = 1
}
else if (Owflag == 0 && currentOWCondition == 1){
      Owflag = 1
      Owstate = 1
}
else if (Owflag == 1 && currentOWCondition == 0){
      Owflag = 0
      Owstate = 0
}
else if (Owflag == 1 && currentOWCondition == 1){
      Owstate = 1
}
else if (Owflag == 0 && currentOWCondition == 0){
      Owstate = 0
}
```

The overwintering sub model is a simplification of its real-world counterpart made in order to reduce the number of parameters required by the model. In reality, winter survival rates are

effected by winter temperatures and not all individuals will be successful at overwintering, due to low temperatures, in adequate shelter or biological complications with freeze avoidance (Bale and Hayward 2010). Consideration for these factors is added to the overwintering sub model through the inclusion of an overwintering success rate parameter and overwintering mortality temperature parameter. The overwintering success rate parameter is a proportion value (between 0 and 1) applied to the insect population as overwintering is induced, to eliminate a certain ratio of the population which represents insects that were unsuccessful at overwintering. In the simplest case, the overwintering success rate can simply use an estimated value based on the understanding that mortality will occur during overwintering. For more accurate overwintering survival, the user can calculate the appropriate overwintering success rate externally, based on winter temperatures and the insect species overwintering response to these temperatures. The overwintering mortality temperature parameter, is the minimum winter temperature below which all insects, overwintering or not, die.

2.4.6 Mortality Event

An additional feature added to the generalized model was the mortality event. The feature was designed to simulate events such as the application of pesticides, or any other natural or anthropogenic event that could severely reduce an insect population. For each of the mortality events, the model parameters specify the Julian day (January 1st is Julian day 1) of the mortality event (mortality event date), the life stage affected by the mortality event (mortality event life stage), and the percentage of the mortality event life stage population killed during the mortality event (mortality event percentage). With the inclusion of the mortality event sub model, the model functions by removing a percentage of the life stage specified, on each of the mortality event dates.

The mortality event sub model is highly simplified from a biological standpoint, with the main simplification being that all mortality occurs within one time step. This simplification is, however, sufficient to approximate a mortality event's effect on an insect population and increase the scope of the general model's applicability.

2.4.7 Environmental Equations

The model's environmental equations are taken verbatim from the *D. suzukii* model by Langille et al. (2016) but are included below for completeness. The equations determine the current number of daylight hours, a value used in the overwintering and reproductive diapause sub models. The daylight hours *h* equation is as follows:

$$h = \frac{24}{\pi} arccos(k') \tag{16}$$

where

$$k' = \begin{cases} -1 & if\ k < 1 \\ 0 & if\ k > 1 \\ k & otherwise \end{cases} \tag{17}$$

where

$$k = tan\left(\frac{\pi L}{180°}\right) tan\left(\left(\frac{\pi R}{180°}\right) cos\left(\frac{\pi Y}{182.625°}\right)\right) \tag{18}$$

where *k* is the exposed radius between the sun's zenith and the solar circle, *L* represents latitude, *Y* the number of days from January 1st and *R* the Earth's current rotational axis 23.439°

Some smooth cosine temperature curve data is provided with the model, each representing the approximate daily average temperature for a year in a certain climatic zone (Table 1). Temperature cosine curves tempA, tempB, tempC and tempD were appropriated from Langille et

al. (2016). More information on the cosine temperature profile curve equations can be found in Langille et al. (2016).

Table 1 List of cosine curve temperature profiles tempA, tempB, tempC and tempD, including their temperature characteristics and the approximate location that they represent. These temperature profiles are provided with the general model and used in the exploration and sensitivity model testing.

Name	Characteristics	Approximate Location
Temp A	Moderate summers, cold winters, large inter seasonal variation	Chicoutimi, QC
Temp B	Moderate summers, cold winters, moderate inter seasonal variation	Clark county, WA
Temp C	Warm summers, moderate winters, reduced inter seasonal variation	Santa Barbara county, CA
Temp D	Hot summers, moderate winters, reduced inter seasonal variation	Hilsborough county, FL

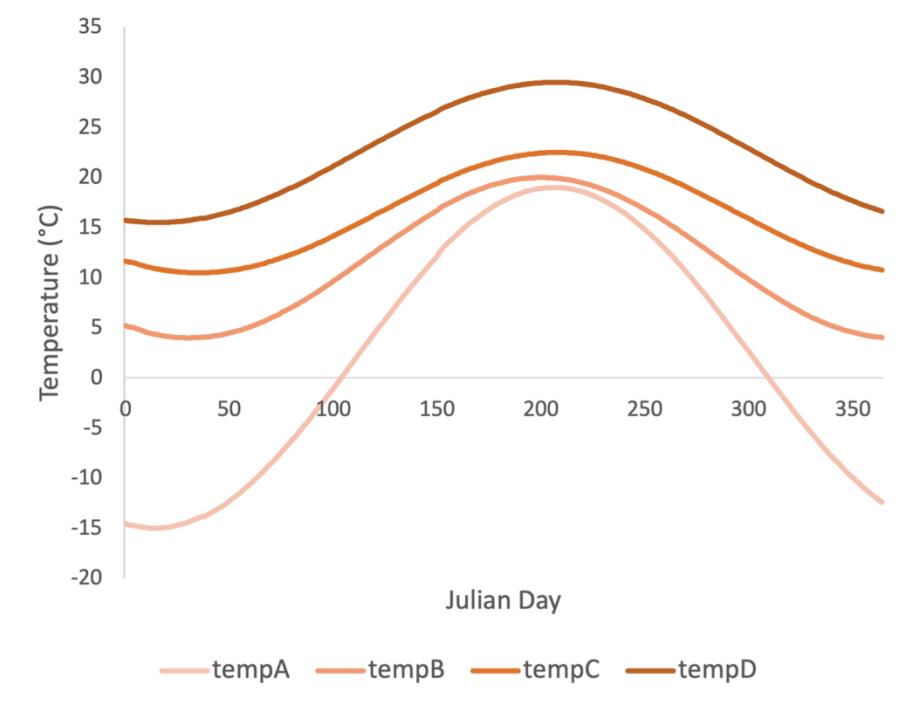

Figure 2.5 Cosine temperature curve profiles tempA, tempB, tempC and tempD, that represent approximate daily average temperatures for a year in a certain climatic zone. These temperature profiles are provided with the general model and used in the exploration and sensitivity model testing.

2.4.8 Model State Equations

The following state equations are used to progress the population through time and through each of the life stages. These equations were adapted from the Langille et al. (2016) model: changing any hardcoded values related to *D. suzukii*'s number of life stages, making the pupal stage state equation optional depending on the species metamorphosis, and adding longevity to the male and final female life stages. The differential equations use the Euler method and follow the general structure: *Change in stage population = development from previous stage – (the current stage population's, intrinsic loss, extrinsic loss, and development).*

The rate of change of the egg stage is represented by the equation:

$$\frac{dE}{dt} = \left(\sum_{i=1}^{n_F} f v_i F_i\right) - E\left(\mu_{in,e} + \mu_{ex,e} + d_e\right) \quad (19)$$

where n_F is the number of adult female stages, f is the female fecundity, v_i is the egg viability at the adult female sub stage i, F_i is the number of adult females at sub stage i, E is the number of eggs at time t, $\mu_{in,e}$ is the daily per capita intrinsic egg mortality (see equation 8), $\mu_{ex,e}$ is the daily per capita extrinsic egg loss obtained through the predation rate and d_e is the daily per capita egg development rate (see equation 6).

The rate of change of the first juvenile instar and subsequent juvenile instar stages is represented by the equations:

$$\frac{dI_1}{dt} = d_e E - I_1\left(\mu_{in,I1} + \mu_{ex,I1} + d_1\right) \quad (20)$$

$$\frac{dI_i}{dt} = d_{i-1} I_{i-1} - I_i\left(\mu_{in,Ii} + \mu_{ex,Ii} + d_i\right) \text{ for } i = 2 \ldots nI \quad (21)$$

where *nI* us the number of juvenile instars, I_i is the number of instars at time *t, i* is the current instar stage and *i-1* the previous life stage, $\mu_{in,Ii}$ is the daily per capita intrinsic instar mortality and $\mu_{ex,Ii}$ is the extrinsic instar mortality (predation rate), d_i is the daily per capita instar development rate.

From the last instar stage the insect may pass through a pupal stage before becoming an adult. The rate of change of the pupal stage is represented by the equations:

$$\frac{dP}{dt} = \begin{cases} d_{nI} I_{nI} - P\left(\mu_{in,P} + \mu_{ex,P} + d_P\right) & if\ hP\ =\ \text{true} \\ NA & if\ hP = \text{false} \end{cases} \tag{22}$$

where d_{nI} is the daily per capita development rate of the last juvenile instar and I_{nI} is the number of juveniles in the last instars stage at time *t*. *P* is the number of pupae at time *t,* $\mu_{in,P}$ is the daily per capita intrinsic pupa mortality and $\mu_{ex,P}$ is the extrinsic pupa mortality (predation rate), d_p is the daily per capita pupa development rate. *hP* is a Boolean value based on the presence of a pupal stage in the species development cycle, *hP* is true when the species has a pupal stage and false otherwise.

The rate of change of the adult male stage is represented by the equations:

$$\frac{dM}{dt} = \begin{cases} \theta\ d_P P - M\left(\mu_{in,M} + \mu_{ex,M} + d_M\right) & if\ hP\ =\ \text{true} \\ \theta\ d_{nI} I_{nI} - M\left(\mu_{in,M} + \mu_{ex,M} + d_M\right) & if\ hP = \text{false} \end{cases} \tag{23}$$

where θ represents the proportion of adult insects that become males, *M* is the number of adult males at time *t,* d_M is the daily per capita longevity for adult males (uses the development rate), $\mu_{in,M}$ is the daily per capita intrinsic adult male mortality and $\mu_{ex,M}$ is the extrinsic adult male mortality (predation rate).

The female life stage can be divided into multiple sub stages with egg viability varying depending on the female's age. The rate of change of the female sub-stages is represented by the equations:

$$\frac{dF_1}{dt} = \begin{cases} (1-\theta)\, d_P P - F_1\left(\mu_{in,F_1} + \mu_{ex,F_1} + d_{F_1}\right) & if\ hP\ =\ \text{true} \\ (1-\theta)\, d_{nI} I_{nI} - F_1\left(\mu_{in,F_1} + \mu_{ex,F_1} + d_{F_1}\right) & if\ hP = \text{false} \end{cases} \quad (24)$$

$$\frac{dF_i}{dt} = d_{F_{i-1}} F_{i-1} - F_i\left(\mu_{in,F_i} + \mu_{ex,F_i} + d_{F_i}\right) \quad for\ i = 2 \ldots nF \quad (25)$$

where $(1 - \theta)$ represents the proportion of adult flies that become females, nF is the number of adult female stages, F_i is the number of adult females at time t, i is the current female stage and d_{Fi} is the daily per capita adult female development rate (or longevity for the last female stage – when $i = nF$) for stage i. $\mu_{in,Fi}$ is the daily per capita intrinsic adult female mortality and $\mu_{ex,Fi}$ is the extrinsic adult female mortality (predation rate).

2.5 Model Differential Equation Solving Method

The model's state equations are solved using Euler's method of numerical approximation. Euler's method was maintained as the differential equation solving method from the original *D. suzukii* model, however, it is known to have issues with rounding errors over long periods and is less accurate with small integration step sizes. Therefore, the effect of the model's integration step size on the model's resulting adult female population was tested (figure 2.6) to ensure the method's suitability for the model's purposes and that other differential equation solving methods such as Runge-Kutta and Heun where not required. It was determined that the errors arising from the differential equation solving method were limited and that Euler's method produced adequate results for the purposes of this model. The model's primary use is not accurate population counts, therefore, the fact that the population shape is maintained is adequate. Additionally, the choice of

the integration step size is left up to the model user and the burden will fall on their hands to choose appropriate values to avoid significant errors.

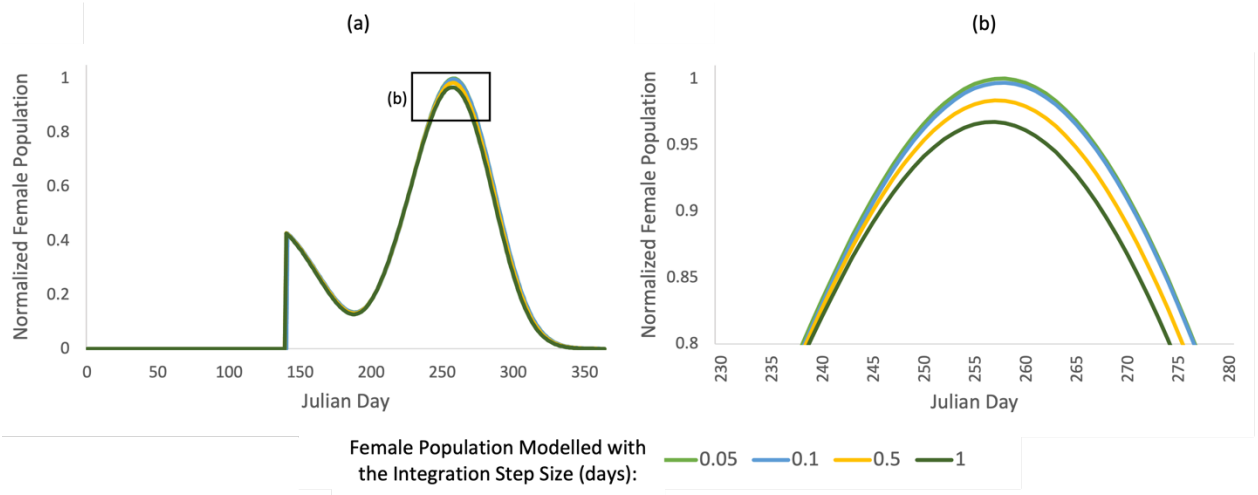

Figure 2.6 (a) Normalized daily female population produced by a one-year general model simulation run with default parameters (Appendix B) with different integration step sizes: 0.05, 0.1, 0.5 and 1 day. (b) Enhanced visualization of the boxed area in (a) (for Julian Days 230 to 280 and normalized female population 0.8 to 1), where the female populations have the greatest size difference between runs with different integration step sizes.

2.6 Technical Details and Model Implementation

The general model was implemented in C++ adding on the existing C++ model code from the *Drosophila suzukii* species-specific model by Langille et al. (2016). The model was compiled using the GNU g++ compiler version 4.2.1 for Linux. All model source code files are available at https://github.com/domdelay/GeneralizedInsectPopulationDynamicsModel in order to provide free open-source access and to encourage further model iterations and modifications along with allowing for study replicability.

The general model takes an object-oriented approach to simulating insect populations. The model is divided into 4 object classes to improve the code's organization and understandability. Each class: SimulatorSingle, CellSingle, Population and Parameters, has their own purpose in the model. The Parameters object represents all the parameters in the CellSingle object, storing the

parameters as a map (String key, double value) and includes methods to retrieve and modify parameters. The Population object tracks each life stage's population over time, includes methods to access and modify current life stage populations, and a method that runs the life stage population through one timestep. The CellSingle object models the population in an environment cell and uses a Parameter object to calculate population vital rates under the environment cell's temperature. The SimulatorSingle object simulates the CellSingle object through a model run under various specified conditions. The object classes' relationships can be seen in the Unified Modelling Language (UML) diagram below (figure 2.7). The model also has a runner class, SingleCellRunner, that takes all required input file names from the user and passes them to the model's object classes. The runner is also responsible for printing the model's results to a specified output data file.

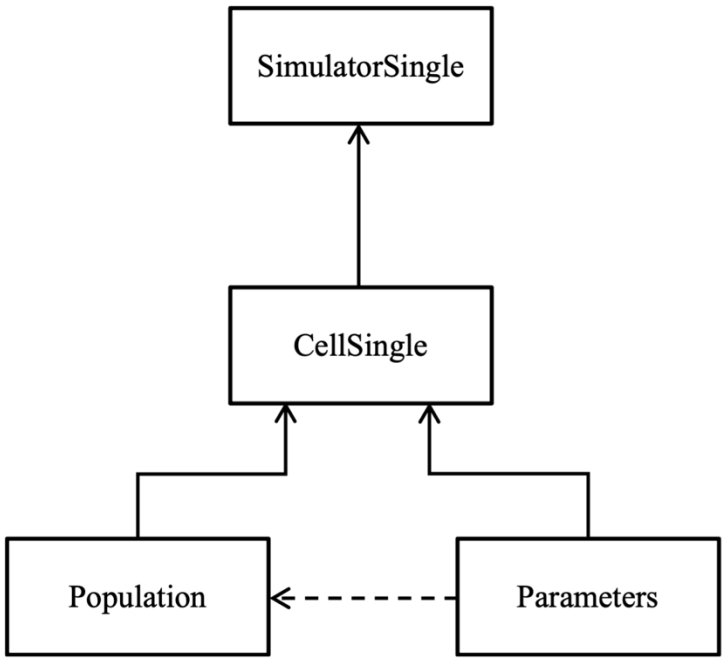

Figure 2.7 Simplified UML (Unified Modelling Language) diagram of the relationships between the model's object classes. Solid arrows represent association relationships and dashed line arrows represent dependency relationships.

The model also has 4 other C++ utility files: SolveParameters, EulersMethod, UtilityMethod and Daylight. SolveParameters contains all vital rate equations along with the reproductive diapause equations and switches. EulersMethod contains all the Euler's method differential equations used to calculate the current populations size for each life stage. UtilityMethod contains any useful methods to simplify code. Daylight contains all the methods required to compute the daylight hours at a certain time step based on the latitude (used by the overwintering and diapause sub models).

3. Chapter 3 Model Exploration and Sensitivity Testing

3.1 Introduction

Sensitivity and exploratory tests were conducted on the general model to demonstrate how the model and its elements respond to a variety of parameters, and to confirm that results are in line with existing knowledge of insect population dynamics. While these tests are not exhaustive, they were chosen based on the model elements that illustrated key model processes or explored new general model functionality. The sensitivity and exploratory tests run in this chapter don't attempt to mimic any specific insect species parameters or real-world circumstances, rather, they are intended to isolate and study specific model behaviors.

Unless otherwise specified, results were produced using the following conditions. The model was configured using "toy" parameters to represent a fictional insect species with six life stages (egg, instar, pupa, male, and two female stages - F1 and F2) each with equal vital rates (development, mortality and fecundity) and egg viabilities equal to 0 for F1 and 1 for F2. This default configuration data did not include any sub model values. The model was initialized with 50 F1 females introduced on Julian day 140 (May 20th) and was run for one year (Julian day 0 to 365). The cosine temperature curve tempB (a smooth cosine temperature curve that represents approximate daily average temperatures for a year in a climatic zone with moderate summers, cool winters and moderate inter seasonal variation) created by Langille et al. (2016) was used as the model's default temperature profile. The complete default toy configuration parameter file is available in appendix B.

When appropriate, test results were normalized by dividing each time step population value by the maximum population value for the data set. This normalization technique results in a peak

population value of 1, deemphasizing the modelled result's absolute scale to focus on the relative comparison of the populations.

3.2 Temperature Tests

Temperature is the principal driver of insect population dynamics in the general model. Through the tests in the section below, the general model's response to changes in temperatures is described and quantified.

3.2.1 Population Response to Constant Temperatures

A series of one-year general model simulations were run at various constant temperatures and the resulting normalized cumulative female populations were graphed on a log scale to demonstrate the model's key population dynamics in response to temperature. Under suitable conditions for development, low mortality, and fecundity, the population grows exponentially until it nears the optimal temperature (figure 3.1). Once the optimal temperature is surpassed, development slows, mortality increases and fecundity decreases resulting in a drop in the cumulative population.

The toy population's optimal temperature of approximately 23°C is determined by a combination of the toy species' optimal vital rate temperatures: 23°C for the optimal development temperature, 17.5°C for the least mortality, and 24°C for optimal fecundity. This result produces a similar constant temperature insect population curve shape as seen in Govindan and Hutchison (2020) for the Brown Marmorated Stink Bug (*Halyomorpha halys*), and in Choudhary et al. (2020) for the Peach Fruit Fly (*Bactrocera zonata*).

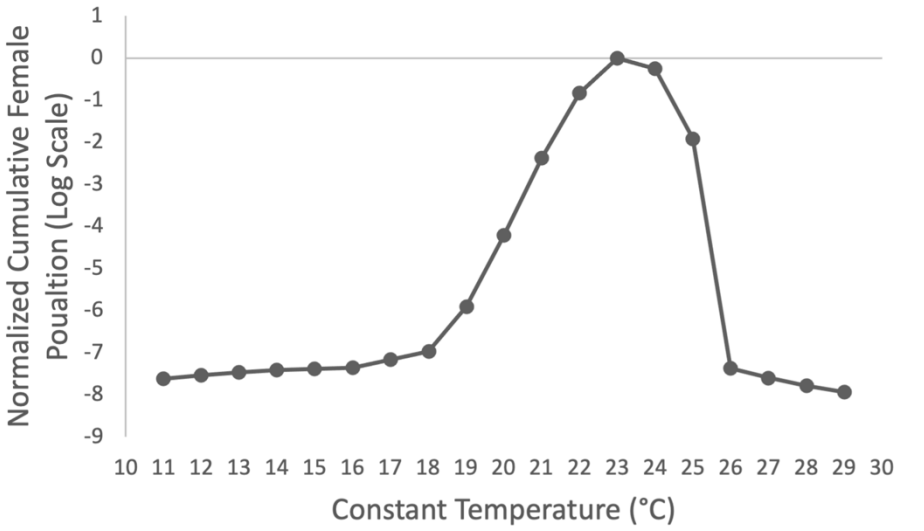

Figure 3.1 Normalized cumulative female population on a log scale for various constant temperature simulations. The general model was run for 365 days with 50 F1 females introduced on Julian day 140. The negative population axis is due to the cumulative female population values being both normalized and log scaled and does not represent real population numbers.

3.2.2 Population Response to Cosine Temperature Profiles

To study the effect of different yearly temperature profiles on modelled insect populations, the general model was run with four synthetic cosine curve temperature profiles (tempA, tempB, tempC and tempD) created by Langille et al. (2016), which are loosely representative of distinct climatic regions daily mean temperature curves (figure 2.5).

The temperature profile tempC produced the biggest population, making it the most suitable climate for the toy species. The temperature profile tempB's peak female population exceeded the size of its initial population, indicating the toy insect's successful establishment. The temperature profiles tempA and tempD, on the other hand, were not suitable for the establishment of the toy insect species and did not produce a population of sufficient size to be sustained the following year (figure 3.2).

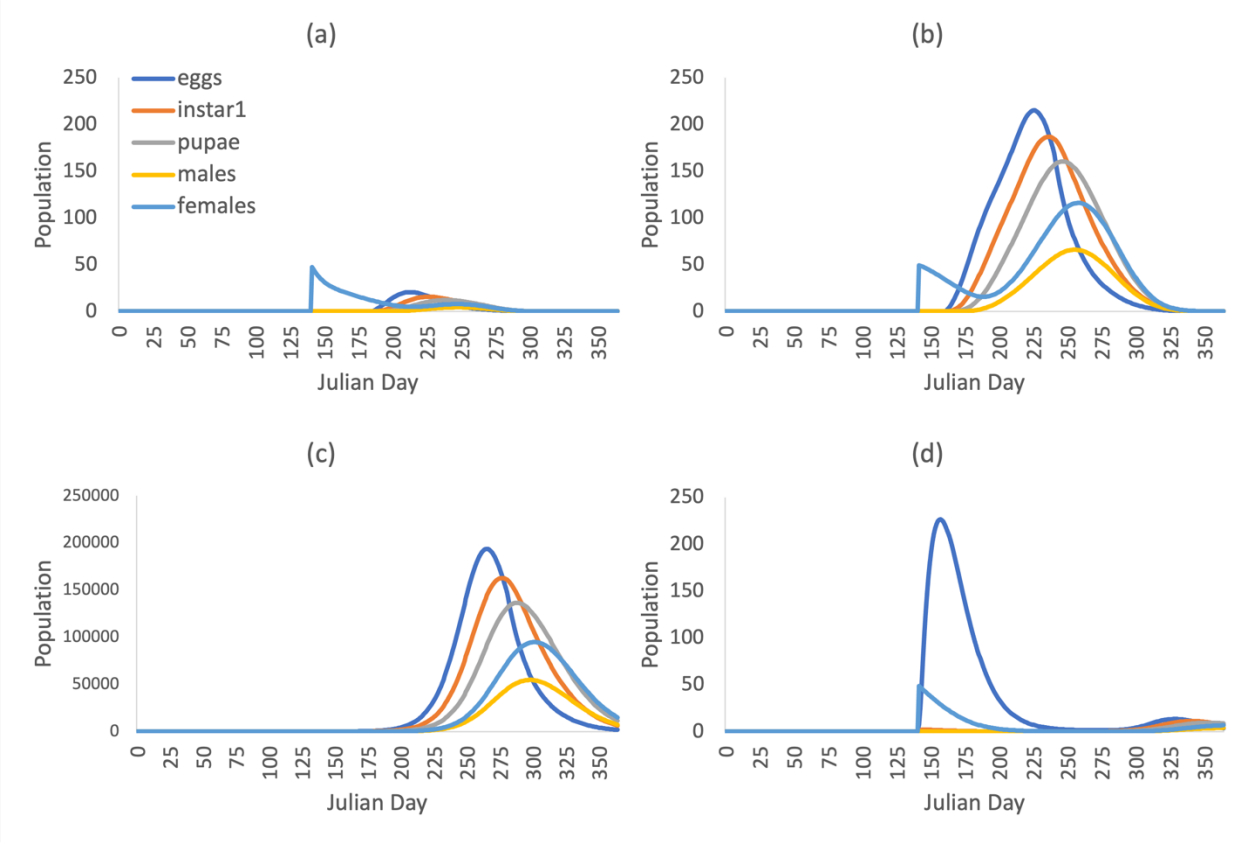

Figure 3.2 Simulated life stage population curves for the toy insect under the cosine temperature profiles (a) tempA, (b) tempB, (c) tempC and (d) tempD (figure 2.5). The general model was run for one year with 50 F1 females introduced on Julian day 140.

A better understanding of the specific causes of the populations' success or failure can be gleaned by examining the species' vital rate values over each temperature profile in figure 3.3. Temperature profiles with daily temperatures that frequently remain below the optimal temperature will produce relatively small populations due to a combination of slow development, high mortality, and low fecundity (tempA). For example, for 225 days out of the year, tempA temperatures are too low for the toy species to develop and has a high mortality rate with a 7% population loss per day. In addition, only 50 days out of the year have suitable conditions for egg production, during which fecundity only reaches a maximum value of approximately 0.25 eggs per day (figure 3.3). Temperature profiles that surpass the optimal temperature will also produce

small populations due to elevated mortality and slower development (tempD). Temperature profiles that remain within the range of a few degrees of the optimal temperature for a prolonged period will produce more successful populations (for example, tempB and tempC). The general model's results under different cosine temperature curves are in agreement with the law of tolerance (Shelford, 1913) - if temperatures are within the optimum range, the population will be abundant; if temperatures are within the range of tolerance, the population will be less successful; if temperatures are in the zone of intolerance the population will be non-existent.

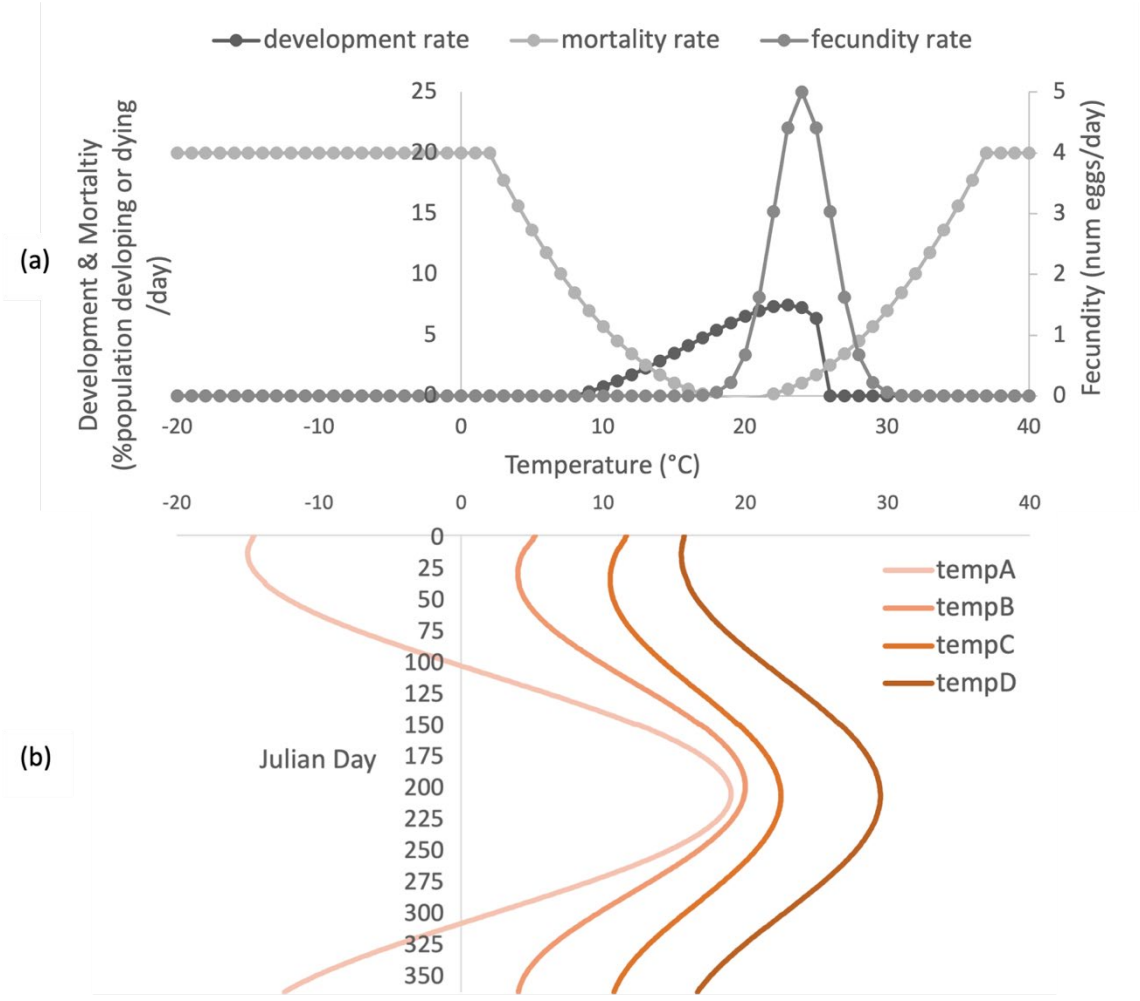

Figure 3.3 (a) vital rates (development, mortality and fecundity) for the toy species at various constant temperatures. (b) temperatures over one year for the cosine temperature profiles tempA, tempB, tempC, and tempD (Note that the temperature and Julian day axes have been switched). The vital rate values for each Julian day under the cosine temperature profiles can be determined by linking these figures through their shared temperature axis.

3.3 Initial Population Tests

In the general model, a simulation's initial insect population can either be comprised of an introduced insect population or an overwintering population terminating its overwintering state. This initial population can vary in size, start date and life stage composition. In this section, the effect of these three initial population factors was explored to have a clear understanding of their effect on the resulting modelled population.

3.3.1 Effect of Starting Population Date and Size

To get a better understanding of the effect of the starting population date and size on total female populations, the model was run multiple times with different introduction dates (Julian day 0, 50, 100, 150, 200, 250, 300, 350) and initial female population sizes (10, 100, 1000, 10000). The model used all other default configuration parameter values (Appendix B) and was run with the default temperature profile (tempB).

The population's introduction date affects its growth potential (figure 3.4). The earlier the introduction date, the more time there is for the population to grow before colder temperatures come with the end of the year. However, if the population is introduced too early, it will experience higher mortality rates due to cold early year temperatures, reducing the population's potential size. The optimal population introduction date can therefore be found at the balancing point between these factors: where a population isn't affected by the early year mortality and still has sufficient time to grow before the end of the year. In this toy species' case, the optimal population introduction date was on Julian day 150. If the model's input temperature profile differs in its rate of increase and in its maximum and minimum temperatures, the optimal population introduction

date will vary. Populations under temperature profiles with less seasonality are less affected by introduction dates.

The initial population's size has a linear scaling effect on any introduction date's simulated population, causing the cumulative population to always be proportional to the model's initial population size. For example, when introduced on Julian day 100, an initial population of 100 females resulted in a population of 5043.17 cumulative simulated females, while an initial population of 1000 females resulted in a population of 50431.7 cumulative simulated females. An initial population that is 10 times larger will result in a 10 times larger cumulative population. This agrees with the established understanding of population growth.

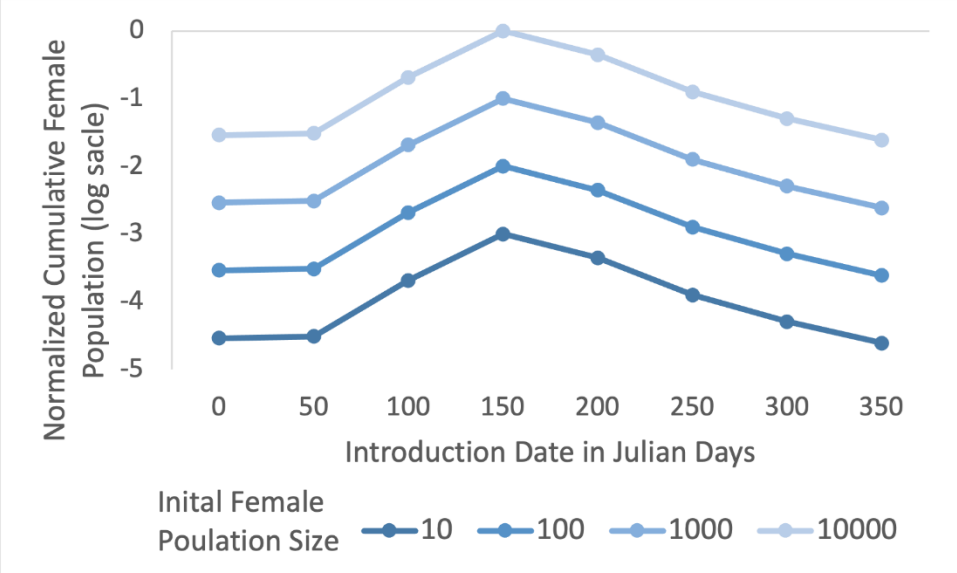

Figure 3.4 Normalized cumulative female population on a log scale produced by general model simulations with various introduction dates and initial population sizes. Each simulation is run for 365 days with the default toy species, under the temperature profile tempB. The negative population axis is due to the cumulative female population values being both normalized and log scaled and does not represent real population numbers.

3.3.2 Effect of Starting Population Life Stage

This test represents an insect species' potential for population growth, based on its initial life stage. The general model was initialized with the default toy data initial population size and

date (50 F1 females on Julian date 140) but used a different starting life stage for each run (egg, instar, pupa and female1). The model used all other default configuration parameter values and was run with the default temperature profile (tempB).

Figure 3.5 explores the effect of the initial population's life stage on the resulting daily female population. A slower population increase was observed in model runs with initial populations composed of early developmental life stages, such as eggs and instars, resulting in a smaller peak female population. Initial populations composed of early developmental life stages must first develop into adults before eggs can be produced and the population can increase. As egg production begins later in the year, populations composed of early developmental life stages have a shorter egg production period, producing fewer new individuals overall. This population lag is most severe with initial egg populations, lessening in severity with initial populations composed of later development life stages. This model behavior matches what would be expected from a real-world system's population if different life stages were introduced on the same date.

It is interesting to note that the peak female populations occur on the same date regardless of the initial population's life stage. This is due to the consistent vital rate for all life stages in the toy data, causing populations to continue growing until the temperature conditions result in mortality rates that are greater than the fecundity rates. Peak female populations wouldn't necessarily occur on the same date, if a more realistic insect species with different life stage vital rates was modelled.

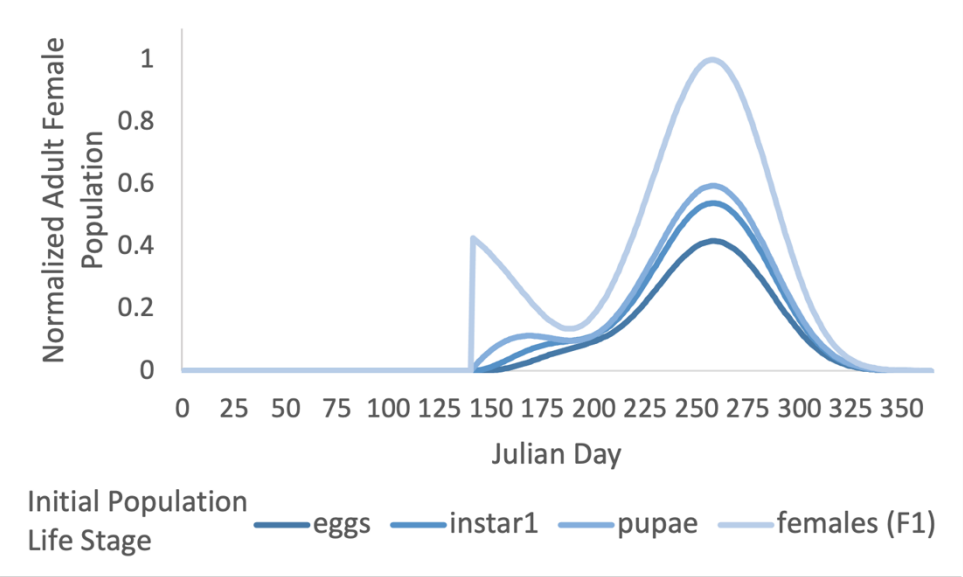

Figure 3.5 Adult female population curve for model simulations initialized with various initial population life stages (egg, instar, pupa and female1) on Julian day 140. The initial population was always composed of 50 females and the model was run with the temperature profile tempB. The spike and subsequent decrease in the females initial population life stage curve (lightest blue line) is caused by the introduction of 50 females on Julian day 140, which quickly decrease due to temperature conditions on the following dates causing high female mortality.

3.4 Overwintering Sub Model Tests

The size of the population that enters an overwintering state determines the specie's potential for success the following year. The general model's overwintering sub model was tested with the goal to identify factors that contribute to the optimal timing for overwintering induction. Due to overwintering juveniles and adults different behavior, both overwintering stages were examined. The date of overwintering induction in relation to the model's population curves was the principle study parameter, disregarding the actual critical induction temperature and daylight hour values.

3.4.1 Effect of Overwintering Induction Date

The model was again configured using the default toy configuration parameters but with additional overwintering sub model parameters. The model was run for each of the overwintering

induction dates associated with the critical induction daylight hours: 15, 14.5, 14, 13.5, 13, 12.5, 12, 11.5, 11, 10.5, 10, 9.5, 9 (see table 2), ignoring temperature as an overwintering induction factor. These 13 runs were repeated twice, once for a juvenile overwintering life stage (instar1) and again for the adult life stage.

Table 2 Overwintering critical induction daylight hours used in each model run for the overwintering induction date tests (figure 3.6 & figure 3.7) along with the associated Julien days of overwintering induction.

Run Number	1	2	3	4	5	6	7	8	9	10	11	12	13
Daylight Hours	15	14.5	14	13.5	13	12.5	12	11.5	11	10.5	10	9.5	9
Julien Day	199	212	225	235	245	254	263	272.5	282	292	302	315	328

It should be noted that the overwintering life stage was also used as the simulation's initial population life stage. The overwintering adult model run had 50 initial adult females (F1) while the overwintering juvenile model run had 50 initial instars. In both cases, the initial population was introduced through the overwintering sub model, when termination conditions were met, mimicking the model having been run for the year prior to this result. For these runs, overwintering was terminated on Julian day 122 with the termination conditions of 10°C and 14 daylight hours. The simulations used the default tempB temperature profile and the latitude of 45°.

The optimal timing for overwintering induction was determined based on the induction date that produced the largest overwintering population, measured on Julian day 365. The factors that determined this optimal induction timing were then explored, including which life stage population curve correlated with the optimal induction timing.

For the adult female life stage, an early overwintering induction date results in a smaller overwintering population; the overwintering population size increases as the induction date occurs later in the year, peaking on the approximate Julian day 225 and decreasing in size again as the

induction date occurs later in the year (figure 3.6-a). The peak overwintering population size is visually correlated with the peak egg population, occurring on nearly the same date (figure 3.6-b). It is logical to associate the peak overwintering female population with an induction date linked to the peak egg population (not the female peak) since adult female overwintering induction stops all new egg production and female mortality. The bigger the egg population on the induction date, the bigger the potential overwintering population. If overwintering induction happens later than the peak egg population the adult female life stage will continue to experience mortality, reducing the potential overwintering population size. This explains why the induction date that produces the largest female overwintering population is on the peak egg population date and not on the peak female population date as might be expected.

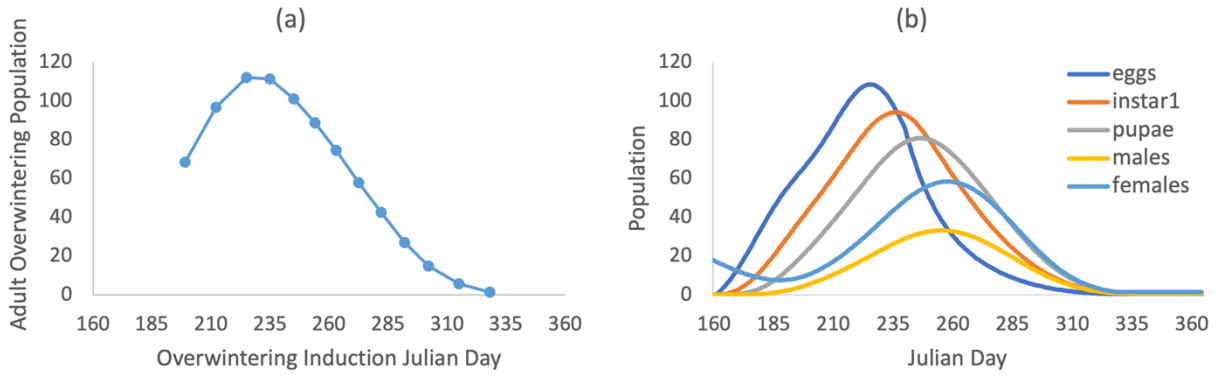

Figure 3.6 (a) Adult overwintering population (measured on Julian day 365) produced when the general model was run with various overwintering induction dates. (b) Life stage population curves for a simulation with the same model parameters as the simulations in (a) but with no overwintering induction date. (b) can be used to visualize the (a) simulations' population size and life stage composition before the overwintering induction dates. For all model simulations in (a) and (b), overwintering was terminated on Julian day 122.

For any juvenile overwintering life stage, an early overwintering induction date results in a larger overwintering population (figure 3.7-a). In the model's overwintering state, juvenile life stages don't experience mortality, therefore, all insects that reach the overwintering life stage will survive into the winter. In addition, adult females can continue to produce new insects which can,

if conditions are suitable, develop to the overwintering life stage and add to the overwintering population. There is, however, a limit to how early overwintering induction can occur. If overwintering is induced too early, the initial juvenile population won't have sufficient time to develop to the adult stage and there won't be sufficient adults to increase the population. The smaller overwintering population size on Julian day 199, was a result of an induction date occurring before sufficient initial instars could develop to the next life stage (figure 3.7-b).

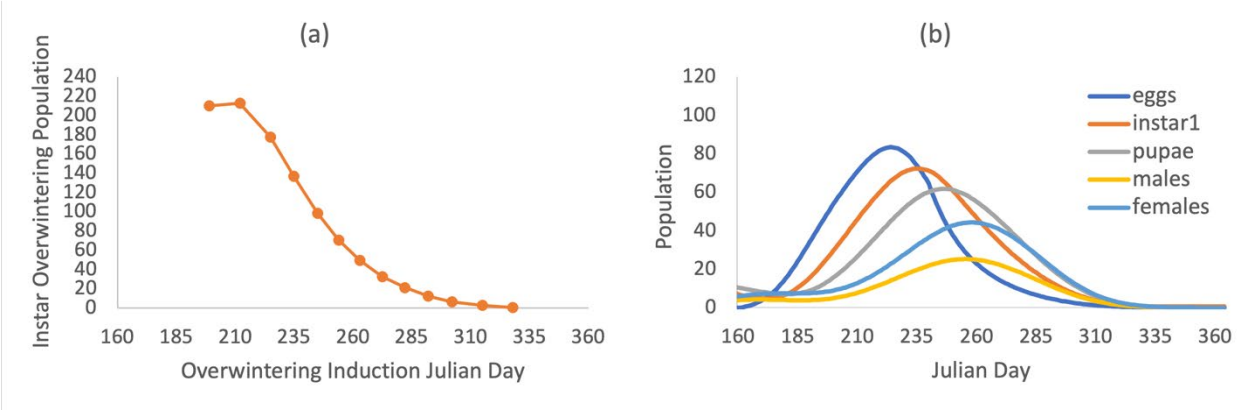

Figure 3.7 (a) Juvenile (instar1) overwintering population (measured on Julian day 365) produced when the general model was run with various overwintering induction dates. (b) Life stage population curves for a simulation with the same model parameters as the simulations in (a) but with no overwintering induction date. (b) can be used to visualize the (a) simulations' population size and life stage composition before the overwintering induction dates. For all model simulations in (a) and (b), overwintering was terminated on Julian day 122.

The general model's overwintering induction dates for adults and juveniles behave differently due to fecundity being paused for adult overwintering. For adults, the simulated induction date must happen late enough that there are sufficient eggs laid to produce the biggest overwintering population but early enough that not too much mortality is applied to any of the adult life stages. For simulated juvenile overwintering, the earlier the induction occurs the bigger the overwintering population will be, since life stages can continue to develop into the overwintering stage. This is true as long as this is balanced with sufficient time for some of the initial overwintering juveniles to reach adulthood.

These optimal overwintering induction date results produced by the general model, for both juvenile and adult overwintering, deviate from actual insect overwintering behavior due to the model not considering the effect of energy stores on overwintering survival. This will be discussed further in the general discussion (section 5.2).

3.5 Life Stage Tests

The model simulates each life stage's population with separate differential equations.

3.5.1 Model Handling of Pre-adult and Pre-egg Laying Life Stages

This section demonstrates the general model's handling of different life stages including pre-adult life stages and pre-egg laying life stages. The general model was run with different life cycles composed of five life stages, each with the same vital rates. The modelled life cycles are as follows: (a) configured with the basic toy species life cycle, (b) replaced the toy specie's pupal stage with a second instar stage and (c) replaced the toy specie's pupal stage with an additional adult female life stage, with an egg viability of zero. All model runs used the default initialization values and the default temperature profile. See table 3 for a full list of life stages and adult female egg viabilities.

The model runs (a) & (b) produced identical population curves with the same total populations peak size and timing (peak of 668.5951 on Julian day 237) (figure 3.8). The model run (c) had the same egg and instar1 population curves, but the total populations peak size and timing don't match those seen in (a) & (b) (peak of 732.38 on Julian day 235). It can be reasoned that if any juvenile life stage is replaced by any other, the same population will be produced by the model, as long as all life stages have the same vital rates. Hence, all pre-adult life stages (egg, instars, and pupa) are treated the same by the general model and behave interchangeably in a

simulated population. On the other hand, if a juvenile life stage is replaced with a non-fecund adult female life stage, the model will not produce the same population. Non-fecund adult female life stage populations behave in a similar way to juvenile stages in the model since they don't increase the population by producing eggs, however due to the model splitting male and female adults into two distinct life stage populations based on a set male ratio, the total adult population will develop at a different rate, even if the non-fecund adult female has the same vital rates as the juvenile life stage.

The general model will produce the same total populations when a simulation is run under conditions where each life stage has the same vital rates, life cycles have the same number of pre-adult stages (of any type) and adult females have the same egg-viability sub-stages.

Table 3 Stages included in simulated life cycles and adult female egg viability values.

Model run	Pre-adult	Adult male	Adult female	Adult female egg viability
(a)	egg, instar1, pupa	male	female1, female2	0, 1
(b)	egg, instar1, instar2	male	female1, female2	0, 1
(c)	egg, instar1,	male	female1, female2, female3	0, 0, 1

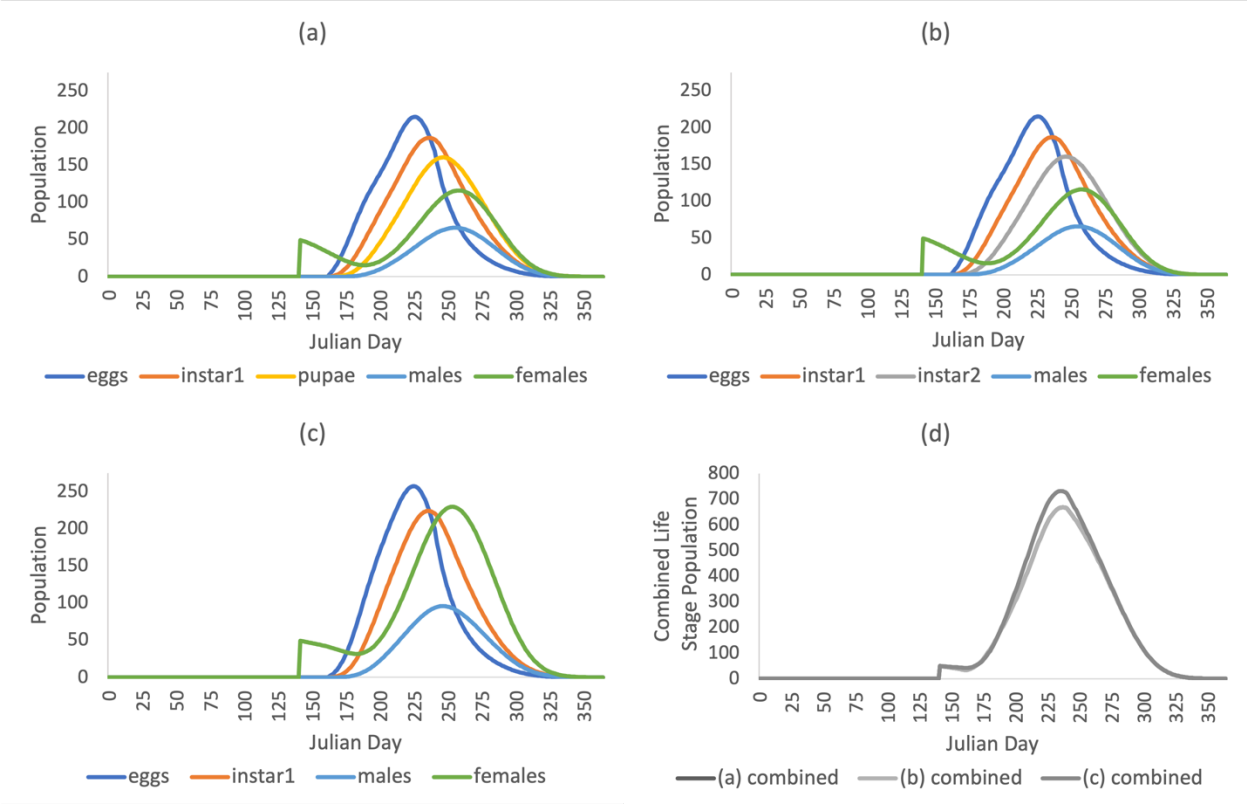

Figure 3.8 (a), (b) and (c) Life stage population curves for model simulations with different life cycles but the same vital rates for each life stage. (a) used the basic toy species life cycle, (b) replaced the toy specie's pupal stage with a second instar stage and (c) replaced the toy specie's pupal stage with an additional adult female life stage with an egg viability of zero. Each simulation was run for one year with 50 introduced F1 females on Julian day 140, under the temperature conditions of tempB. (d) Combined life stage population on each Julian day for the simulated life cycles seen in (a), (b) and (c). Note that in (d), the combined life stage population (a) is not visible since the combined life stage population (b) is nearly perfectly superposed due to their near identical curves.

3.6 Mortality Event Sub Model Tests

The mortality event sub model implemented in the general model is intended to function as a natural or anthropogenic event that kills a certain percentage of a specified life stage's population on a specified date. The following tests explore the effect of the mortality event's timing, mortality percentage and affected life stage, to get a better understanding of the model's functionality and to ensure that the model behaves similarly to what would be expected from a real-life system.

All tests conducted for the mortality event used the default toy configuration parameters with additional mortality event parameter values.

3.6.1 Effect of Mortality Event Date and Mortality Event Percentage

This section illustrates the effect of a mortality event's timing and mortality percentage on the resulting peak female population. The general model was run for multiple separate simulations with mortality events applied to the instar life stage between Julian day 170 and 300, with 10 day intervals (chosen to study the mortality events when the population was non-zero), and with the mortality event percentages killing 0%, 25%, 50%, 75% and 100% of the instar life stage on the mortality event's date (mortality event date). All other parameters were kept constant, including the life stage (instar) affected by the mortality event (mortality event life stage). All peak female population values were normalized with the largest peak female population which occurred on the model run where no mortality event was applied. Normalized peak female populations equal to 1 represent populations that are unchanged by mortality events, while smaller normalized values can be interpreted as the proportion of the unchanged population that remains under the effect of a mortality event.

The date of the mortality event has a direct impact on the peak female population (figure 3.9-a). Mortality events early in the year result in less substantial peak female population decreases. As the mortality event date occurs later in the year, its effect increases, reaching its peak female population reduction of 28.41%, with a 100% instar mortality event, on Julian day 220. Mortality events beyond this date result in a smaller reduction of the female population. The peak population reduction of the mortality event is correlated with the timing of the mortality event life stage's peak population date, in this case the instar's peak population date (figure 3.9-b). The

mortality event results in the greatest population reduction when it is applied a few days prior to the instar's peak population date, in this case approximately 15 days before the instar peak population. A mortality event a few days prior to the peak population, keeps the maximum population size of the instar life stage lower and in turn reduces the adult female population's peak (supplementary figure 8.1). The timing of the highest population reduction is therefore based on model factors that determined the mortality event life stage's peak population date, such as, daily temperature, insect life cycle, and life stage vital rates. While the mortality timing's correlation with the peak population will specifically vary depending on the life stage's development rate and parameters.

The percentage of insets killed during the mortality event (mortality event percentage) has a direct impact on the size of the population's reduction. The percentage of the mortality event life stage population that is eliminated determines the reduction of the peak female population. 100% effective mortality events produce the biggest peak female population reduction for any mortality event dates (figure 3.9-a). Any other mortality event percentage results in peak female population reductions that are proportional to the mortality event's percentage of effectiveness (figure 3.9-a). For example, the 100% mortality event resulted in a peak female population reduction of 0.284; while the 25% mortality event resulted in a peak female population reduction of 0.071, a reduction equal to 25% of the 100% mortality reduction. The general model's mortality event could be used as a tool to determine the effect and optimal timing of mortality events, however, there is insufficient research on the effect of natural and anthropogenic mortality events on insect populations to undoubtably state the model's results as factual representations of real-world behavior.

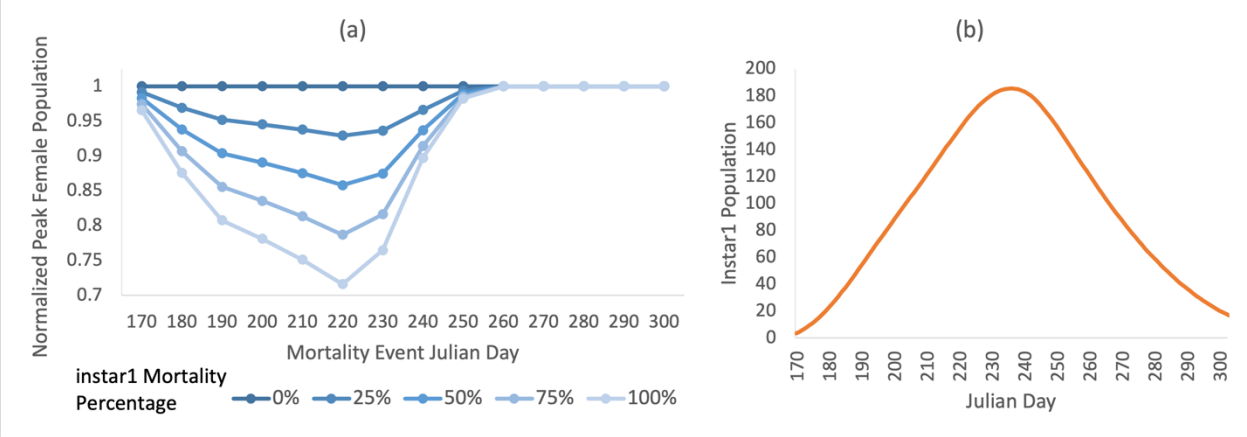

Figure 3.9 (a) Peak adult female population produced by general model simulations where mortality events were applied to the instar life stage on various days (Julian day 170 to 300 with 10 day intervals) and with various mortality event percentages (0%, 25%, 50%, 75% and 100%). Each simulation was initialized with an initial population of 50 F1 females on Julian day 140 and run for one year with the default toy parameters, under the temperature profile tempB. (b) Instar1 population curve for a one year simulation, using the same parameters and initial conditions as in (a) but with no mortality events applied. (b) can be used to determine the instar mortality event life stage's population size on the date of each mortality event in (a). For example, on the mortality event Julian day 220, the instar life stage has a population of 154 instars.

3.6.2 Effect of Mortality Event Life Stage

This test explores the effect of mortality events being applied to different life stages (mortality event life stage) on the resulting population reduction to identify factors that contribute to the optimal mortality event life stage and mortality event timing. The general model was run for multiple simulations with mortality events applied to various life stages (egg, instar, pupa and adult female) on dates between Julian day 170 and 300, with 10 day intervals (chosen to study the mortality events when the population was non-zero), and with a 50% mortality event percentage. The resulting normalized peak female population and normalized cumulative female populations can be seen in figure 3.10.

For any mortality event life stage other than adult females, the general model produced the greatest reduction in the cumulative and peak female populations when the date of the mortality event was a few days prior to the mortality event life stage's peak population date (figure 3.10).

The female life stage mortality event on the other hand produced the greatest population reduction when it was applied early in the year. There was also an increase in the mortality event life stage's population reduction near the insect introduction date or overwintering termination date (Julian day 170), for mortality events applied to the introduced initial life stage (female1) or its subsequent development life stage (female2). The mortality event's increased effectiveness was a result of the population's life stage composition at that time, being made-up mainly of the initial life stage. A mortality event applied to the initial life stage, therefore, effects nearly the entire insect population.

When considering each mortality event life stage on their optimal mortality event date and excluding the adult female mortality event life stage itself, the pupal mortality event caused the biggest reduction to the peak adult female population, while the egg mortality event caused the biggest reduction to the cumulative adult female population (figure 3.10). Since the pupal life stage occurs directly prior to the adult female life stage in this toy insect's life cycle, the pupal life stage mortality event has a more direct impact on the female peak population. The mortality event is applied to the pupal stage's peak population resulting in fewer pupae being available to develop into the adult stages. This reduced number of pupae developing into adults dramatically reduced the female's peak population size. The egg mortality event, on the other hand, as an early developmental life stage, affects the population when it is at its most vulnerable, near its introduction date. Through earlier tests (section 3.3.1) it was determined that the initial population's size has a linear scaling effect on the resulting population's size. The mortality event applied to the egg stage, for all intents and purposes reduces the insect population's initial population size and in turn proportionally reduces its cumulative population, resulting in a large cumulative population reduction.

Overall, the female life stage produced the greatest reduction in population as a mortality event life stage, irrespective of the mortality event date (figure 3.10). The adult female life stage is the population driver, responsible for producing all new eggs, therefore, it's logical that when the adult female population experiences a mortality event, and egg production is reduced, the insect population as a whole would experience a substantial reduction in size. Adult female mortality events early in the year resulted in the greatest population reduction since populations earlier in the year are smaller making them more vulnerable to mortality events.

In this test structure, the female mortality event life stage produced the largest population reduction, however, this could be a result of the female life stage also being used as the life stage measured to evaluate population reduction and as the overwintering stage. To ensure that the results obtained in this test and the subsequent conclusions that were drawn don't only hold for this specific model test structure, supplementary model tests were conducted where the measured and overwintering adult female life stage were replaced by the instar life stage (supplementary figure 8.2 and supplementary figure 8.3). The supplementary test results were in agreement with the findings above, confirming that mortality events applied to the initial population life stage near its introduction date greatly reduces both the peak and cumulative populations. Mortality events applied to early developmental life stages (a few days prior to the life stage peak population) cause the biggest reduction to the measured cumulative population and that mortality events applied to life stages preceding the measured life stage in the insect's life cycle (a few days prior to the life stage peak population) cause the biggest reduction to the measured peak population. It also confirmed that even under the modified test structure, a mortality event applied to the adult female life stage has the greatest reductive effect on the population.

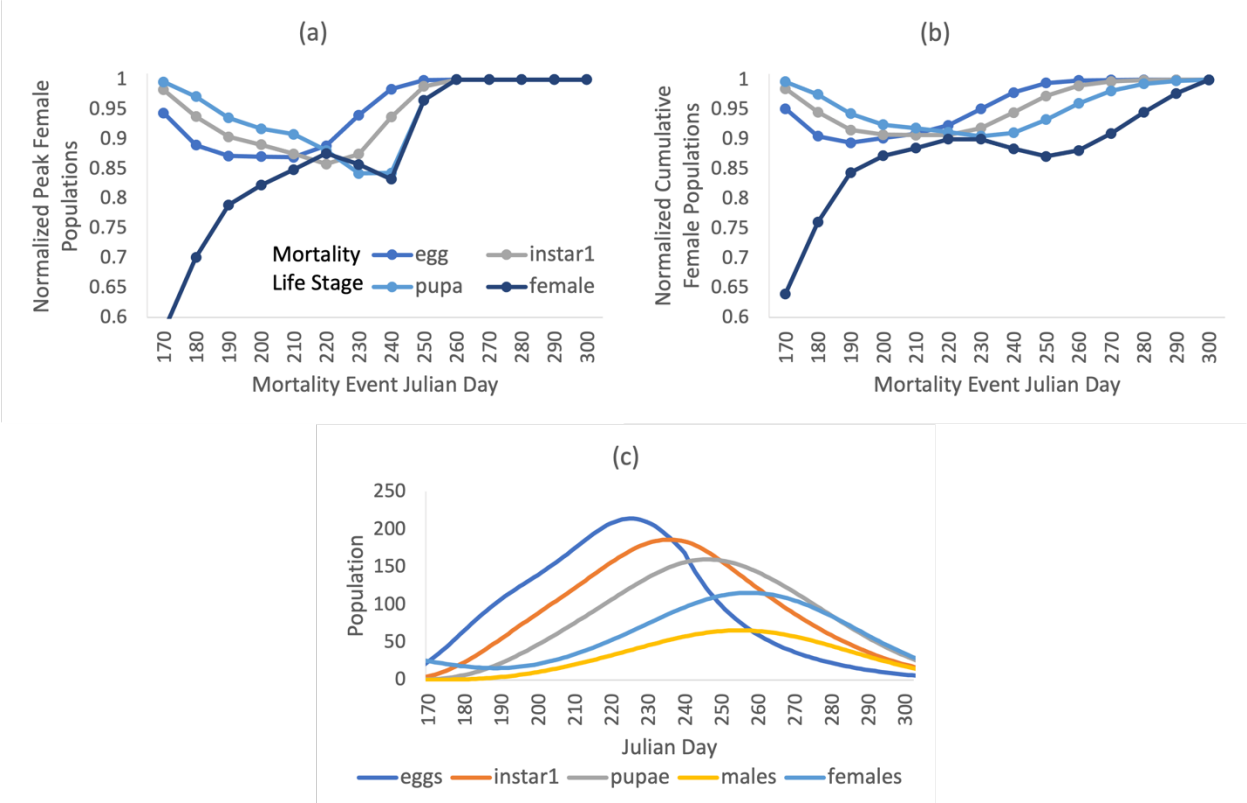

Figure 3.10 (a) Peak and (b) cumulative adult female population produced by general model simulations where 50% mortality events were applied on various days (Julian day 170 to 300 with 10 day intervals) and to various life stages (egg, instar1, pupa, female). Each simulation was initialized with an initial population of 50 F1 females on Julian day 140 and run for one year with the default toy parameters, under the temperature profile tempB. (c) All life stage population curves for a one year simulation, using the same parameters and initial conditions as in (a) and (b) but with no mortality events applied. (c) can be used to determine a mortality event life stage's population size on the date of each mortality event in (a) and (b). For example, on the mortality event Julian day 240, the egg, instar1, pupa and female life stages have populations of 91, 101, 85 and 51 respectively.

4. General Model Validation

4.1 Introduction

Although sometimes overlooked, model testing and validation is an essential part of new model development, determining under which conditions the model works best and identifying its limits. If model processes and results are not appropriately evaluated, mistakes arising from improper use, expectations not being aligned or model use beyond its bounds, can be extremely costly (Getz et al. 2018). When evaluating models, the term "model validation" is often used. Although comparing a model's results to empirical data is a common model validation method (e.g. Baker 1991; Jia et al. 2016; Petrice et al. 2021), model validation doesn't always indicate a model's ability to accurately predict its real world counterpart, rather, a model is said to be valid when it meets specified performance requirements making it acceptably accurate for its intended use (Rykiel 1996). Performance requirements vary depending on the objective of the model and can be both quantitative and qualitative.

In this chapter, the general mechanistic model, described previously, is validated based on its intended use as an exploratory model. The general model is not intended to predict exact population sizes under specific conditions but rather to produce potential insect population dynamics under the model's existing constraints, which include working with an isolated population and only considering a limited number of insect population dynamics driving factors, excluding extrinsic mortality, density dependent mortality and food or resource availability.

The validation criteria used to determine the success of this general model's simulations when compared to published population dynamics studies were chosen based on the model's intended use and are as follows:

- produces results with similar overall population curve shapes

- approximately mimics key species population dynamics characteristics
- has comparable life stage timing, and peak population dates
- has similar population start and end dates, when applicable with reproductive diapause and overwintering

The chapter objectives are to (1) confirm the model's ability to use existing laboratory collected data as input, (2) verify that the model can reach its validation criteria for various insect species, and (3) identify the model's optimal species and limits as a general model.

4.2 Methods

In order to validate the general model, insect species parameters were obtained from published papers (appendix D) and used to simulate the species' population dynamics. General model results were then compared to modelled or observed population dynamics data from other published papers.

Published Population Data Sources:

The population data used to test the general model's results for specific insect species were obtained from published insect population field studies or model studies. The general model results were compared directly to published population dynamics figures due to raw population dynamics data not being available in published papers.

Temperature Data:

The general model used daily temperature data obtained from a variety of sources due to temperature data used by the published study commonly not being made available. General model

tests used: exact daily temperature data from published studies, smoothed daily temperature data from published studies, smoothed approximate temperature data extrapolated from a study location's monthly mean temperature, and smoothed approximate temperature data extrapolated from monthly mean temperatures for a location near the study location. The latter two temperature data types were obtained from online historic temperature data sources. The list of temperature data sources are in order of most to least specific. For all validation tests, the type of temperature data used to produce the results are specified. All temperature files used in the model's validation tests can be found at https://github.com/domdelay/GeneralizedInsectPopulationDynamicsModel

Model Initialization:

For all model comparison runs, a starting population size and date that matched the published population's initial conditions was used. Otherwise, known overwintering termination conditions were used to introduce the population at an appropriate date for the study region. The specifics of these initial conditions are stated for each species' tests.

Model Comparison Method:

The general model was run and its results were adapted to facilitate comparison to the published result's format: adult population, total daily life stage populations, proportional life stage distribution or other population representations. As discussed previously, the published population study's data was commonly not available, therefore the general model's results were adapted to match the published graph's population format. Most testing methods were limited to a visual and graphical comparison of the results, a common model validation method (Rykiel 1996) however, in certain cases where numerical values could be helpful in analysing the comparability of the

results, the absolute or percent error was calculated. The absolute error (the magnitude of the error between measured and real values) and percent error (the size of the error relative to the real value expressed as a percentage) are both common methods for determining the error between values.

The population size of the raw model results will not be compared since the general model is not spatially explicit. The raw population values represent the computed population level but not the actual number of individuals in any specified dimension or area. Therefore, any general model result comparisons will be with normalized populations. Normalized results produce populations on the same relative scale making it possible to compare the effect of models run with different input parameters, starting population size, temperature profiles and any other model elements. If not normalized, the model should only be used to better understand the timing of changes in the population.

Test Species:

Validation tests were conducted on a variety of insect species from different orders. Species were chosen based on the availability of both model parameter data and published population data (a form of convenience sampling), including their response to temperature. These species tend to be crop or forest pest insects due to human's vested interest in these species. A limited number of species were tested to get an initial idea of the general model's ability to produce meaningful exploratory results for various insect species. Model validation tests were run for five insect species: the spotted wing fruit fly (*Drosophila suzukii)*, the mountain pine beetle (*Dendroctonus ponderosae),* the brown marmorated stink bug (*Halyomorpha halys),* the swede midge (*Contarinia nasturti)* and the cotton aphid *(Aphis Gossypii)*.

4.3 Model Validation Test Results

4.3.1 *Drosophila suzukii* (Spotted Wing Fruit Fly)

The general model was first compared to the Spotted wing fruit fly *Drosophila suzukii* a soft-skinned fruit pest originally from southeast Asia which has spread to America and Europe. The general model was build based on the species-specific *D. suzukii* model by Langille et al. (2016), therefore the following test were run to ensure that the model could still produce appropriate results after being generalized. The general model was compared to results produced by the species-specific Langille et al. (2016) model when run with four different smooth cosine temperature profiles and when run with observed daily temperatures.

Langille et al. *Drosophila suzukii* Cosine Temperature Curve Model Results

General model validation was conducted with *D. suzukii* data output by the Langille et al. (2016) model. Both models were run with the cosine temperature profiles (tempA, tempB, tempC, and tempD) created by Langille et al. (2016) and discussed in section 2.4.7. Both models were initialized with an initial population of 50 females (F1) on Julian day 120 and all sub models were turned off. A full list of general model configuration parameters can be found in appendix A. Figure 4.1 compares the normalized life stage population curves for one year, output by each model.

The results output by the general model were visually comparable to the results produced by the species-specific Langille et al. (2016) model. The two models had similar life stage peak population values and peak timing, along with comparable one year life stage population curves (figure 4.1).

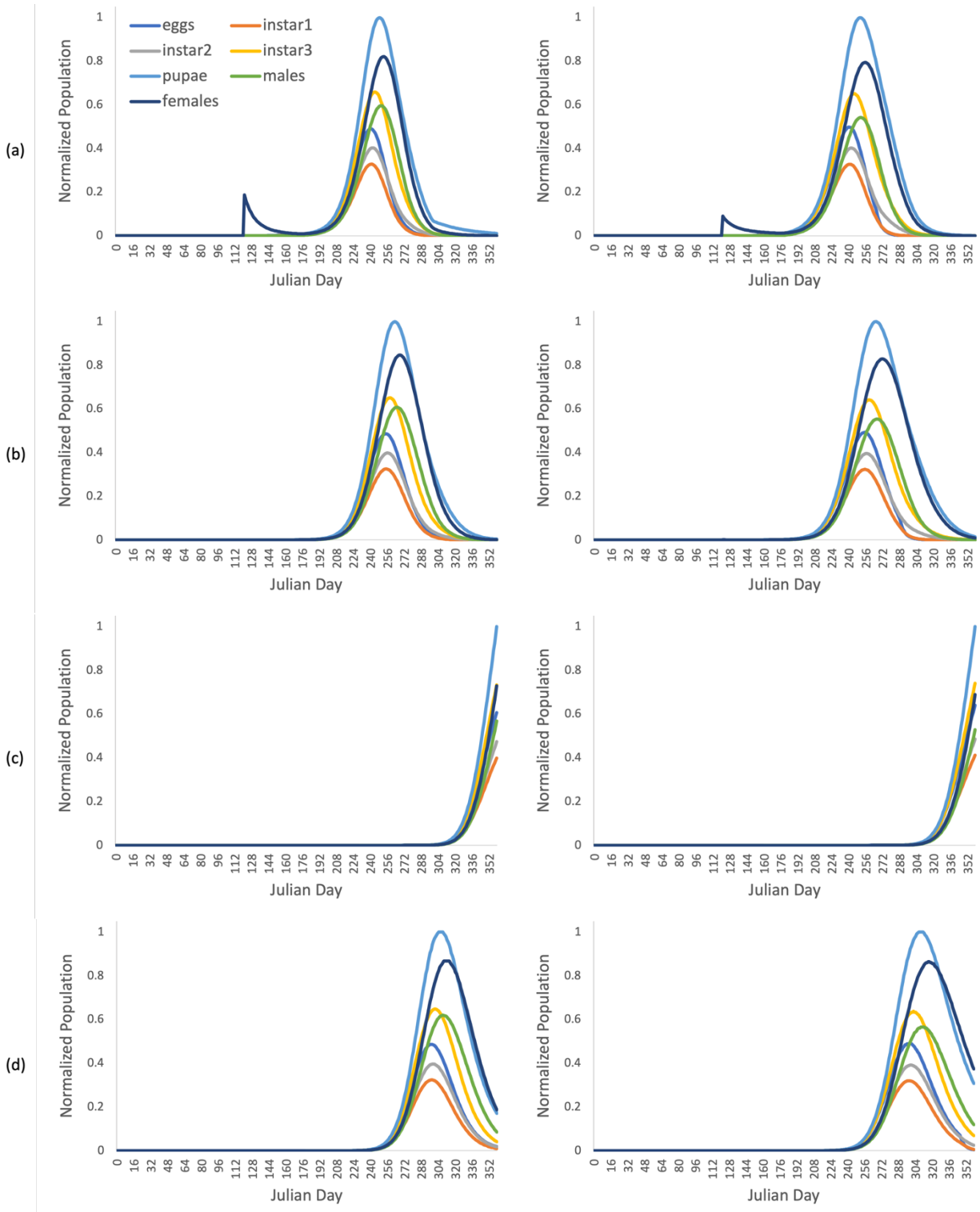

Figure 4.1 Normalized *Drosophila suzukii* life stage population curves under the temperature profiles (a) tempA, (b) tempB, (c) tempC, and (d) tempD. Simulations were run for one year with an initial population of 50 F1 females on Julian day 120, using the Langille et al. (2016) model (left column) and the general model (right column).

The qualitative visual comparison was further quantified by calculating the normalized peak and cumulative population's percent error for each temperature profile and life stage (figure 4.2). The models' cumulative populations had more variation in percent error between different temperature profiles, especially for earlier development life stages. The adult male life stage for both the peak and cumulative population had the biggest percent error for all temperature profiles. Overall, the peak and cumulative population's percent error remained low for all life stages and temperature profiles, with a maximum percent error of 15.2% and a minimum percent error of 0%. These quantitative results confirm that the general model can still produce qualitatively-similar results for *Drosophila suzukii* after being generalized.

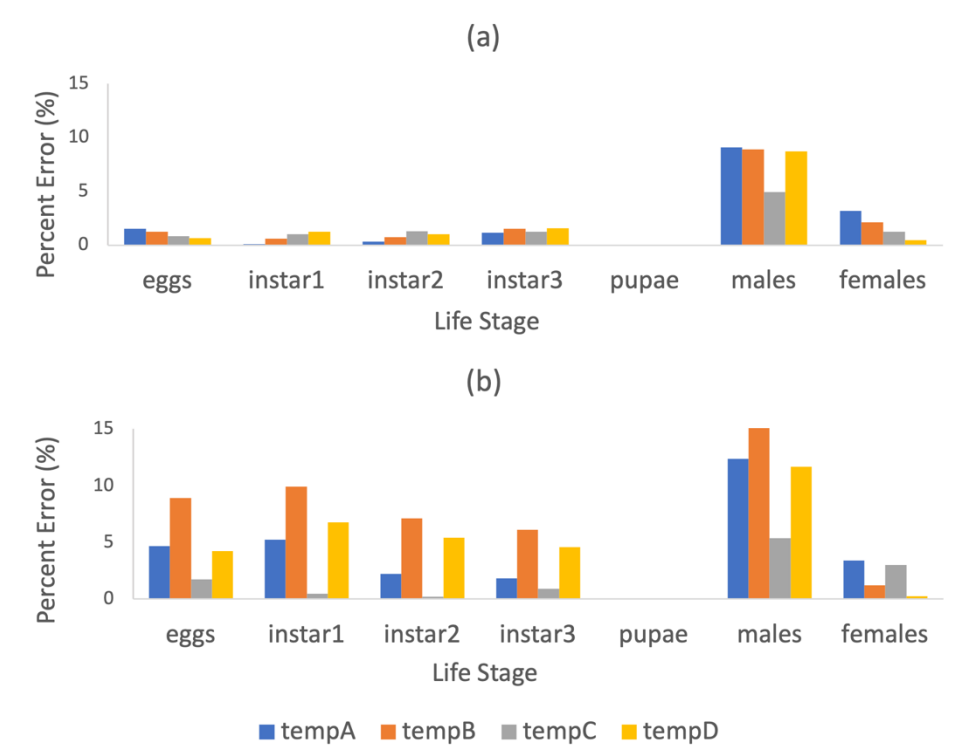

Figure 4.2 Comparison of the Langille et al. (2016) and general model simulated *Drosophila suzukii* population from figure 4.1. (a) percent error of the general model's normalized peak *D. suzukii* population for each life stage simulated with each cosine temperature profile. (b) percent error of the general model's normalized cumulative *D. suzukii* population for each life stage simulated with each cosine temperature profile.

A final test was conducted to compare the non-normalized simulated cumulative population size of the general and species-specific model to better understand the effect of the changes made to the general model. The simulated population's scale is compared in this test even though, as stated in the chapter's methods, the raw general model's population size results should usually be ignore since the model is spatially ambiguous. This test is only intended as an interesting exploration of the elements in the model generalization that resulted in changes to the population size compared to the species-specific model. Any differences between the model's scales don't indicate that the general model is not well-suited for modelling *D. suzukii* since the order of suitability of each temperature profile has been shown to be the same between the two models in the normalized results.

To determine the scale difference between the general model and the species-specific model under each temperature profile, the models' cumulative population size ratio was calculated. The general model's average cumulative life stage population was divided by the species-specific model's average cumulative life stage population at each temperature profile. A cumulative population size ratio of one represents equal model populations, ratios greater than one indicate that the general model's population is larger than the species-specific population, while ratios less than one indicate that the general model's population is smaller than the species-specific population; the more the ratio diverges from one the bigger the models' population scale difference. The general model produced a bigger cumulative population than the species-specific model under the tempA temperature profile with a population size ratio of 2.25 while the general model produced a smaller population under the tempB, tempC and tempD profiles with a population size ratio of 0.72, 0.0037 and 0.17 respectively (figure 4.3). The two models' difference in scale can be explained by changes made to the way the general model simulates populations.

Logically, changes made when generalizing the species-specific model, will influence the general model's population results. In the general model, adult development was made temperature-dependent, following the same curve shape as other life stage development curves, in order to better match a variety of insect species adult development rate data, in published papers. Temperature-dependent adult development was parameterized for *D. suzukii* in the generalized model so that development would not occur at temperatures below 9.8504°C. As a result, under temperature profiles with daily temperatures commonly below, 9.8504°C, such as seen in tempA, females stay in fecund life stages longer and produce more eggs. The general model's cumulative population is therefore larger under the tempA temperature profile. The general model's temperature-dependent mortality curve equation was also modified to be a better fit for a variety of insect species. A comparison of the general model and the species-specific model temperature-dependent mortality curves can be seen in figure 4.4. The modified general model temperature-dependent mortality curve produces similar mortality rates to the species-specific curve, for most life stages, when temperatures are between 10°C and 20°C or when temperatures are beyond the bounds of 0°C and 35°C. Temperatures outside these conditions produce a higher mortality in the general model. If a temperature profile is commonly outside these temperature conditions, the general model will produce smaller populations (tempC and tempD). The temperature profile tempB is frequently within the range of temperatures (~4°C to 18°C) with the least change in mortality values between the two models resulting in the smallest population size ratio seen for any of the cosine temperature profiles (figure 4.3).

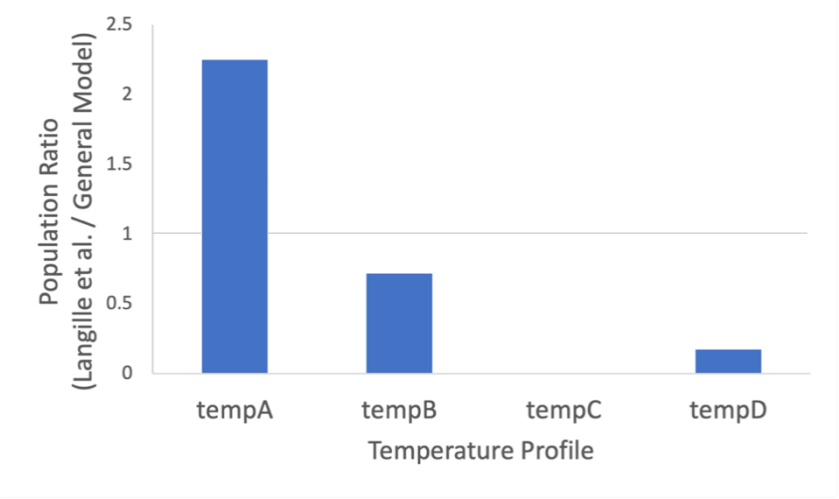

Figure 4.3 Ratio between the Langille et al. (2016) model and the general model's average life stage cumulative *Drosophila suzukii* population when simulated under each cosine temperature profile (figure 4.1). Note that the tempC population's ratio is not visible but has the value of 0.00367.

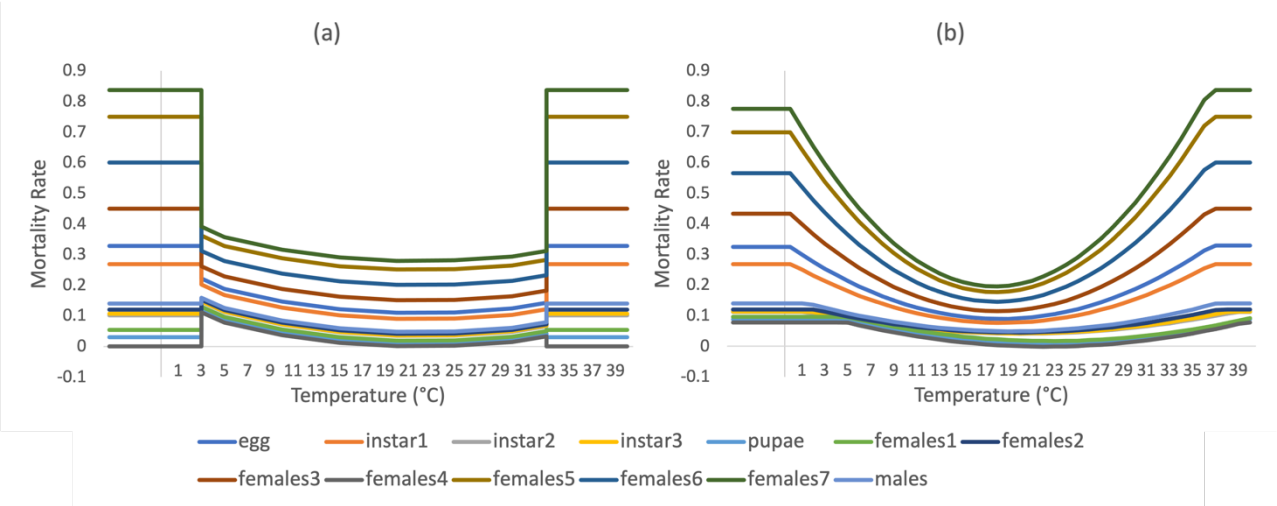

Figure 4.4 *Drosophila suzukii* life stage mortality rate, at various constant temperatures, used in (a) the species-specific Langille et al. (2016) model and (b) the general model.

Langille et al. *Drosophila suzukii* Observed Daily Mean Temperature Curve Model Results

Langille et al. (2016) produced normalized per-day female *D. suzukii* population dynamics results using daily observed mean temperatures in Clark County, Washington, for each year between 1993 and 2013, and for the daily mean temperatures averaged over 20 years. In order to compare the general model's ability to reproduce these results, the general model was run with

each of these temperature profiles and the same initial model conditions: 100 females introduced on the date of the termination of reproductive diapause. The species-specific and general model simulation results can be seen in figure 4.5 where model output was normalized using the maximum female population value for all simulation years.

It can be noted that all general model simulation diapause termination dates matched those obtained by Langille et al. (2016), confirming that changes made to the reproductive diapause sub model have not affected the sub model's functionality for *D. suzukii*. The general model's results have a similar shape and scale to those produced by the species-specific model (figure 4.5). The temperature profile that produced the largest population with the species-specific model, 2003, remains the largest population for the general model. General model daily female populations results are suitably similar to the Langille et al. (2016) model results.

The difference between the model results was again quantified, by calculating the percent error. The daily percent error between the species-specific *D. suzukii* and general model female population can be seen in figure 4.6. On average there was a greater percent error near the end of the 1-year simulation. The percent error varied between years, with the daily mean temperatures for 1996 resulting in the biggest percent error. These high percent errors are both cause by changes to the general model's vital rate equations, discussed previously.

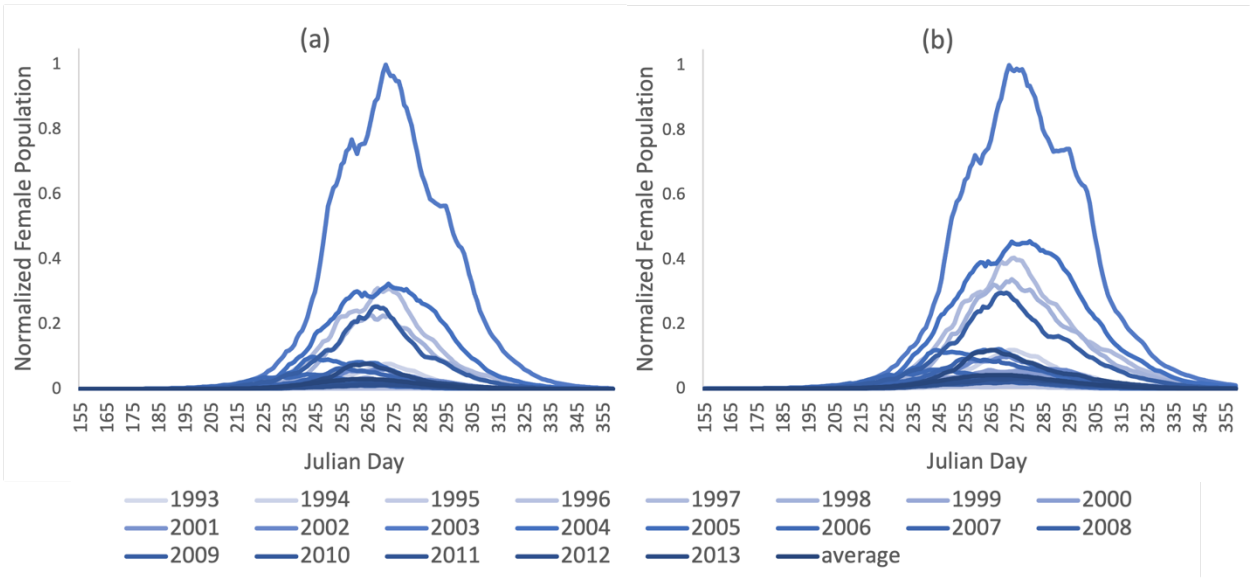

Figure 4.5 Normalized daily number of *Drosophila suzukii* females simulated under the temperature conditions of Clark county, WA for the years 1993 to 2013 and the 20 year average temperature. An initial population of 100 females was introduced on the termination date of reproductive diapause. (a) results from the species-specific Langille et al. (2016) model and (b) results from the general model.

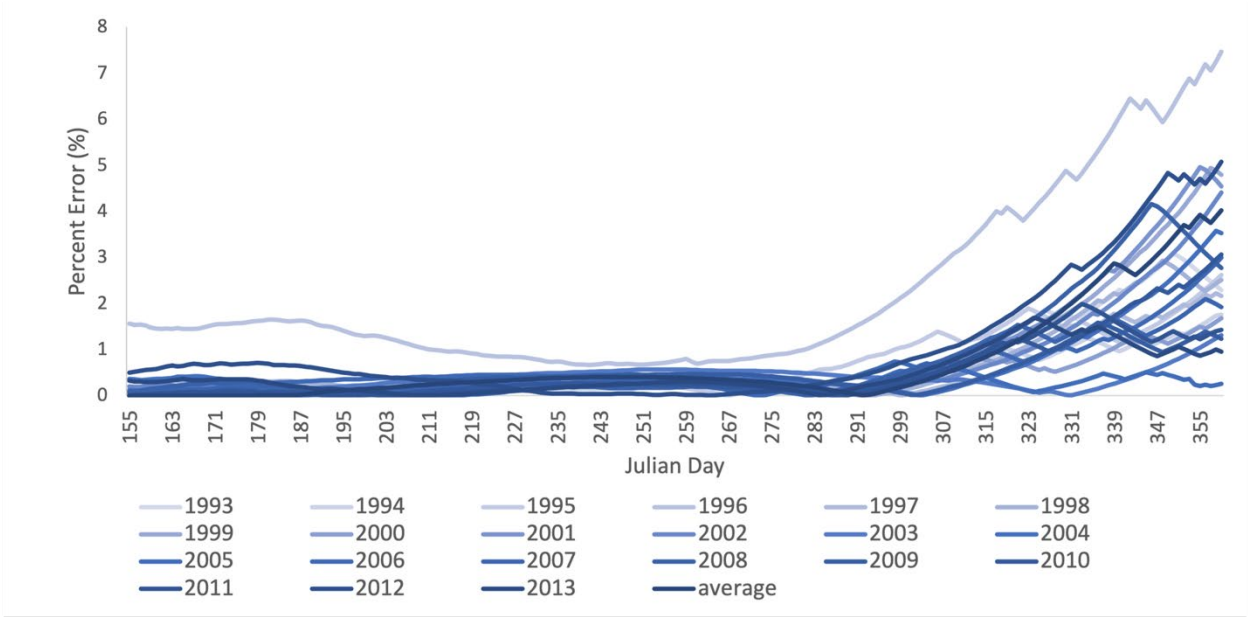

Figure 4.6 Daily percent error between the species-specific Langille et al. (2016) and the general model's normalized *Drosophila suzukii* female populations under Clark county, WA temperatures for the years 1993 to 2013 and the 20 year average temperature (figure 4.5).

Drosophila suzukii Conclusion

Based on the comparison of the Langille et al. (2016) model and the general model's results under cosine and observed temperature profiles, it appears that the general model can produce qualitatively-similar results for *D. suzukii* after being generalized. All population curves maintained similar curve shapes and approximate peak population timing, fulfilling the validation criteria set in the introduction.

4.3.2 *Halyomorpha halys* (Brown Marmorated Stink Bug)

The general model's second test species was the brown marmorated stink bug *Halyomorpha halys,* an agricultural pest species native to Asia which has spread to North America. The general model simulation results were compared to a survival rate model by Govindan and Hutchison (2020) and field studies conducted by Haye et al. (2014).

Govindan and Hutchison *Halyomorpha halys* Published Model Results

Govindan and Hutchison (2020) developed an age-stage, two-sex life table for *Halyomorpha halys* where population survival was based on laboratory observations of development, survival, and reproduction rates at different constant temperatures. The general model was run at each of the population study's constant temperatures to compare the general model's population dynamics results to the Govindan and Hutchison (2020) population study. The general model was initialized with a starting population of one egg on day zero of the simulation and had fecundity turned off.

One population life cycle (egg to peak adult female population) under each constant temperature lasted a similar number of days under the constant temperatures 20, 23, 27, 30 and 33

°C with the species-specific model requiring 105.25, 75.5, 36.0, 36.5 and 31.2 days to develop and the general model requiring 119.9, 85.4, 58.2, 46.85 and 37.35 days to develop. Life stage population curves produced by the general model had similar peak dates as those in Govindan and Hutchison (2020) (figure 4.7). The general model's life stage population curves however are much flatter and taper off more slowly than the population study curves resulting in greater life stage overlap. This curve shape is common in differential equation models because of the use of development rates. The general model's differential equations tend towards but never reach zero due to exponential decreases. This results in a portion, however small, of the population always remaining in previous development life stages. Curves produced by development rates can be interpreted as the probability that the insect population will be in a life stage rather than the number of individuals in a life stage. The proportion of eggs to survive to adulthood in both models was also compared (figure 4.8). Simulated survival in the general model was significantly lower for the constant temperatures of 27°C and 30°C. The general model's juvenile mortality parameterization data was obtained from a laboratory study by Nielsen et al, 2008 where survival was at its highest at approximately 22.5°C a noticeably different peak survival temperature than 27°C used in the Govindan and Hutchison (2020) model. Since model parameters determine the model's behavior, it is reasonable to expect different results from models that were parameterized with different data. The difference seen between the models' proportion of eggs to survive to adulthood, therefore, do not indicate inaccuracies in the general model's design making the general model a good match for *H. halys* population development and mortality.

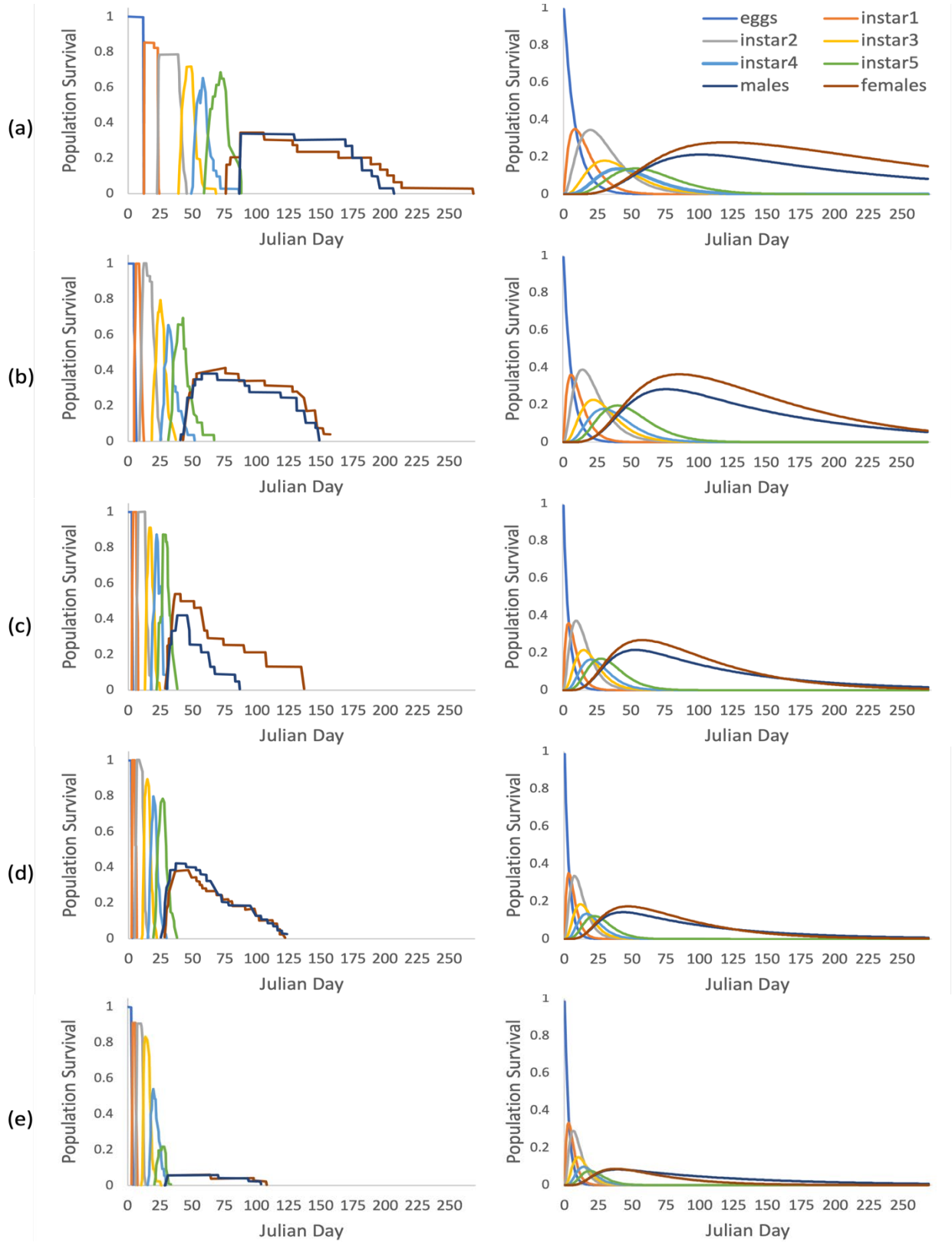

Figure 4.7 *Halyomorpha halys* life stage progression and population survival at constant temperatures (a) 20°C, (b) 23°C, (c) 27°C, (d) 30°C, (e) 33°C produced by the Govindan and Hutchison (2020) model (left column) and general model (right column).

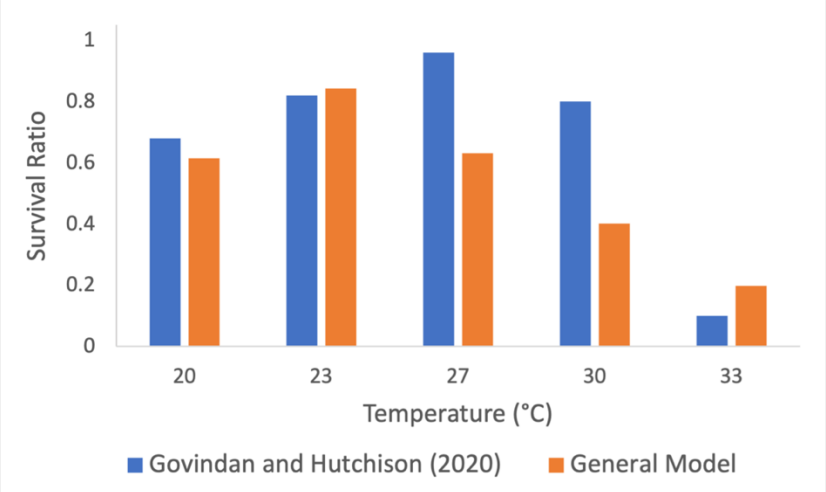

Figure 4.8 Comparison of the proportion of *Halyomorpha halys* eggs to survive to adulthood in the Govindan and Hutchison (2020) model and the general model.

Haye et al. *Halyomorpha halys* Published Field Observation Results

Three results obtained by the Haye et al. (2014) field study of *Halyomorpha halys* were compared to those produced by the general model run with the insect species' parameters. The field study was conducted under the temperature conditions of Delémont, Canton Jura, Switzerland in 2013 while the general model used 2013 daily average temperatures from a nearby location in Switzerland, Zurich-Wollishofen, due to field temperatures not being available.

The first field result found in Haye et al. (2014) was the number of eggs produced per week by *H. halys*. This value was converted to the cumulative number of eggs produced, a value that can also be obtained by the general model by setting both the egg development and mortality rates to zero. The general model was run with an initial population of 23 females on April 15th to imitate the conditions in the field study. The cumulative number of eggs between April 15 and November 17, 2013 simulated by the general model was a good visual match for those observed in the Haye et al. (2014) field study with both curves following a similar shape (figure 4.9). The total number

of eggs for both the observed and simulated populations have similar start dates where egg production increased (June 10th vs June 6th) and end of egg production dates (September 15th vs September 11th).

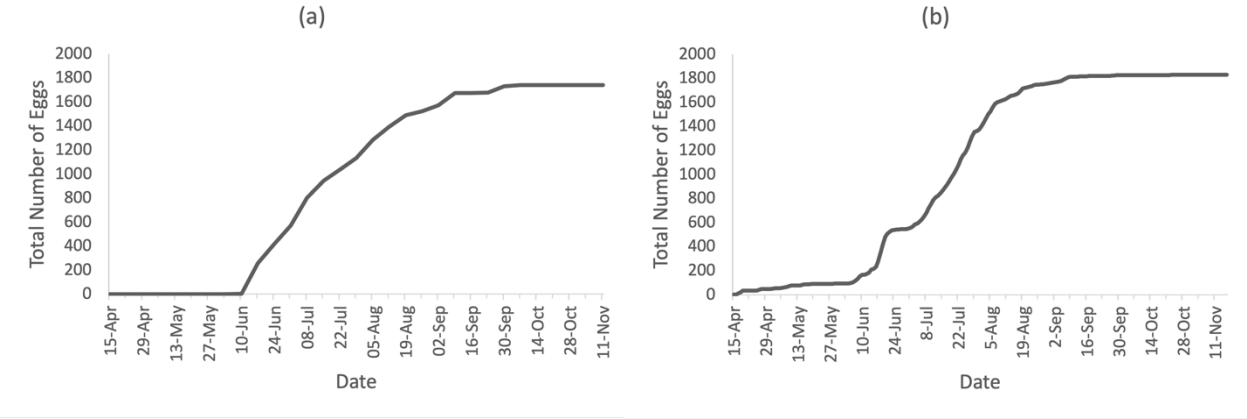

Figure 4.9 Total cumulative number of eggs laid by a *Halyomorpha halys* population, composed of 23 females, under daily average temperatures in Switzerland, 2013, (a) observed by Haye et al. (2014) and (b) modelled by the general model.

The second published field result compared to the general model was the observed percentage of *H. halys* adults alive over the observed time period between Apr 15 and Dec 1, 2013. The general model was initialized with 100 males and 100 females starting on Apr 15 to match the field population values. The general model's male and female survival curves generally mimicked the field study's survival (figure 4.10). The percentage of surviving adults remains relatively constant before the week of June 17th and is reduced to 10% adult survival after the week of October 21st, for both the simulated and observed populations. Between these dates, simulated male and female populations diverge from observed populations. The general model adult survival results, however, are meaningful, since, as stated previously, the general model is not intended for forecasting and model results that are generally comparable to published results can be deemed successful.

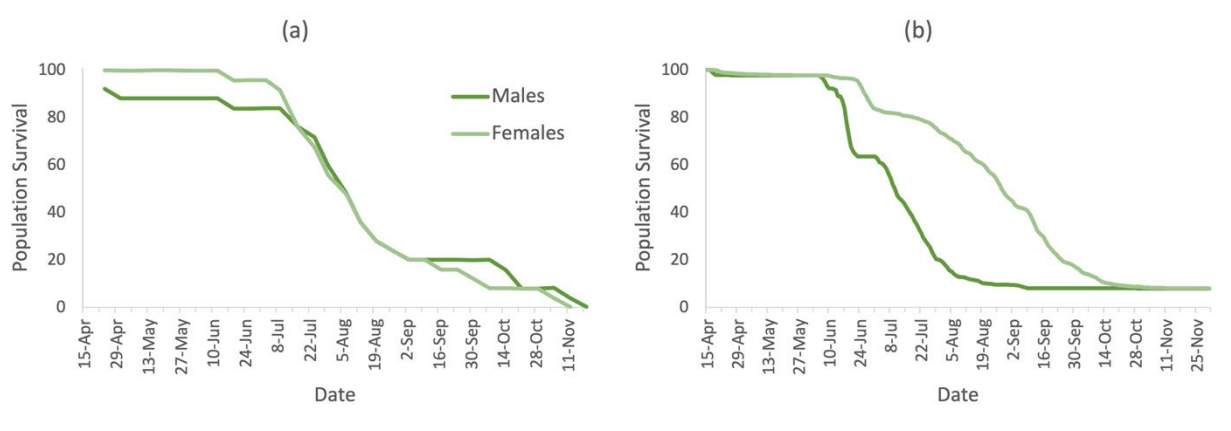

Figure 4.10 Adult male and adult female *Halyomorpha halys* population survival under daily average temperatures in Switzerland, 2013, (a) observed by Haye et al. (2014) and (b) modelled by the general model.

The third published result displays field collected data on the proportion of the *H. halys* population in each life stage, known as the population's age structure, on different observed dates. The population proportion was only measured seven times over the five-month period resulting in a higher potential error margin due to possible undetected population fluctuations. The general model was run with the reproductive diapause critical induction daylength of 14 hours based on a study by Nielsen et al. (2008). To avoid errors caused by daily fluctuations of the simulated population, the general model's life stage proportion values for each date measured in the field study was composed of the 7-day average simulated life stage proportion value (3 before the date 3 after the date). The general model produced population proportions results that were visually comparable to those observed in the field study however, there was some discrepancies with the early developmental life stage proportions (figure 4.11). The proportion of the population in adult life stages (overwintering or new adults) at each observed date was similar, as confirmed by the very low calculated absolute error for each measured date (average absolute error for overwintering adults 0.06332 and 0.03551 for new adults) (figure 4.12). The proportion of insects in each instar stage in the model does not match observations. For each displayed date, the

observed Haye et al. (2014) population proportion is mainly composed of one dominate life stage and very few residual insects from any of the previous instar life stages. There is a clear transition between dominant life stages over the observation period (figure 4.11-a). Each of the general model's population proportions, on the other hand, are partially composed of a combination of all previous instar life stages. There isn't as clear a transition from one life stage to the next with a proportion of the population always being composed of previous life stages (figure 4.11-b). These discrepancies result in high absolute errors for the instar life stage populations proportion (figure 4.12). High instar absolute errors can be explained by the flat, tapered characteristic of differential equation model curves discussed previously, and discrete observed time steps being compared to a continuous model. A comparison of the field data's total daily population size was also conducted which indicated that both the simulated and observed total daily populations followed very similar population growth and reduction timing (figure 4.13). Regardless of differences in the instar life stage proportions, this result remains promising for the general model since the most important population driver is the adult female life stage, which in this case was the life stage where the model most closely matched the observed proportions.

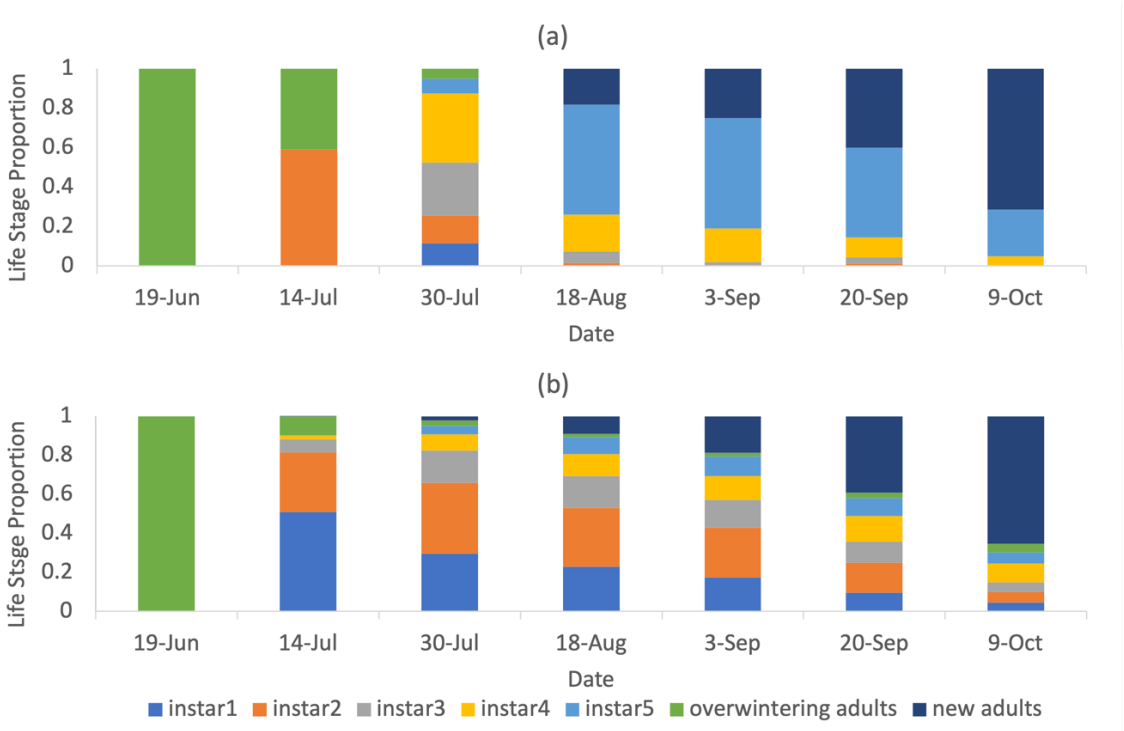

Figure 4.11 *Halyomorpha halys* life stage proportion under daily average temperatures in Switzerland, 2013, (a) observed by Haye et al. (2014) and (b) modelled by the general model. Note that the life stage population proportions were measured on dates that are not equally distributed over the observed and simulated time period.

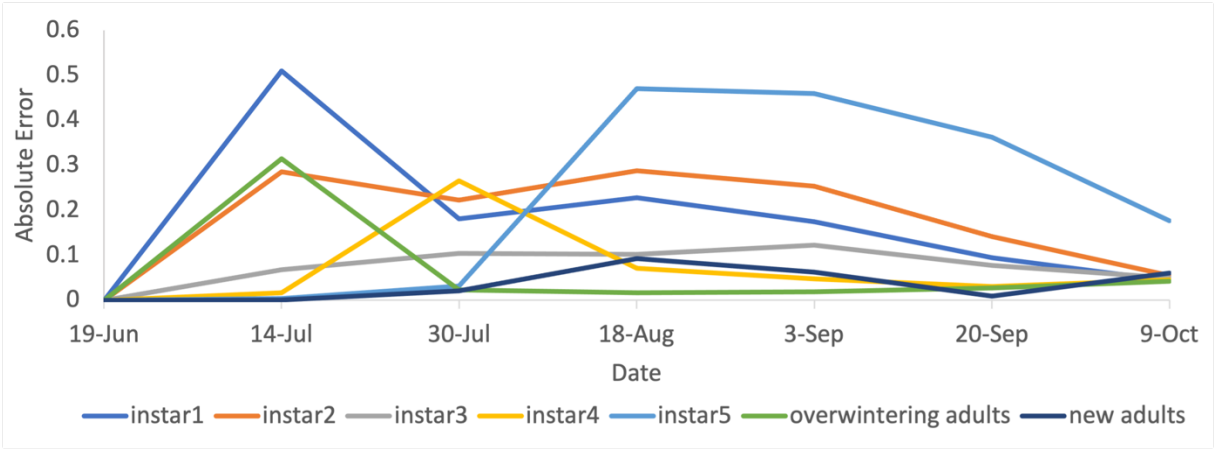

Figure 4.12 Absolute error between the Haye et al. (2014) and the general model's *Halyomorpha halys* life stage population proportion for each life stage (figure 4.11).

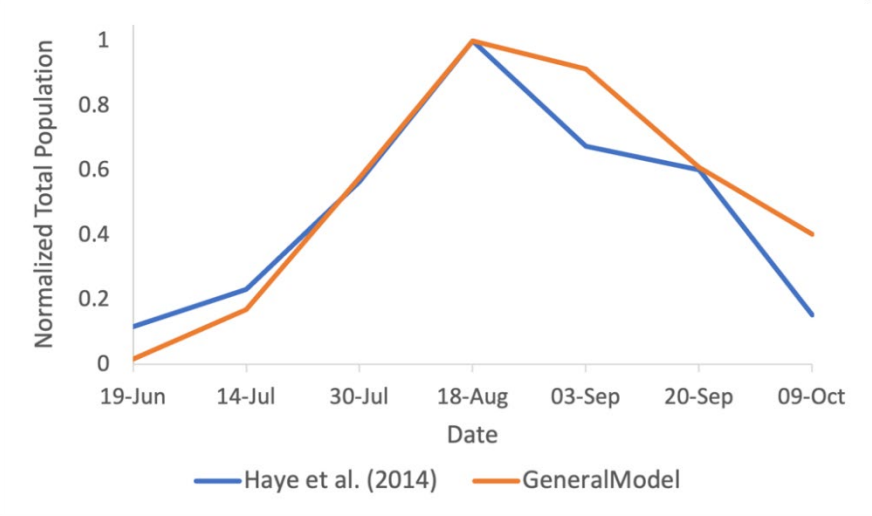

Figure 4.13 Normalized daily *Halyomorpha halys* combined life stage population size observed by Haye et al. (2014) and simulated by the general model.

Halyomorpha halys Conclusion

Although the general model produced population results with flattened tapering curves for the Govindan and Hutchison (2020) constant temperature life cycle and the Haye et al. (2014) life stage proportion, the general model remains a valid method for simulating *H. halys* population dynamics since test species results fulfilled the validation criteria.

4.3.3 *Dendroctonus ponderosae* (Mountain Pine Beetle)

General model validation was also conducted on the mountain pine beetle *Dendroctonus ponderosae*, a forestry pest species native to western North America. The general model's results were compared to the published *D. ponderosae* population studies by Bentz et al. (1991) and Mitton and Ferrenberg (2012).

Bentz et al. *Dendroctonus ponderosae* Published Model Results

Bentz et al. (1991) developed a phenology model to describe the effect of temperature on the temporal distribution of life stages, based on conducted constant-temperature laboratory experiments. The Bentz et al. (1991) phenology model results were produced using phloem temperature data from an infested lodgepole pine in Sawtooth National Recreation Area, ID. The general model was parameterized to *D. ponderosae* data including the overwintering termination critical temperature of 5°C and the overwintering induction critical temperature of 15°C (Bentz and Mullins 1999; Bentz and Hansen 2018). The model run was initialized with 100 eggs on Julian day 222 and used smoothed phloem temperature data from the published Bentz et al. (1991) *D. ponderosae* study.

Figure 4.14 compares the life stage density graph from Bentz et al. (1991) with the one produced by the general model. The general model results have the same tapering life stage curves seen and explained in previous species tests, resulting in small overlapping life stages. Disregarding this, the density curves produced by the general model are a good match for the Bentz et al. (1991) model. The combined egg and first three instar life stages last a similar duration as seen in Bentz et al. (1991). When measuring the instar3 life stage's end date as the day where the life stage's population is less than 0.1, the simulated Bentz et al. population lasts 84 days and the simulated general model population lasts 109 days (29.76% error). Overwintering induction and termination occurs on comparable Julian days. The general model starts overwintering on Julian day 225 and ends overwintering on Julian day 532 while the Bentz et al. (1991) model start overwintering on Julian day 253 and ends on Julian day 533. Finally, the model's post overwintering pupal life stage timing is a good match for the observed population. Both peak pupae

populations occur on the same date, July 1st (Julian day 547). Overall, the general model produced good qualitative life stage density results for *D. ponderosae.*

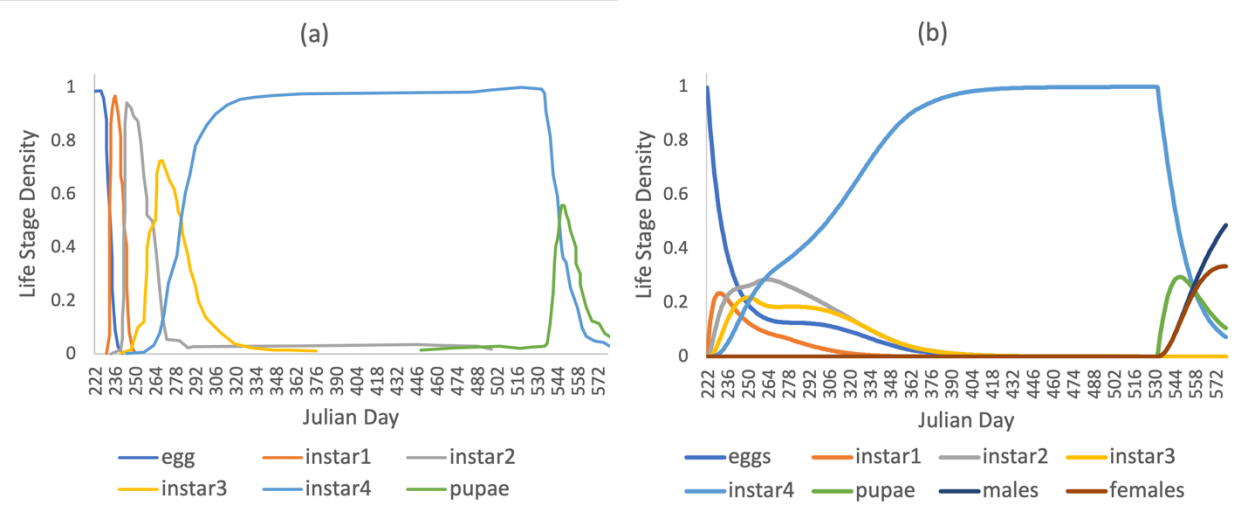

Figure 4.14 *Dendroctonus ponderosae* population life stage density (ratio) between Julian day 222 and 590 under the phloem temperature of an infested lodgepole pine in Sawtooth National Recreation Area, ID, (a) produced by the Bentz et al. (1991) model and (b) the general model.

Mitton and Ferrenberg *Dendroctonus ponderosae* Published Field Observation Results

Mitton and Ferrenberg (2012) conducted a population field study of *D. ponderosae* in Colorado in 2008 and 2009 and compared their finding to historic *D. ponderosa* phenology. They determined that with increased annual temperatures, *D. ponderosa* populations increase due to a longer flight season, increased reproductive output and increased number of generations and broods (from one to two generations). An approximation of the historic (1970-1979) and recent (2000-2008) temperature profile in Colorado (figure 4.15) where created to be used in the general model based on monthly temperature ranges described in Mitton and Ferrenberg (2012), since the study region's daily temperature was not available in the paper. The goal with this test was to confirm the findings described in Mitton and Ferrenberg (2012), that *D. ponderosa* populations are larger under recent temperatures as compared to populations under historic temperatures in Colorado.

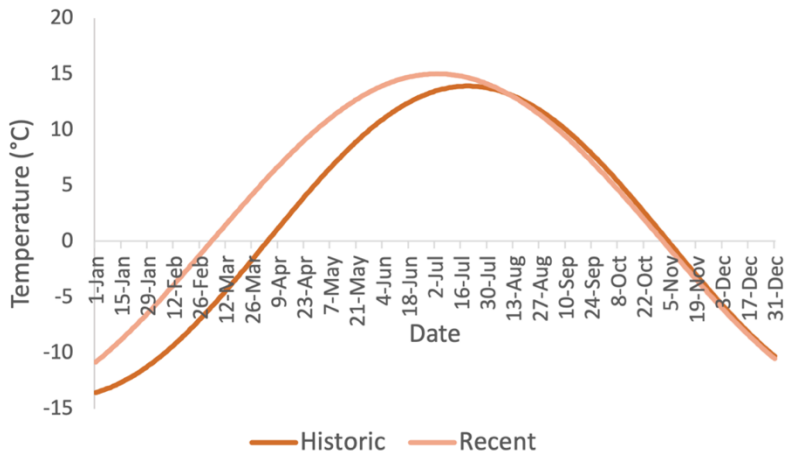

Figure 4.15 Historic (1970-1979) and recent (2000-2008) smoothed daily average temperature curves in Colorado for one year.

The model was run for one year with an initial population of 100, overwintering fourth instar juveniles, that resumed their natural metabolism when temperatures were greater than the overwintering critical temperature of 5°C. Figure 4.16 shows the general model's life stage population curves over the simulation period under historic and recent Colorado temperature profiles. It should be noted that both graphs were normalised using the population's initial size in order to maintain an equal population (y-axis) scale between the historic and recent temperature graphs. The overwintering fourth instar population at the end of the one-year historic temperature simulation was approximately equal to the initial overwintering population (figure 4.16-a), while the overwintering fourth instar population under recent temperatures was nearly three times larger than the initial population at the end of the one year simulation (figure 4.16-b). These results, as expected, match the assertion made by Mitton and Ferrenberg (2012) that under warmer recent temperatures *D. ponderosa* populations increase.

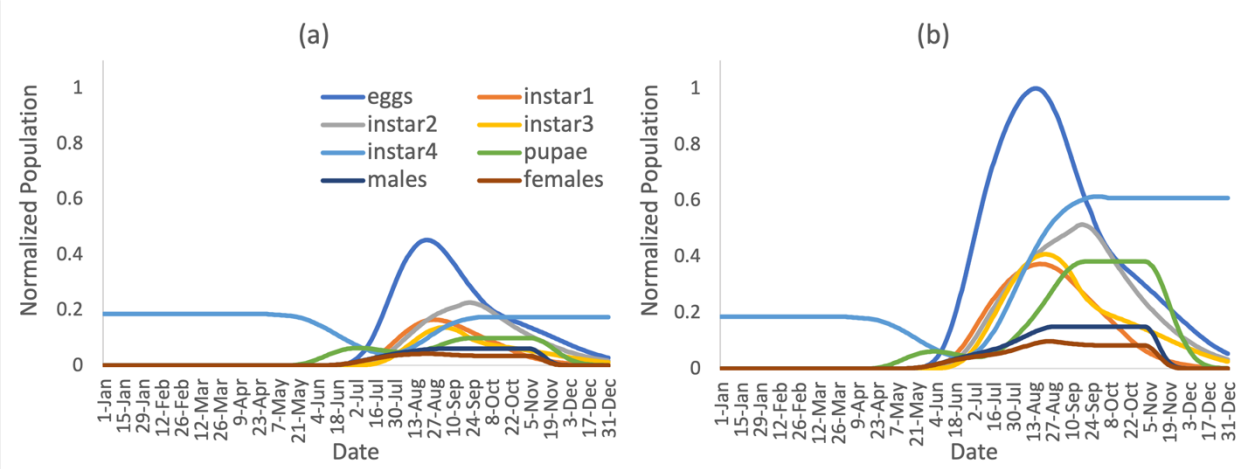

Figure 4.16 Normalized *Dendroctonus ponderosae* life stage population curves produced by the general model under (a) historic and (b) recent Colorado temperatures (figure 4.15).

Dendroctonus ponderosae Conclusion

The results produced by the general model were comparable to the published Bentz et al. (1991) and Mitton and Ferrenberg (2012) *D. ponderosae* population studies. Validation criteria were achieved by the life stage density simulation and observations made about *D. ponderosae's* success under different temperature profiles was confirmed by the model. The general model is, therefore, well suited to simulating *D. ponderosae* populations

4.3.4 *Contarinia nasturtii* (Swede Midge)

The general model was parameterized and run for the swede midge *Contarinia nasturtii*, a crop pest originally native to Europe and Asia. The general model was only compared to one published *C. nasturtii* population study from Liu (2019) that included field and modelled data.

Liu *Contarinia nasturtii* Published Field Study and Model Results

Liu (2019) compared mean relative adult *C. nasturtii* emergence field data (provided by R. Hallett) with results produced by the MidgEmerge model (Hallett et al. 2009), a *C. nasturtii* model

created with DYMEX (Hearne Software, 2021), run with weather data from a site at the University of Guelph Elora Research Station. The observed and simulated adult populations from Liu (2019) can be seen in figure 4.17 and were used to validate the general model results through a visual comparison. The general model was run using the same 2009 daily mean temperature data used in the MidgEmerge model, obtained from the Elora Research Station Meteorological Records Dataverse (dataverse.scholarsportal.info/dataverse/ersmr). The general model used an initial population of 100 pupae, leaving overwintering with the critical termination conditions of 6°C and 14 daylight hours based on values tested in the MidgeEmerge model and research by Hallett et al. (2009).

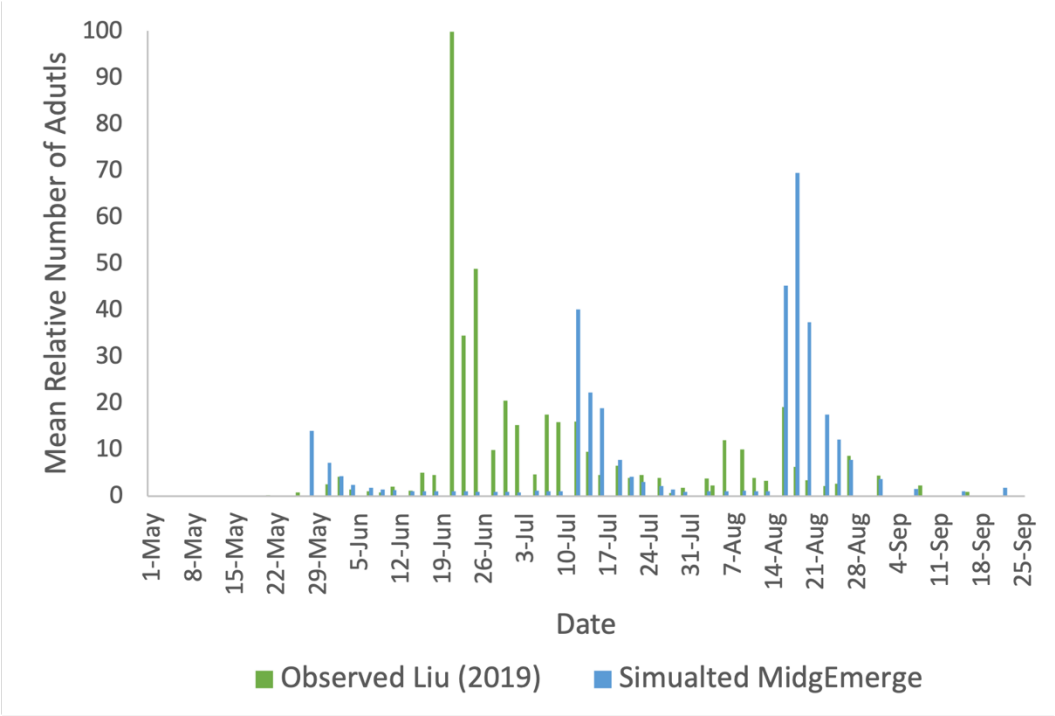

Figure 4.17 Mean relative number of *Contarinia nasturtii* adults in the observed population and in the simulated MidgEmerge model population under the temperature conditions at the University of Guelph Elora Research Station between the months of May and September 2009. Figure from Liu (2019).

Adult population results produced by a normal run of the general model can be seen in figure 4.18. The general model's adult population peaked on September 30 (Julian day 272) later

in the year than either of the Liu (2019) species-specific observed or modelled results (figure 4.17) which occurred on June 21 and August 18 (Julian day 173 and Julian day 231).

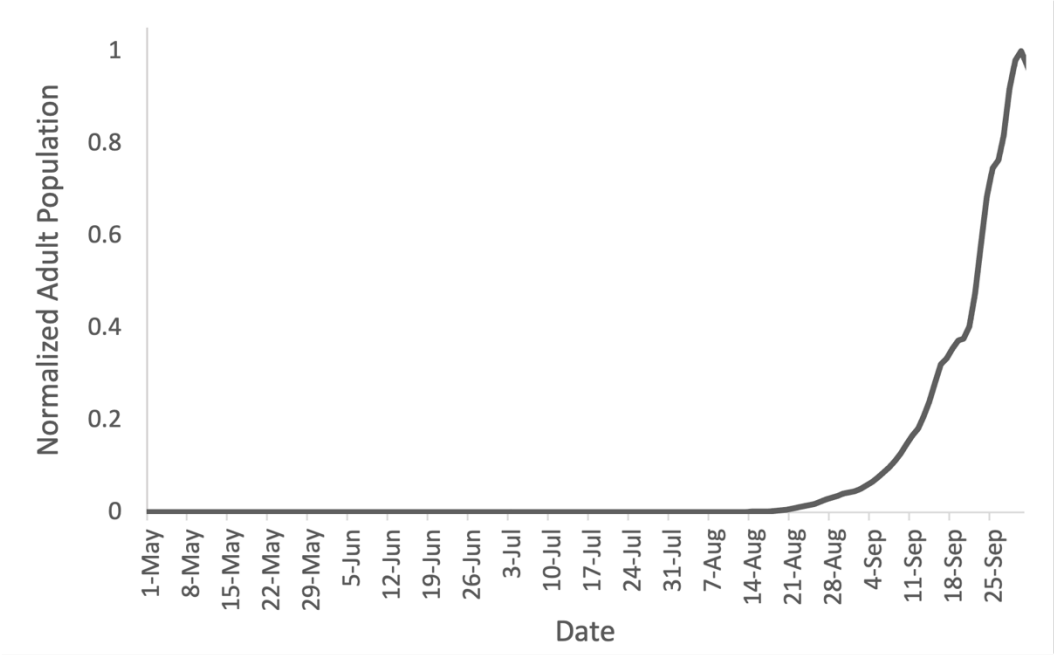

Figure 4.18 Normalized adult *Contarinia nasturtii* population simulated by the general model under the temperature conditions at the University of Guelph Elora Research Station in 2009. This figure's population is compared to figure 4.17's populations.

Adult *C. nasturtii* populations seen in Liu (2019) are very generational. The Liu (2019) observed population has multiple generations with distinct peak emergence dates, while the MidgEmerge model populations has 3 distinct adult peaks on May 28, July 12 and August 18 (Julian day 149, 194 and 231) (figure 4.17). Generations can be difficult to perceive with the general model due to its continuous nature, however, potential generations can be recognized by visually identifying the peaks of steeper population increases on a log scale curve. The general model results were converted to a log scale in figure 4.19 to identify the potential timing of the general model's population generations. The general model's potential *C. nasturtii* generations were determined to occur at the approximate dates of May 8, July 3 and August 26 (Julian days: 128, 184, 238). The general model, like the MidgEmerge model simulated a total of three *C.*

nasturtii generations per year and the timing of these generations were also comparable to those produced by the MidgEmerge model. Like the MidgEmerge model, the general model's results don't match observed *C. nasturtii* adult populations.

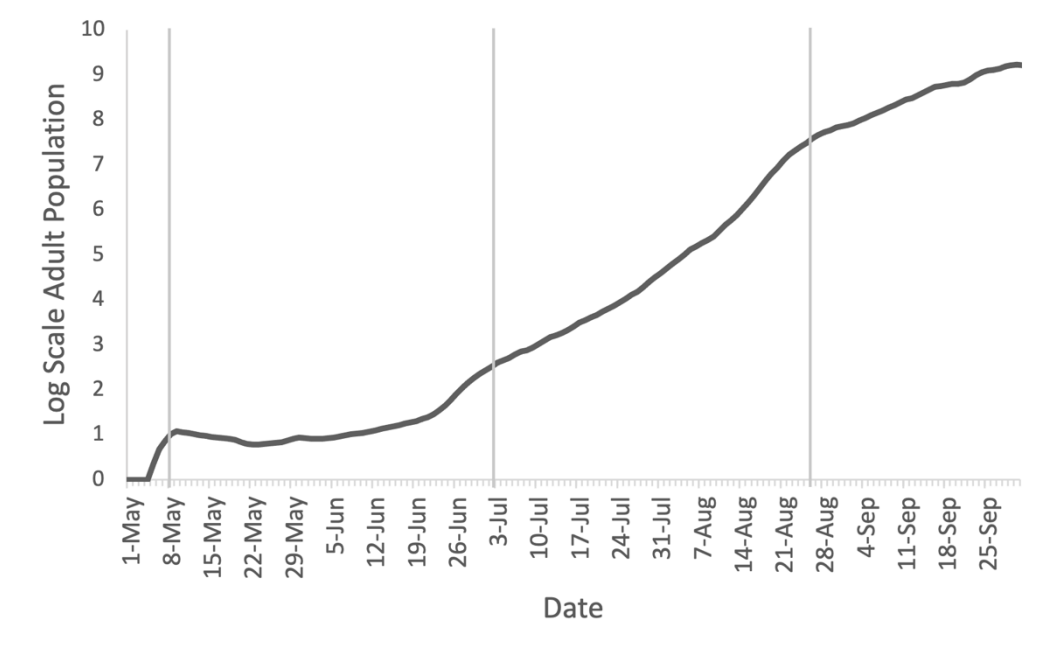

Figure 4.19 Normalized adult *Contarinia nasturtii* population simulated by the general model under the temperature conditions at the University of Guelph Elora Research Station in 2009, converted to a logarithmic scale to extract the population's approximate generation timing (May 8, July 3 and August 26). This figure's population is compared to figure 4.17's populations.

An additional general model experiment was conducted to test a different technique for "extracting" an insect population's generations. The general model was run 3 separate times (with no fecundity) ending each run when the adult female population was at its peak and beginning the next run with the number of eggs produced by the previous run's peak female population. The combination of each run's adult population can be seen in figure 4.20. This running method produced generations on May 22, June 30 and August 05 (Julian Day 141, 180 and 216). The results produced by this method are comparable to those obtained by MidgEmerge (figure 4.17) and by the normal general model run (figure 4.19), but are again very different from the observed population (figure 4.17). This method confirmed the validity of extracting population generations

by log transforming the general model results, although, with this multi-run method, the third generation occurred earlier than with the log scale method.

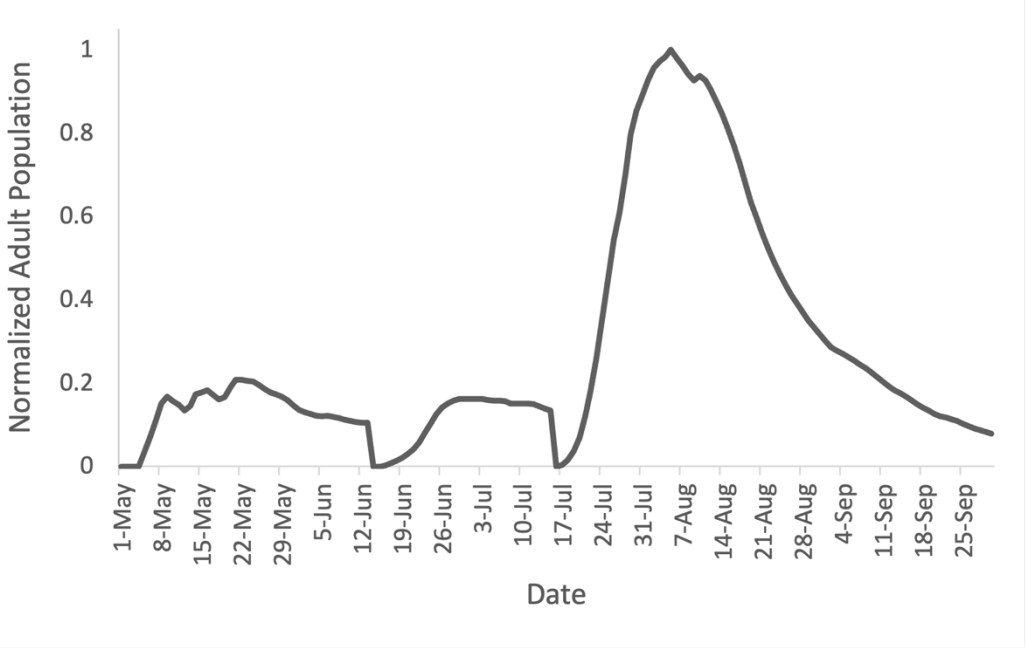

Figure 4.20 Normalized adult *Contarinia nasturtii* population produced by three separate general model simulations terminated on the peak female population date and initialized with the number of eggs produced by the previous simulation's peak female population. All general model runs used the temperature conditions at the University of Guelph Elora Research Station in 2009. This figure's population is compared to figure 4.17's populations.

In this validation model test, the general model was able to produce *C. nasturtii* results with similar generation timing and equal yearly generations as the MidgEmerge model through two "extraction" methods. The general model can be considered to be valid as a general, exploration model for this insect species since it reaches the result standards produced by other models, specifically the MidgEmerge model. The general model's results can provide insight into *C. nasturtii* simplified population dynamics and generations, yet is not able to mimic actual observed populations.

Contarinia nasturtii Conclusion

The general model was not able to mimic the Liu (2019) observed populations peak dates or the overall shape of the observed population curve, due to the specie's complex population dynamics beyond the general model's simulation abilities. *C. nasturtii* is known to be a difficult insect species to simulate, it has three confirmed emergence phenotypes (Goodfellow 2005; Hallett et al. 2009; Des Marteaux et al. 2015), more than one overlapping generation per year in southern Ontario (Hallett 2007; Hallett et al. 2009) and its population emergence peaks have not been found to correlate with common causational factors such as temperature during development, day length when developing out of its overwintering pupal stage and precipitation levels prior to emergence (Des Marteaux et al. 2015).

With all this considered, the results produced by the general model reproduce observed *C. nasturtii* populations as closely as can be expected from a general model. Liu (2019) was able to produce population results that more closely match observed *C. nasturtii* populations with the use of a more refined species-specific model, however, it used a statistical parameterization method that iteratively adjusted species parameters that didn't have reliable measured values, to better match Ontario populations. Unless the swede midge's complex life cycle, which isn't fully understood, is fully replicated in a computer model, exact population results cannot be expected from a mechanistically parameterized general model.

4.3.5 *Aphis gossypii* (Cotton Aphid)

The general model's final test species was the Cotton Aphid, *Aphis gossypii*, an agricultural crop pest found in tropical and temperate regions of the world. The general model results where compared to a field study by Parajulee et al. (1997).

Parajulee et al. *Aphis gossypii* Published Field Study Results

Parajulee et al. (1997) monitored cotton aphid and predator (75.4% Ladybeetle *Harmonia dimidiata*) populations in a monoculture, cotton crop treatment at the Texas Agricultural Experiment Station in Munday, Texas, USA, for the years of 1992, 1993 and 1994. As seen in figure 4.21, three-year average cotton aphid population peaked on August 25, followed by a predator population peak one week later on September 2. Parajulee et al. (1997) determined that this time lag suggested a strong density-dependent relationship between these species. Based on Parajulee et al.'s (1997) findings, it can be expected that the general model won't be able to accurately simulate this species population in part due to its strong predator prey interaction which isn't considered in the general model.

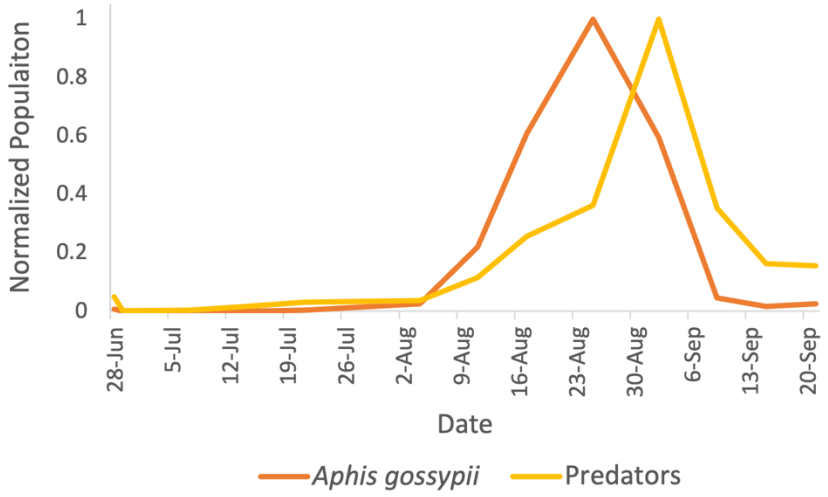

Figure 4.21 Normalized three year average (1992, 1993 and 1994) *Aphis gossypii* and predator species (75.4% *Harmonia dimidiata*) populations observed by Parajulee et al. (1997) at the Texas Agricultural Experiment Station in Munday, TX.

The general model was initialized with 100 cotton aphid eggs on May 20th and run for one year using the three-year average mean daily temperature for 1992, 1993 and 1994 in Abilene,

Texas. The model's egg development rate was set to a very large value to cause new insects produced by adult females to transition directly to the first juvenile life stage, skipping the egg stage, in order to account for *A.* gossypii's complex life cycle that only includes eggs as a hardy overwintering life stage.

The simulated combined life stage daily *A. gossypii* population grew exponentially and peaked in the fall on October 27th (Julian day 300) (figure 4.22). This peak population date didn't match the observed Parajulee et al. (1997) peak population date on August 25 (Julian day 237) (figure 4.21). The model didn't produce meaningful results due to the specie's complex life cycle, and population dynamics that are greatly influenced by factors not included in the model. The production of live young was approximated in the model by skipping the egg stage, however, the full complexity of aphid life cycles including sexual vs asexual reproduction, egg overwintering, and winged adults, could not be replicated because of the general model's design. The primary population dynamics driving factor, predator-prey relationships, could not be accounted for in the general model causing the model to be unable to determine the timing of *A. gossypii* population increases and decreases.

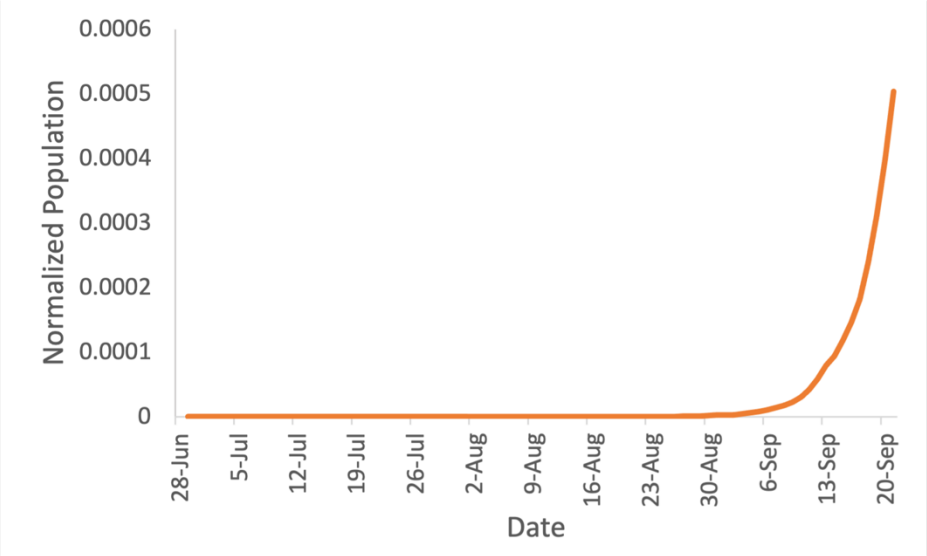

Figure 4.22 Normalized *Aphis gossypii* population simulated by the general model under the three-year average (1992, 1993 and 1994) mean daily temperatures in Abilene, TX. The general model was initialized with 100 eggs on May 20th. This figure's population is compared to figure 4.21's populations. Note that the *Aphis gossypii* population continues to grow exponentially outside of the range of the figure and peaks on October 29th with the normalized peak value of 1.

Aphis gossypii Conclusion

The general model is not suited for simulating *A. gossypii* populations. The model's inability to simulate predator prey interactions can be ignored in the model's validation since the general model is not intended for simulating this population dynamics driving factor, never the less, the general model's inability to simulate *A. gossypii*'s complex life cycles makes it unusable for this species.

5. Discussion and Conclusion

5.1 Generalized Mechanistic Insect Population Dynamics Model Discussion

General Model Summary

A mechanistic general model was created to simulate various insect species through their life stages under specified temperature profiles. This model was successfully adapted from the species-specific *Drosophila suzukii* model by generalizing its differential and vital rate equations while maintaining its overall structure. The model includes sub models that can represent insect overwintering, reproductive diapause and natural or anthropogenic mortality events. The general model requires a limited number of parameters to simulate insect population dynamics, making it easier to parameterize and use. Parameters were minimized during model creation by using vital rate equations that require few parameters and simplifying insect population dynamics mechanisms without greatly affecting their functionality.

General Model Vital Rate Equations

The general model's vital rate equation curves were chosen based on their good fit to insect species' vital rate values at measured constant temperatures and their limited and accessible parameters that represent real ecological values. Although these equations produce a reasonable fit for the vital rates of a number of insect species, other equations may be more suited for certain species. For example, the general model's parabolic mortality rate equation is commonly used to model temperature-dependent mortality (e.g. Gilioli et al. 2016; Esbjerg and Sigsgaard 2019), however, a smoothed square wave has also been used (Tanga et al. 2018; Otieno et al. 2019). Insect species with temperature-dependent mortality rates better described by a smoothed square wave can still be fit to the parabolic curve used in the general model, but some differences will exist

between real and modelled mortality rate values. Though the differences in mortality rate values are relatively small, they may potentially result in significant errors in simulated insect populations.

As the general model is open source, this possible error could be resolved by the users themselves. Users have the option to modify the vital rate equations in the general model's code to be better suited to their study species and to better match its response to temperature. However, this requires the user to have programing experience, a barrier to access that the general model aims to avoid. Future work on the general model could focus on determining, through analytical methods, the best vital rate equations for a large number of insect species' published temperature-dependent development, mortality and fecundity data. Alternatively, the general model could provide an easy way to switch between several vital rate equation options to best fit the insect species of interest.

General Model Simplifications

Many of the model's elements and sub models are based on simplified representations of their real world counterparts. The limitations that arise from model simplifications were balanced with the simplifications' advantages. For example, the general model bases insect temperature-dependent mortality on the daily mean temperature value since it was the most commonly measured mortality value in published laboratory studies, however, more complex models also consider the length of time that the insect is exposed to these temperatures (Nedved et al. 1998; Diaz et al. 2008; Régnière et al. 2012b). The inaccuracies that can arise from ignoring the exposure time were deemed to be less important than the accessibility provided by modelling mortality with the most commonly available data, since one of the general model's goals was to be simple to use

without requiring users to conduct supplementary research on the insect species of interest. Additionally, the general model includes a simplified overwintering sub model that only accounts for basic insect overwintering behavior where insect development and mortality is halted during overwintering. Though the general model doesn't fully mimic real insect overwintering, the inclusion of a sub model that accounts for the broad role of overwintering was determined to be advantageous since it can provide users with a tool to simulate insect species for multiple years. Finally, populations simulated by the general model operate within a closed system which does not consider emigration and immigration. This doesn't accurately reflect real population dynamics but does reduce model complexity which can be advantageous. As it was clearly stated that results produced by the model are only intended as initial explorations of insect population dynamics and are not necessarily indications of any real-world insect population response, approximate simplified results are considered acceptable.

Overall, the general model could be made more complex to simulate insect population dynamics more accurately, however this would require additional input parameters, a change that is counter to the model's goals of simplicity and ease of use.

5.2 Model Exploration and Sensitivity Testing Discussion

Exploration and Sensitivity Test Results

Exploration and sensitivity tests were run for the general model. Exploration results that were only intended as sensitivity tests, without any real world meaning, adequately demonstrated the function of the model. All results with real world parallels behaved as expected for real insect populations other than the overwintering sub model. The general model's overwintering behavior, especially for the juvenile overwintering life stage, was unrealistic. Very early induction overwintering dates

produced the biggest overwintering populations (section 3.4.1). In reality, insects accumulate energy stores, most commonly lipids, during the active season and use these as fuel for the overwintering and post-overwintering season (Brent and Marshall, 2018). Insufficient energy stores significantly affect overwintering mortality and post-overwintering starvation (Knapp and Rericha, 2020). If insects enter an overwintering state as early as suggested by the general model exploration results, they would not likely have sufficient time to build energy stores and would not have adequate stored energy to survive the overwintering and post-overwintering period. More realistic optimal overwintering induction timing would take energy stores into account and result in a later induction date. Overwintering energy stores is one of the overwintering survival factors that were overlooked in the overwintering sub model in favor of model simplicity. Energy stores and other overwintering survival factors can be approximated by using the sub model's survival percentage, but this parameter must be measured or calculated by hand and was not considered in this exploratory test. Since the overwintering sub model doesn't take energy stores into consideration, the general model should not necessarily be used as a tool to determine the overwintering induction date that will result in the largest overwintering population.

5.3 General Model Validation Discussion

Data Availability for Model Validation Test Parametrization

The general model achieved its goal of simplicity and accessibility, as sufficient published data was available to parameterize the model for validation tests for multiple insect species. The general model's required input parameters consisted of common temperature-dependent insect species data, frequently collected for other laboratory studies unrelated to the general model. Temperature-dependent life-tables, for example, are created for insects through laboratory studies

in order to better understand their response to temperature (e.g., Ning et al. 2017; Otieno et al. 2019). Constant temperature insect development, longevity, mortality and fecundity life table values, are one of the best sources of species data that can be used to fit the model's equations and obtain the model's configuration parameters.

Though the model was parameterized with published data for five insect species, data availability issues may still be present for other species. Certain insects are simply unstudied or under studied making data unavailable or inaccurate. Even if data exists, it may not produce accurate model results if data were collected in a different region than the specific region of interest since insects species have been known to demonstrate different population dynamics based on their geographical distribution (Liu et al. 2002; Golizadeh and Zalucki 2012; Liu 2019). In other cases, research has been conducted but data is not shared or presented in a way that can be used in models. The publication of raw data for laboratory studies or standardized metrics could allow modellers to use research data more easily. It is strongly recommended that theorist (modelers) and non-theorist (researchers) collaborate to ensure that both data and ecological knowledge can be shared in order to ameliorate theoretical understanding of insects population dynamics in the field of ecology.

Further data availability issues were experienced when obtaining temperature data from population studies, used to validate the model. The problem was that they didn't publish location specific or lab temperature data for the population results, so daily temperature data was approximated using alternative sources, e.g. historic climate databases. As shown in Langille (2017), small differences in temperature curves can have a big impact on the model's resulting population. It is recommended that researchers record and publish temperature data from their experiment location.

Validation Test Results for Multiple Insect Species

In four of five insect species tested, the general model is able to produce acceptable insect population dynamics results for the model's intended use and validation criteria.

Drosophila suzukii, *Dendroctonus ponderosae* and *Halyomorpha halys* simulations produced good population dynamics results that accurately approximated the published population's overall shape, key species population characteristics, life stage peak population timing, and, whenever applicable, diapause termination and induction dates and overwintering termination and induction dates. Yet, the general model notably deviated from certain published population life stage curve results, producing less steep, flatter, more tapered life stage curves due to differential equation model characteristics causing populations to tend towards but not reach zero. These deviations are, however, negligible as they do not affect the modelled populations most important result, the life stage timing.

Like the first three species, *Contarinia nasturti* achieved many of the validation criteria. The *Contarinia nasturti* general model simulations mimicked other published model results relatively accurately, but the general model was not able to approximate published observed populations and their peak timing due to *Contarinia nasturti*'s complex generations and multiple phenotypes with emergence patterns whose environmental triggers aren't fully understood.

Finally, the *Aphis Gossypii* general model simulation did not produce qualitatively acceptable results due to *Aphis Gossypii*'s complex life cycle, and population dynamics driving factors that are not included in the general model, such as predator prey interactions.

As expected, no general model results exactly matched published population results since the model is not designed or intended for precise predictive population dynamics. Rather, the

general model is intended for exploration, producing approximate populations that generally behave as expected from an insect species.

Validation tests were limited to five insect species, a good first step in identifying the general model's limits and the type of insect species that it is capable of accurately simulating. However, further tests on additional insect species with diverse behaviors and life histories would need to be conducted to draw any decisive conclusions about the model's ability to simulate the broad range of insect species that general models are intended to simulate.

Model Limits and Best Use

Based on the validation test findings, the model is well suited to simulating insect species with simple life cycles, however, more complex life cycles are not as easily simulated due to the general model progressing linearly through life stages. The general model is not suited to simulating eusocial insect populations, such as aphids (as seen in the *Aphis* gossypii validation test), bees, termites, wasps, and others, due to the complexity of their life cycles and life stage longevity that differs between insects with different roles (e.g., in bees: queen, worker and drone). The general model is also not suited to simulating species with complex developmental dormancies that don't behave like the simplified overwintering or reproductive diapause sub models. Finally, as mentioned in the validation test results, the model is not capable of producing meaningful results for insect species populations that greatly depend on population dynamics driving factors not considered by the model including abiotic factors like humidity, snow fall, micro climates and biotic factors including resource availability (Monro 1967), predator-prey interactions (Parajulee et al. 1997) and density dependent mortality (Haridas et al. 2016).

General Model Validation Conclusion

The general model should be used and applied based on its known best use cases and limitations listed above. Users should consider the insect specie's population dynamics driving factors to decide if this general model is suited to produce accurate population results. For insect species populations that are not greatly dependent on factors not included in the general model, and with suitable parameters, general model simulations produce populations that follow the overall shape and have similar life stage peak population dates as previously simulated or observed insect populations.

5.4 Final Thoughts and Future Work

Thesis Summary

The primary objective of this thesis was to create and validate a generalized insect population dynamics model that could accurately simulate various insect species while remaining simple and easy to use. Through exploration (sensitivity) and validation tests, the model was found to produce insect populations that behaved as expected for the real-life system and to be effective at simulating various insect species' with simple life cycles. It was also demonstrated that the general model can use readily accessible published laboratory data to run simulations, making the model well suited for rapid modelling for both researchers and non-researchers. The general model's ease of use is further improved by the inclusion of a GUI (graphical user interface; appendix G) that can help the user input insect species parameters, run the model, and visualize the resulting populations.

Other General Models

This general model is simpler than many existing general models (e.g. CLIMEX (Sutherst 1985; Kriticos et al. 2015), DYMEX (Maywald et al. 2007), BioSim (Régnière 1996; Régnière et al. 2014), and ILCYM (Sporleder et al. 2009)); it has fewer parameters, the parameters are based on real measurements (e.g. the maximum and minimum temperature for survival), and it uses a more condensed set of population dynamics driving factors than other models. The model simplifications that make it less complex might reduce the accuracy of population dynamics results produced, however, as shown in the validation results, the general model remains capable of producing acceptable exploratory results within its set constraints. The general model could be made more complex by adding considerations for more population dynamics driving factors such as precipitation, humidity, wind, air pressure, snow, solar radiation (BioSim), and competition between species (CLIMEX & DYMEX) to increase the range of insect species that the general model can accurately simulate, but since this model is intended for rapid simple insect population dynamics exploration, increasing the model's complexity and difficulty of use would be counter to its goals. Maintaining the general model's simplicity and ease of use is essential to making the model accessible to a wide audience with diverse backgrounds including those with no research or modelling experience. This general model contributes to the range of models that can produce qualitatively good results for various but not all insect species making it essential in the field of ecological modelling.

General Model Applications

The general model is a simple, easy to use insect population dynamics model making it perfect for study ideation or prototyping and for rapid exploration of insect species basic

population dynamics. Due to its simplicity the general model can be used by both scientists and industry professionals. The model is not intended to produce predictive results, rather it's intended to simulate approximate insect population dynamics. The general model can be used for numerous purposes because of its mechanistic and split life stage population simulations that can provide not only population size information, but also information about the population's life stage progression, life stage peak timing, along with specific life stage survival, mortality, longevity and egg production values. Some ways the general model can be used include:

- Exploring and improving theoretical understanding of an insect's population dynamics (life stage timing, number of generations per year, overwintering, diapause, phenology and more).
- Determining a foreign or invasive species' potential success if introduced in a new region.
- Informing pest species' mitigation and management strategies in order to save money and reduce the environmental impact of pesticide applications.
- Studying insect species' potential response to changing climates.
- Exploring a number of other "what-if" insect species scenarios.

Future Work

The main addition that should be considered for the general model's future work is the implementation of multi-cell simulations. This would allow the model to create a map of the insect species range, based on suitable temperatures, by simulating the insect species population for multiple cells each with its own temperature profile. Mapping is a feature in many general models, and was also a feature in the species-specific Langille et al. (2016) (Langille et al. 2017) model

that this general model was based on. The addition of a multi-cell simulation option to the general model would be relatively straightforward and would greatly increase the model's application cases.

6. Bibliography

Abbott, K.C., and Dwyer, G. 2007. Food Limitation and Insect Outbreaks: Complex Dynamics in Plant-Herbivore Models. J Anim Ecology **76**(5): 1004–1014. doi:10.1111/j.1365-2656.2007.01263.x.

Abbott, K.C., and Dwyer, G. 2008. Using Mechanistic Models to Understand Synchrony in Forest Insect Populations: The North American Gypsy Moth as a Case Study. The American Naturalist **172**(5): 613–624. doi:10.1086/591679.

Abram, P.K., Haye, T., Mason, P.G., Cappuccino, N., Boivin, G., and Kuhlmann, U. 2012. Biology of Synopeas myles, a parasitoid of the swede midge, Contarinia nasturtii, in Europe. BioControl **57**(6): 789–800. doi:10.1007/s10526-012-9459-x.

Adler, P.B., and Lauenroth, W.K. 2003. The Power of Time: Spatiotemporal Scaling of Species Diversity. Ecol Letters **6**(8): 749–756. doi:10.1046/j.1461-0248.2003.00497.x.

Aldyhim, Y.N., and Khalil, A.F. 1993. Influence of Temperature and Daylength on Population Development of Aphis gossypii on Cucurbita Pepo. Entomologia Experimentalis et Applicata **67**(2): 167–172. John Wiley & Sons, Ltd. doi:10.1111/j.1570-7458.1993.tb01665.x.

Baker, C.R.B. 1991. The Validation and Use of a Life-Cycle Simulation Model for Risk Assessment of Insect Pests. EPPO Bulletin **21**(3): 615–622. doi:10.1111/j.1365-2338.1991.tb01295.x.

Baker, R.E., Peña, J.-M., Jayamohan, J., and Jérusalem, A. 2018. Mechanistic Models Versus Machine Learning, a Fight Worth Fighting for the Biological Community? Biol. Lett. **14**(5). doi:10.1098/rsbl.2017.0660.

Bale, J.S. 2002. Insects and Low Temperatures: From Molecular Biology to Distributions and Abundance. Phil. Trans. R. Soc. Lond. B **357**(1423): 849–862. doi:10.1098/rstb.2002.1074.

Bale, J.S., and Hayward, S. a. L. 2010. Insect overwintering in a changing climate. Journal of Experimental Biology **213**(6): 980–994. The Company of Biologists Ltd. doi:10.1242/jeb.037911.

Balenghien, T., Carron, A., Sinègre, G., and Bicout, D.J. 2010. Mosquito Density Forecast from Flooding: Population Dynamics Model for Aedes caspius (pallas). Bull. Entomol. Res. **100**(3): 247–254. doi:10.1017/S0007485309990745.

Baumgärtner, S., Becker, C., Frank, K., Müller, B., and Quaas, M. 2008. Relating the Philosophy and Practice of Ecological Economics: The Role of Concepts, Models, and Case Studies in Inter- and Transdisciplinary Sustainability Research. Ecological Economics **67**(3): 384–393. doi:10.1016/j.ecolecon.2008.07.018.

Belles, X. 2011. Origin and Evolution of Insect Metamorphosis. *In* Encyclopedia of Life Sciences. John Wiley & Sons, Ltd. p. 11. doi:10.1002/9780470015902.a0022854.

Bentz, B.J., and Hansen, E.M. 2018. Evidence for a Prepupal Diapause in the Mountain Pine Beetle (Dendroctonus ponderosae). Environmental Entomology **47**(1): 175–183. doi:10.1093/ee/nvx192.

Bentz, B.J., Logan, J.A., and Amman, G.D. 1991. Temperature-Dependent Development of the Mountain Pine Beetle (Coleoptera: Scolytidae) and Simulation of Its Phenology. Can Entomol **123**(5): 1083–1094. doi:10.4039/Ent1231083-5.

Bentz, B.J., and Mullins, D.E. 1999. Ecology of Mountain Pine Beetle (Coleoptera: Scolytidae) Cold Hardening in the Intermountain West. Environ Entomol **28**(4): 577–587. doi:10.1093/ee/28.4.577.

Bleiker, K.P., and Smith, G.D. 2019. Cold Tolerance of Mountain Pine Beetle (Coleoptera: Curculionidae) Pupae. Environmental Entomology **48**(6): 1412–1417. doi:10.1093/ee/nvz116.

Boggs, C.L., and Inouye, D.W. 2012. A Single Climate Driver Has Direct and Indirect Effects on Insect Population Dynamics. Ecology Letters **15**: 502–508. doi:10.1111/j.1461-0248.2012.01766.x.

Bommireddy, P.L., Parajulee, M.N., and Porter, D.O. 2004. Influence of Constant Temperatures on Life History of Immature Lygus elisus (Hemiptera: Miridae). en **33**(6): 1549–1553. doi:10.1603/0046-225X-33.6.1549.

Brière, J.-F., Pracros, P., Le Roux, A.-Y., and Pierre, J.-S. 1999. A Novel Rate Model of Temperature-Dependent Development for Arthropods. Environ Entomol **28**: 22–29. doi:10.1093/ee/28.1.22.

Bugmann, H. 1994. On the Ecology of Mountainous Forests in a Changing Climate: A Simulation Study. Swiss Federal Institute of Technology, Zürich, Switzerland.

Choudhary, J.S., Mali, S.S., Naaz, N., Mukherjee, D., Moanaro, L., Das, B., Singh, A.K., Rao, M.S., and Bhatt, B.P. 2020. Predicting the Population Growth Potential of Bactrocera zonata (saunders) (Diptera: Tephritidae) Using Temperature Development Growth Models and Their Validation in Fluctuating Temperature Condition. Phytoparasitica **48**(1): 1–13. doi:10.1007/s12600-019-00777-4.

Corlay Herrera, F.R. 2008. Seasonal Development and Natural Enemies of an Invasive Exotic Species, the Swede Midge Contarinia Nasturtii (kieffer), in Québec. Library and Archives Canada = Bibliothèque et Archives Canada, Ottawa.

Cuddington, K., Sobek-Swant, S., Crosthwaite, J.C., Lyons, D.B., and Sinclair, B.J. 2018. Probability of Emerald Ash Borer Impact for Canadian Cities and North America: A Mechanistic Model. Biol Invasions **20**(9): 2661–2677. doi:10.1007/s10530-018-1725-0.

Denlinger, D. 2002. Regulation of Diapause. Annual review of entomology **47**: 93–122. doi:10.1146/annurev.ento.47.091201.145137.

Des Marteaux, L.E., Schmidt, J.M., Habash, M.B., and Hallett, R.H. 2015. Patterns of Diapause Frequency and Emergence in Swede Midges of Southern Ontario: Patterns of Swede Midge Diapause. Agr Forest Entomol **17**(1): 77–89. doi:10.1111/afe.12083.

Diaz, R., Overholt, W.A., Samayoa, A., Sosa, F., Cordeau, D., and Medal, J. 2008. Temperature-Dependent Development, Cold Tolerance, and Potential Distribution of Gratiana boliviana (Coleoptera: Chrysomelidae), a Biological Control Agent of Tropical Soda Apple, Solanum Viarum (solanaceae). Biocontrol Science and Technology **18**(2): 193–207. doi:10.1080/09583150701861543.

Dixon, A.F.G. 1977. Aphid Ecology: Life Cycles, Polymorphism, and Population Regulation. Annu. Rev. Ecol. Syst. **8**: 329–353. doi:10.1146/annurev.es.08.110177.001553.

Duarte, C.M., Amthor, J.S., DeAngelis, D.L., Joyce, L.A., Maranger, R., Pace, M.L., Pastor, J., and Running, S.W. 2003. The Limits to Models in Ecology. *In* Models in Ecosystem Science. *Edited by* C.D. Canham, J.J. Cole, and W.K. Lauenroth. Princeton University Press. p. 19. Available from http://www.jstor.org/stable/j.ctv1dwq0tq.

Emiljanowicz, L.M., Ryan, G.D., Langille, A., and Newman, J. 2014. Development, Reproductive Output and Population Growth of the Fruit Fly Pest Drosophila suzukii

(Diptera: Drosophilidae) on Artificial Diet. j econ entomol **107**(4): 1392–1398. doi:10.1603/EC13504.
Esbjerg, P., and Sigsgaard, L. 2019. Temperature Dependent Growth and Mortality of Agrotis segetum. Insects **10**(1): 7. doi:10.3390/insects10010007.
Estay, S.A., Lima, M., and Labra, F.A. 2009. Predicting Insect Pest Status Under Climate Change Scenarios: Combining Experimental Data and Population Dynamics Modelling. Journal of Applied Entomology **133**(7): 491–499. doi:10.1111/j.1439-0418.2008.01380.x.
Getz, W.M., Marshall, C.R., Carlson, C.J., Giuggioli, L., Ryan, S.J., Romañach, S.S., Boettiger, C., Chamberlain, S.D., Larsen, L., D'Odorico, P., and O'Sullivan, D. 2018. Making Ecological Models Adequate. Ecol Lett **21**(2): 153–166. doi:10.1111/ele.12893.
Gilioli, G., Pasquali, S., and Marchesini, E. 2016. A Modelling Framework for Pest Population Dynamics and Management: An Application to the Grape Berry Moth. Ecological Modelling **320**: 348–357. doi:10.1016/j.ecolmodel.2015.10.018.
Golizadeh, A., and Zalucki, M. 2012. Estimating Temperature-Dependent Developmental Rates of Potato Tuberworm, Phthorimaea operculella (Lepidoptera: Gelechiidae). Insect Science **19**(5): 609–620. doi:10.1111/j.1744-7917.2012.01503.x.
Goodfellow, S.A. 2005. Population Dynamics and Predictive Modelling of the Swede Midge, Contarinia nasturtii (Kieffer). The University of Guelph, Guelph, Ontario, Canada.
Govindan, B.N., and Hutchison, W.D. 2020. Influence of Temperature on Age-Stage, Two-Sex Life Tables for a Minnesota-Acclimated Population of the Brown Marmorated Stink Bug (Halyomorpha halys). Insects **11**(2): 108. doi:10.3390/insects11020108.
Grevstad, F.S., Wepprich, T., Barker, B., Coop, L.B., Shaw, R., and Bourchier, R.S. 2022. Combining Photoperiod and Thermal Responses to Predict Phenological Mismatch for Introduced Insects. Ecological Applications **32**(3): 16. doi:10.1002/eap.2557.
Grimm, V. 1994. Mathematical Models and Understanding in Ecology. Ecological Modelling **75–76**: 641–651. doi:10.1016/0304-3800(94)90056-6.
Hahn, D., and Denlinger, D. 2011. Energetics of Insect Diapause. Annual review of entomology **56**: 103–21. doi:10.1146/annurev-ento-112408-085436.
Hallett, R.H. 2007. Host Plant Susceptibility to the Swede Midge (Diptera: Cecidomyiidae). Journal of Economic Entomology **100**(4): 1335–1343. doi:https://doi.org/10.1093/jee/100.4.1335.
Hallett, R.H., Goodfellow, S.A., Weiss, R.M., and Olfert, O. 2009. Midgemerge, a New Predictive Tool, Indicates the Presence of Multiple Emergence Phenotypes of the Overwintered Generation of Swede Midge. Entomologia Experimentalis et Applicata **130**(1): 81–97. doi:10.1111/j.1570-7458.2008.00793.x.
Haridas, C.V., Meinke, L.J., Hibbard, B.E., Siegfried, B.D., and Tenhumberg, B. 2016. Effects of Temporal Variation in Temperature and Density Dependence on Insect Population Dynamics. Ecosphere **7**(5). doi:https://doi.org/10.1002/ecs2.1287.
Hartig, F., and Dormann, C.F. 2013. Does model-free forecasting really outperform the true model? Proceedings of the National Academy of Sciences **110**(42): E3975–E3975. National Academy of Sciences. doi:10.1073/pnas.1308603110.
Hartley, S., Krushelnycky, P.D., and Lester, P.J. 2010. Integrating Physiology, Population Dynamics and Climate to Make Multi-Scale Predictions for the Spread of an Invasive Insect: The Argentine Ant at Haleakala National Park, Hawaii. Ecography **33**(1): 83–94. doi:10.1111/j.1600-0587.2009.06037.x.

Haye, T., Abdallah, S., Gariepy, T., and Wyniger, D. 2014. Phenology, Life Table Analysis and Temperature Requirements of the Invasive Brown Marmorated Stink Bug, Halyomorpha halys, in Europe. J Pest Sci **87**(3): 407–418. doi:10.1007/s10340-014-0560-z.

Herman, W.S. 1981. Studies on the Adult Reproductive Diapause of the Monarch Butterfly, Danaus plexippus. Biol. Bull. **160**(1): 89–106. doi:10.2307/1540903.

Hilborn, R., and Mangel, M. 1997. The Ecological Detective: The Ecological Detective: Confronting Models with Data. Princeton University Press. Available from http://www.jstor.org/stable/j.ctt24hqnx [accessed 3 November 2022].

Huis, A. van. 2014. The Global Impact of Insects. Wageningen University & Research, Wageningen, Netherlands.

Jackson, L.J., Trebitz, A.S., and Cottingham, K.L. 2000. An Introduction to the Practice of Ecological Modeling. BioScience **50**(8): 694–706. doi:10.1641/0006-3568(2000)050[0694:aittpo]2.0.CO;2.

Jandricic, S.E., Wraight, S.P., Bennett, K.C., and Sanderson, J.P. 2010. Developmental Times and Life Table Statistics of Aulacorthum solani (Hemiptera: Aphididae) at Six Constant Temperatures, With Recommendations on the Application of Temperature-Dependent Development Models. Environ Entomol **39**(5): 1631–1642. doi:10.1603/EN09351.

Jaworski, T., and Hilszczański, J. 2013. The Effect of Temperature and Humidity Changes on Insects Development Their Impact on Forest Ecosystems in the Expected Climate Change. Forest Research Papers **74**(4): 345–355. doi:10.2478/frp-2013-0033.

Jia, P., Lu, L., Chen, X., Chen, J., Guo, L., Yu, X., and Liu, Q. 2016. A Climate-Driven Mechanistic Population Model of Aedes Albopictus with Diapause. Parasites Vectors **9**(175). doi:10.1186/s13071-016-1448-y.

Johnson, A.R., Wiens, J.A., Milne, B.T., and Crist, T.O. 1992. Animal Movements and Population Dynamics in Heterogeneous Landscapes. Landscape Ecol **7**(1): 63–75. doi:10.1007/BF02573958.

Kehoe, R., Sanders, D., and van Veen, F.J. 2022. Towards a Mechanistic Understanding of the Effects of Artificial Light at Night on Insect Populations and Communities. Current Opinion in Insect Science **53**: 100950. doi:10.1016/j.cois.2022.100950.

Kendall, B.E., Ellner, S.P., McCauley, E., Wood, S.N., Briggs, C.J., Murdoch, W.W., and Turchin, P. 2005. Population Cycles in the Pine Looper Moth: Dynamical Tests of Mechanistic Hypotheses. Ecological Monographs **75**(2): 259–276. doi:10.1890/03-4056.

Kersting, U., Satar, S., and Uygun, N. 1999. Effect of Temperature on Development Rate and Fecundity of Apterous Aphis gossypii Glover (hom., Aphididae) Reared on Gossypium hirsutum L. Journal of Applied Entomology **123**(1): 23–27. John Wiley & Sons, Ltd. doi:10.1046/j.1439-0418.1999.00309.x.

Khaliq, A., Javed, M., Sohail, M., and Sagheer, M. 2014. Environmental Effects on Insects and Their Population Dynamics. JEZS **2**(2): 1–7.

Khan, J., and Saljoki, A.-U.-R. 2016. Effect of Temperature on Biological Attributes and Predatory Potential of Harmonia dimidiata (fab.) (coleoptera: Coccinellidae) Fed on Rhopalosiphum padi Aphid. Journal of Entomology and Zoology Studies **4**(5): 1016–1022.

Kim, K.C. 2009. Taxonomy and Management of Insect Biodiversity. *In* Insect Biodiversity. *Edited by* R.G. Foottit and P.H. Adler. Wiley-Blackwell, Oxford, UK. pp. 561–574. doi:10.1002/9781444308211.ch24.

Kocourek, F., Berankova, J., and Jarosik, V. 1993. Introduction of Predatory Midge Aphidoletes aphidimyza for Control of Cotton Aphid, Aphis gossypii, on Greenhouse Cucumbers. Ochrana Rostlin-UZPI (Czech Republic).

Kriticos, D.J., Maywald, G.F., Yonow, T., Zurcher, E.J., Herrmann, N.I., and Sutherst, R.W. 2015. CLIMEX. Version 4. Exploring the Effects of Climate on Plants, Animals and Diseases. CSIRO Publishing, Melbourne, Australia.

Kumar, S., Neven, L.G., and Yee, W.L. 2014. Evaluating Correlative and Mechanistic Niche Models for Assessing the Risk of Pest Establishment. Ecosphere **5**(7): 86. doi:10.1890/ES14-00050.1.

Lactin, D.J., Holliday, N.J., Johnson, D.L., and Craigen, R. 1995. Improved Rate Model of Temperature-Dependent Development by Arthropods. Environmental Entomology **24**(1): 68–75. doi:10.1093/ee/24.1.68.

Ladányi, M., and Horváth, L. 2010. A Review of the Potential Climate Change Impact on Insect Populations – General and Agricultural Aspects. Appl Ecol Env Res **8**(2): 143–151. doi:10.15666/aeer/0802_143151.

Lagergren, J., Reeder, A., Hamilton, F., Smith, R.C., and Flores, K.B. 2018. Forecasting and Uncertainty Quantification Using a Hybrid of Mechanistic and Non-mechanistic Models for an Age-Structured Population Model. Bull Math Biol **80**(6): 1578–1595. doi:10.1007/s11538-018-0421-7.

Langille, A.B., Arteca, E.M., and Newman, J.A. 2017. The Impacts of Climate Change on the Abundance and Distribution of the Spotted Wing Drosophila (Drosophila suzukii) in the United States and Canada. PeerJ **5**: e3192. doi:10.7717/peerj.3192.

Langille, A.B., Arteca, E.M., Ryan, G.D., Emiljanowicz, L.M., and Newman, J.A. 2016. North American Invasion of Spotted-Wing Drosophila (Drosophila suzukii): A Mechanistic Model of Population Dynamics. Ecological Modelling **336**: 70–81. doi:10.1016/j.ecolmodel.2016.05.014.

Langille, B.A.B. 2017. A Mechanistic Model of Drosophila Suzukii Population Dynamics in Contemporary and Future Climates. The University of Guelph, Guelph, Ontario, Canada.

Liu, J. 2019. Modelling Swede Midge (Contarinia nasturtii kieffer) Population Dynamics in Its Invasive Range. The University of Guelph, Guelph, Ontario, Canada. Available from http://hdl.handle.net/10214/16000.

Liu, S.-S., Chen, F.-Z., and Zalucki, M.P. 2002. Development and Survival of the Diamondback Moth (Lepidoptera: Plutellidae) at Constant and Alternating Temperatures. Environ Entomol **31**(2): 221–231. doi:10.1603/0046-225X-31.2.221.

Liu, Y.H., and Tsai, J.H. 2000. Effects of Temperature on Biology and Life Table Parameters of the Asian citrus psyllid, Diaphorina citri Kuwayama (Homoptera: Psyllidae). Ann Applied Biology **137**(3): 201–206. doi:10.1111/j.1744-7348.2000.tb00060.x.

Logan, J.A., Régnière, J., and Powell, J.A. 2003. Assessing the Impacts of Global Warming on Forest Pest Dynamics. Frontiers in Ecology and the Environment **1**(3): 130–137. doi:10.2307/3867985.

Logan, J.A., Wollkind, D.J., Hoyt, S.C., and Tanigoshi, L.K. 1976. An Analytic Model for Description of Temperature Dependent Rate Phenomena in Arthropods. Environmental Entomology **5**(6): 1133–1140. doi:10.1093/ee/5.6.1133.

Maino, J.L., Kong, J.D., Hoffmann, A.A., Barton, M.G., and Kearney, M.R. 2016. Mechanistic Models for Predicting Insect Responses to Climate Change. Current Opinion in Insect Science **17**: 81–86. doi:10.1016/j.cois.2016.07.006.

Matis, T.I., Parajulee, M.N., Matis, J.H., and Shrestha, R.B. 2008. A Mechanistic Model Based Analysis of Cotton Aphid Population Dynamics Data. Agricultural and Forest Entomology **10**(4): 355–362. doi:10.1111/j.1461-9563.2008.00389.x.

Maywald, G.F., Bottomley, W., Sutherst, R.W., and Kriticos, D. 2007. DYMEX Model Simulator Version 3: User's Guide. CSIRO Publishing, Melbourne, Australia.

Mitton, J.B., and Ferrenberg, S.M. 2012. Mountain Pine Beetle Develops an Unprecedented Summer Generation in Response to Climate Warming. The American Naturalist **179**(5): E163–E171. doi:10.1086/665007.

Monro, J. 1967. The Exploitation and Conservation of Resources by Populations of Insects. The Journal of Animal Ecology **36**(3): 531. doi:10.2307/2810.

Nedved, O., Lavy, D., and Verhoef, H.A. 1998. Modelling the Time-Temperature Relationship in Cold Injury and Effect of High-Temperature Interruptions on Survival in a Chill-Sensitive Collembolan: Modelling Cold Injury and Recovery. Functional Ecology **12**(5): 816–824. doi:10.1046/j.1365-2435.1998.00250.x.

Nielsen, A.L., Chen, S., and Fleischer, S.J. 2016. Coupling Developmental Physiology, Photoperiod, and Temperature to Model Phenology and Dynamics of an Invasive Heteropteran, Halyomorpha halys. Front. Physiol. **7**. doi:10.3389/fphys.2016.00165.

Nielsen, A.L., Hamilton, G.C., and Matadha, D. 2008. Developmental Rate Estimation and Life Table Analysis for Halyomorpha halys (Hemiptera: Pentatomidae). Environmental Entomology **37**(2): 348–355. doi:10.1603/0046-225X(2008)37[348:DREALT]2.0.CO;2.

Ning, S., Zhang, W., Sun, Y., and Feng, J. 2017. Development of Insect Life Tables: Comparison of Two Demographic Methods of Delia Antiqua (Diptera: Anthomyiidae) on Different Hosts. Scientific Reports **7**(4821). doi:10.1038/s41598-017-05041-5.

Otieno, M.H.J., Ayieko, M.A., Niassy, S., Salifu, D., Abdelmutalab, A., Fathiya, K.M., Subramanian, S., Fiaboe, K.K.M., Roos, N., Ekesi, S., and Tanga, C.M. 2019. Integrating Temperature-Dependent Life Table Data into Insect Life Cycle Model for Predicting the Potential Distribution of Scapsipedus Icipe Hugel & Tanga. PLOS ONE **14**(9): e0222941. doi:10.1371/journal.pone.0222941.

Parajulee, M.N. 2007. Influence of Constant Temperatures on Life History Parameters of the Cotton Aphid, Aphis gossypii, Infesting Cotton. Environmental Entomology **36**(4): 666–672. doi:10.1093/ee/36.4.666.

Parajulee, M.N., Montandon, R., and Slosser, J.E. 1997. Relay Intercropping to Enhance Abundance of Insect Predators of Cotton Aphid (Aphis gossypii glover) in Texas Cotton. International Journal of Pest Management **43**(3): 227–232. doi:10.1080/096708797228726.

Peck, S.L. 2004. Simulation as Experiment: A Philosophical Reassessment for Biological Modeling. Trends in Ecology & Evolution **19**(10): 530–534. doi:10.1016/j.tree.2004.07.019.

Pener, M.P. 1992. Environmental Cues, Endocrine Factors, and Reproductive Diapause in Male Insects. Chronobiology international **9**(2): 102–113. doi:10.3109/07420529209064521.

Pener, M.P., Girardie, A., and Joly, P. 1972. Neurosecretory and Corpus Allatum Controlled Effects on Mating Behavior and Color Change in Adult Locusta migratoria migratorioides Males. General and Comparative Endocrinology **19**(3): 494–508. doi:10.1016/0016-6480(72)90248-1.

Penning De Vries, F.W.T. 1983. Modeling of Growth and Production. *In* Physiological Plant Ecology IV: Ecosystem Processes: Mineral Cycling, Productivity and Man's Influence.

Edited by O.L. Lange, P.S. Nobel, C.B. Osmond, and H. Ziegler. Springer Berlin Heidelberg, Berlin, Heidelberg. pp. 117–150. doi:10.1007/978-3-642-68156-1_5.
Pertierra, L.R., Bartlett, J.C., Duffy, G.A., Vega, G.C., Hughes, K.A., Hayward, S.A.L., Convey, P., Olalla-Tarraga, M.A., and Aragón, P. 2020. Combining Correlative and Mechanistic Niche Models with Human Activity Data to Elucidate the Invasive Potential of a Sub-Antarctic Insect. J Biogeogr **47**(3): 658–673. doi:10.1111/jbi.13780.
Petrice, T.R., Bauer, L.S., Miller, D.L., Poland, T.M., and Ravlin, F.W. 2021. A Phenology Model for Simulating Oobius agrili (Hymenoptera: Encyrtidae) Seasonal Voltinism and Synchrony with Emerald Ash Borer Oviposition. Environmental Entomology **50**(2): 280–292. doi:10.1093/ee/nvaa169.
Phillips, S.J., Anderson, R.P., and Schapire, R.E. 2006. Maximum Entropy Modeling of Species Geographic Distributions. Ecological Modelling **190**(3–4): 231–259. doi:10.1016/j.ecolmodel.2005.03.026.
Phillips, S.J., and Dudík, M. 2008. Modeling of Species Distributions with Maxent: New Extensions and a Comprehensive Evaluation. Ecography **31**(2): 161–175. doi:10.1111/j.0906-7590.2008.5203.x.
Pimentel, D. 2009. Pesticides and Pest Control. *In* Integrated Pest Management: Innovation-Development Process: Volume 1. *Edited by* R. Peshin and A.K. Dhawan. Springer Netherlands, Dordrecht. pp. 83–87. doi:10.1007/978-1-4020-8992-3_3.
Poggi, S., Sergent, M., Mammeri, Y., Plantegenest, M., Le Cointe, R., and Bourhis, Y. 2021. Dynamic Role of Grasslands as Sources of Soil-Dwelling Insect Pests: New Insights from in Silico Experiments for Pest Management Strategies. Ecological Modelling **440**: 13. doi:10.1016/j.ecolmodel.2020.109378.
Ragland, G.J., and Kingsolver, J.G. 2008. The Effect of Fluctuating Temperatures on Ectotherm Life-History Traits: Comparisons Among Geographic Populations of Wyeomyia smithii. Evolutionary Ecology Research **10**: 16.
Readshaw, J.L. 1961. The Biology and Ecology of the Swede Midge Contarinia nasturii (kieffer) (Diptera; Cecidomyidae). Durham University, Durham, United Kingdom. Available from http://hdl.handle.net/10443/1074.
Readshaw, J.L. 1966. The Ecology of the Swede Midge, Contarinia nasturtii (kieff.) (Diptera, Cecidomyiidae). I.—Life-History and Influence of Temperature and Moisture on Development. Bulletin of Entomological Research **56**(4): 685–700. Cambridge University Press. doi:10.1017/S0007485300056686.
Régnière, J. 1996. Generalized Approach to Landscape-Wide Seasonal Forecasting with Temperature-Driven Simulation Models. Environmental Entomology **25**(5): 869–881. doi:10.1093/ee/25.5.869.
Régnière, J., Powell, J., Bentz, B., and Nealis, V. 2012a. Effects of temperature on development, survival and reproduction of insects: Experimental design, data analysis and modeling. Journal of Insect Physiology **58**(5): 634–647. doi:10.1016/j.jinsphys.2012.01.010.
Régnière, J., Saint-Amant, R., and Béchard, A. 2014. Biosim 10: User's Manual. Laurentian Forestry Centre, Québec, Québec.
Régnière, J., St-Amant, R., and Duval, P. 2012b. Predicting Insect Distributions Under Climate Change from Physiological Responses: Spruce Budworm as an Example. Biol Invasions **14**(8): 1571–1586. doi:10.1007/s10530-010-9918-1.
Rogerson, J.P. 1963. SWEDE MIDGE ON TWO NORTHUMBERLAND FARMS, 1959?61. Plant Pathology **12**(4): 161–171. doi:10.1111/j.1365-3059.1963.tb00242.x.

Rosenberger, D.W., Aukema, B.H., and Venette, R.C. 2017. Cold Tolerance of Mountain Pine Beetle Among Novel Eastern Pines: A Potential for Trade-Offs in an Invaded Range? Forest Ecology and Management **400**: 28–37. doi:10.1016/j.foreco.2017.05.031.

Ryan, G.D., Emiljanowicz, L., Wilkinson, F., Kornya, M., and Newman, J.A. 2016. Thermal Tolerances of the Spotted-Wing Drosophila *Drosophila suzukii* (Diptera: Drosophilidae). J Econ Entomol **109**(2): 746–752. doi:10.1093/jee/tow006.

Rykiel, E.J. 1996. Testing ecological models: the meaning of validation. Ecological Modelling **90**(3): 229–244. doi:https://doi.org/10.1016/0304-3800(95)00152-2.

Safranyik, L. 1998. Mortality of mountain pine beetle larvae, Dendroctonus ponderosae (Coleoptera: Scolytidae) in logs of lodgepole pine (Pinus contorta var. latifolia) at constant low temperatures. Journal of the Entomological Society of British Columbia **95**: 81–88.

Satar, S., Kersting, U., and Uygun, N. 2005. Effect of Temperature on Development and Fecundity of Aphis gossypii Glover (Homoptera: Aphididae) on Cucumber. J Pest Sci **78**(3): 133–137. doi:10.1007/s10340-005-0082-9.

Scheffer, M., and Beets, J. 1994. Ecological Models and the Pitfalls of Causality. Hydrobiologia **275**(1): 115–124. doi:10.1007/BF00026704.

Scudder, G.G.E. 2017. The Importance of Insects. *In* Insect Biodiversity. pp. 9–43. doi:10.1002/9781118945568.ch2.

Singh, K., and Singh, R. 2015. Effect of Temperature on the Life History Traits of Aphis gossypii Glover (Homoptera: Aphididae) on Bottle Gourd, Laginaria Siceraria (Molina) Standl. (Cucurbitaceae). International Journal of Life Sciences Biotechnology & Pharma Research **4**(4): 179–182.

Sporleder, M., Chavez, D., Gonzales, J.C., Juarez, H., Simon, R., and Kroschel, J. 2009. ILCYM- Insect Life Cycle Modeling: Software for Developing Temperature-Based Insect Phenology Models with Applications for Regional and Global Pest Risk Assessments and Mapping. ISTRC: 216–223.

Stange, E.E., and Ayres, M.P. 2010. Climate Change Impacts: Insects. *In* Encyclopedia of Life Sciences (ELS). John Wiley & Sons, Ltd. doi:10.1002/9780470015902.a0022555.

Stokes, B.M. 1953. Biological Investigations into the Validity of Contarinia Species Living on the Cruciferae, with Special Reference to the Swede Midge, Contarinia nasturtii (kieffer). Annals of Applied Biology **40**(4): 726–741. John Wiley & Sons, Ltd. doi:10.1111/j.1744-7348.1953.tb01110.x.

Stork, N.E. 2018. How Many Species of Insects and Other Terrestrial Arthropods Are There on Earth? Annu. Rev. Entomol. **63**: 31–45. doi:10.1146/annurev-ento-020117-043348.

Sutherst, R. 1985. A Computerised System for Matching Climates in Ecology. Agriculture, Ecosystems & Environment **13**(3–4): 281–299. doi:10.1016/0167-8809(85)90016-7.

Sutherst, R.W., Maywald, G.F., and Russell, B.L. 2000. Estimating Vulnerability Under Global Change: Modular Modelling of Pests. Agriculture, Ecosystems & Environment **82**(1–3): 303–319. doi:10.1016/S0167-8809(00)00234-6.

Tanga, C.M., Khamis, F.M., Tonnang, H.E.Z., Rwomushana, I., Mosomtai, G., Mohamed, S.A., and Ekesi, S. 2018. Risk Assessment and Spread of the Potentially Invasive Ceratitis Rosa Karsch and Ceratitis Quilicii De Meyer, Mwatawala & Virgilio Sp. Nov. Using Life-Cycle Simulation Models: Implications for Phytosanitary Measures and Management. PLoS ONE **13**(1): e0189138. doi:10.1371/journal.pone.0189138.

Tatar, M., and Yin, C. 2001. Slow Aging During Insect Reproductive Diapause: Why Butterflies, Grasshoppers and Flies Are Like Worms. Exp Gerontol **36**(4–6): 723–738. doi:10.1016/s0531-5565(00)00238-2.

Tauber, M.J., Tauber, C.A., and Masaki, S. 1986. Seasonal Adaptations in Insects. Oxford University Press, Oxford, UK.

Taylor, F. 1981. Ecology and Evolution of Physiological Time in Insects. The American Naturalist **117**(1): 1–23. doi:10.1086/283683.

Van Steenis, M.J. 1995. Evaluation of four aphidiine parasitoids for biological control of Aphis gossypii. Entomologia Experimentalis et Applicata **75**(2): 151–157. John Wiley & Sons, Ltd. doi:10.1111/j.1570-7458.1995.tb01921.x.

Van Steenis, M.J., and El-Khawass, K.A.M.H. 1995. Life History of Aphis gossypii on Cucumber: Influence of Temperature, Host Plant and Parasitism. Entomologia Experimentalis et Applicata **76**(2): 121–131. John Wiley & Sons, Ltd. doi:10.1111/j.1570-7458.1995.tb01954.x.

Vinatier, F., Tixier, P., Duyck, P.-F., and Lescourret, F. 2011. Factors and Mechanisms Explaining Spatial Heterogeneity: A Review of Methods for Insect Populations. Methods in Ecology and Evolution **2**(1): 11–22. doi:10.1111/j.2041-210X.2010.00059.x.

Xia, J.Y., Van Der Werf, W., and Rabbinge, R. 1999. Temperature and Prey Density on Bionomics of Coccinella septempunctata (Coleoptera: Coccinellidae) Feeding on Aphis gossypii (Homoptera: Aphididae) on Cotton. Environ Entomol **28**(2): 307–314. doi:10.1093/ee/28.2.307.

Zamani, A.A., Talebi, A.A., Fathipour, Y., and Baniameri, V. 2006. Effect of Temperature on Biology and Population Growth Parameters of Aphis gossypii Glover (Hom., Aphididae) on Greenhouse Cucumber. J Appl Entomology **130**(8): 453–460. doi:10.1111/j.1439-0418.2006.01088.x.

7. Appendix A: List of General Model Parameters

Table 4 List of all general model parameters including the graphical user interface (GUI) section, the equation in which they appear, the value's type, the value's units, whether the parameter is required to run the model and a description of the parameter. Note that the names of the parameters listed below are the parameter names used in the user interface and are not written as they should appear in the species' parameter file. For the proper parameter file parameter names see appendix B.

GUI Section	Eqn number	Name	Value Type	Value Unit	Required	Description
1. Setup	NA	Days to simulate	double	days	true	Number of days for the simulation to run
1. Setup	NA	Time step size	double	days	true	Size of differential equation time step used to calculate the population
1. Setup	NA	Print interval	double	days	true	Interval between population values being output to file
1. Setup	(18)	Latitude	double	degrees (°)	true	The latitude of the region where the population will be simulated (influences daylight length)
1. Setup	(21)	Number of instar stages	integer	individuals	true	The number of instar stages for the species
1. Setup	(22)	Has pupal stage	Boolean	dimensionless	true	Whether the species has a pupal stage
1. Setup	(25)	Number of female stages	integer	individuals	true	Number of adult female sub-stages, based on different egg viabilities
1. Setup	(23) (24)	Male proportion	double	Males per total individuals	true	Proportion of the total eggs laid that are male
2. Initial	NA	Initial population (each stage)	integer	individuals	true	The number of individuals that will be introduced to the population on the "add insect date" (Note: if starting population is overwintering, do not include in these values. See overwintering submodel)
2. Initial	NA	Add insect date	integer	Julian day	true	The Julian day when the initial insects will be added to the model population
3. Development	(6)	Development a (each stage)	double	dimensionless	true	Development rate parameter that affects the shape of the temperature-dependent development curve (seen in the Brière et al. (1999) equation 2 (briere2) temperature-dependent development rate equation)
3. Development	(6)	Development tmin (each stage)	double	degrees Celsius (°C)	true	The minimum temperature below which the species development stops
3. Development	(6)	Development tmax (each stage)	double	degrees Celsius (°C)	true	The maximum temperature above which the species development stops

4. Mortality	(9) (10) (11)	mortality min (each stage)	double	individuals per day	true	The lowest possible daily mortality rate when temperatures are optimal
4. Mortality	(8) (9) (10) (11)	mortality max (each stage)	double	Individuals per day	true	The highest possible daily mortality rate when temperatures are beyond the minimum and maximum mortality temperatures
4. Mortality	(8) (9) (10) (11) (12) (13)	mortality min temperature (each stage)	double	degrees Celsius (°C)	true	The minimum temperature, below which the mortality rate is at its maximum
4. Mortality	(8) (9) (10) (11) (12) (13)	mortality max temperature (each stage)	double	degrees Celsius (°C)	true	The maximum temperature, above which the mortality rate is at its maximum
5. Egg values	(19)	Egg viability (each female stage)	double	viable egg/total eggs	true	Ratio of eggs laid that are viable
5. Egg values	(3)	Fertility max	double	eggs/day	true	The maximum number of eggs laid by a female in one day
5. Egg values	(2) (4)	Fertility tmin	double	degrees Celsius (°C)	true	The minimum temperature below which insects are infertile
5. Egg values	(2) (4) (5)	Fertility tmax	double	degrees Celsius (°C)	true	The maximum temperature above which insects are infertile
6. Submodels	NA	Ignore mortality temperature	Boolean	dimensionless	true	When set to 1 (true), temperature has no effect on the species mortality
6. Submodels	NA	Ignore diapause	Boolean	dimensionless	true	When set to 1 (true), the reproductive diapause submodel is ignored
6. Submodels	NA	Ignore Overwintering	Boolean	dimensionless	true	When set to 1 (true), the overwintering submodel is ignored
6. Submodels	NA	Ignore kill	Boolean	dimensionless	true	When set to 1 (true), the mortality event submodel is ignored
6. Submodels	NA	Ignore predation	Boolean	dimensionless	true	When set to 1 (true), the extrinsic mortality (predation) submodel is ignored
7. Submodel: reproductive diapause	NA	Diapause critical temperature	double	degrees Celsius (°C)	false	The temperature at which diapause is induced and terminated
7. Submodel: reproductive diapause	NA	Diapause daylight hours	double	hours	false	The number of daylight hours at which diapause is induced and terminated
7. Submodel: reproductive diapause	(14)	Daylight hours half in diapause	double	hours	false	The number of daylight hours for half of the female population to be in reproductive diapause
7. Submodel: reproductive diapause	(14)	Diapause rate per daylight hours	double	individuals per day	false	The rate at which insects enter and leave diapause base on daylight hours
8. Submodel: overwintering	NA	Overwintering stage	integer	dimensionless	false	The life stage that overwinters (0 = egg)
8. Submodel: overwintering	NA	Initial Overwintering Insects	integer	individuals	false	The number of individuals that are overwintering on day 0 of the simulation. These insects

						will leave overwintering when conditions are favorable
8. Submodel: overwintering	NA	Overwintering success	double	successful individuals per total individuals	false	Overwintering population ratio to survive the overwintering process (Note: not dependent on winter temperatures)
8. Submodel: overwintering	(15)	Overwintering critical induction temperature	double	degrees Celsius (°C)	false	The temperature at which insects enter overwintering
8. Submodel: overwintering	(15)	Overwintering induction daylight hours	double	hours	false	The number of daylight hours at which insects enter overwintering
8. Submodel: overwintering	(15)	Overwintering critical termination temperature	double	degrees Celsius (°C)	false	The temperature at which insects leave overwintering
8. Submodel: overwintering	(15)	Overwintering termination daylight hours	double	hours	false	The number of daylight hours at which insects leave overwintering
8. Submodel: overwintering	NA	Overwintering mortality temperature	double	degrees Celsius (°C)	false	The minimum winter temperature below which all insects, overwintering or not, die
9. Submodel: mortality event	NA	Kill date	integer	Julian day	false	The Julian day when part of a life stage's population will be removed
9. Submodel: mortality event	NA	Stage kill	integer	dimensionless	false	The life stage that experiences the mortality event and loses part of its population (0 = egg)
9. Submodel: mortality event	NA	Percent kill	double	percentage	false	The percentage of the mortality event life stage population to be eliminated on the mortality event date
10. Submodel: predation mortality	NA	Mortality due to predation (each stage)	double	individuals predated per total individuals (per day)	false	The ratio of each life stage population lost to predation each day

8. Appendix B: Default Toy Species' Configuration Parameter File

```
numDaysToSim: 365
integrationStep: 1.0
printInterval: 1.0

numInstars: 1
hasPupalStage: 1
numFemStages: 2

male proportion: 0.5
latitude: 45.7

addInsectsDate: 140
initial eggs: 0
initial instar1: 0
initial pupae: 0.0
initial males: 0.0
initial females1: 50
initial females2: 0

eggs development a: 0.00015
eggs development tmin: 8
eggs development tmax: 26
instar1 development a: 0.00015
instar1 development tmin: 8
instar1 development tmax: 26
pupae development a: 0.00015
pupae development tmin: 8
pupae development tmax: 26
males development a: 0.00015
males development tmin: 8
males development tmax: 26
females1 development a: 0.00015
females1 development tmin: 8
females1 development tmax: 26
females2 development a: 0.00015
females2 development tmin: 8
females2 development tmax: 26

eggs mortality min: 0
eggs mortality max: 0.2
eggs mortality min temp: 2
eggs mortality max temp: 37
instar1 mortality min: 0
instar1 mortality max: 0.2
instar1 mortality min temp: 2
instar1 mortality max temp: 37
pupae mortality min: 0
pupae mortality max: 0.2
pupae mortality min temp: 2
pupae mortality max temp: 37
females1 mortality min: 0
females1 mortality max: 0.2
females1 mortality min temp: 2
females1 mortality max temp: 37
females2 mortality min: 0
females2 mortality max: 0.2
females2 mortality min temp: 2
females2 mortality max temp: 37
males mortality min: 0
males mortality max: 0.2
males mortality min temp: 2
males mortality max temp: 37

females1 egg viability: 0
females2 egg viability: 1
fecundity max: 10
fecundity tmin: 18
fecundity tmax: 30

ignoreOverwintering: 1
ignoreMortTemp: 0
ignoreKill: 1
ignorePredation: 1
ignoreDiapause: 1

diapause critical temp: 0
diapause daylight hours: 0
daylight hours half in diapause: 0
diapause rate per daylight hours: 0

overwinteringStage: 0
initialOverwintering: 0
overwintering success: 0
overwintering critical induction temp: 0
overwintering induction daylight hours: 0
overwintering critical termination temp: 0
overwintering termination daylight hours: 0
overwintering mortality temp: -20

numKillDates: 0
killDate1: 0
stageKill: 0
percentKill: 0

eggs mortality due to predation: 0
instar1 mortality due to predation: 0
pupae mortality due to predation: 0
males mortality due to predation: 0
females1 mortality due to predation: 0
females2 mortality due to predation: 0
```

Figure 8.1 Content of the Toy specie's configuration parameters file including all model parameters.

9. Appendix C: Supplementary Figures

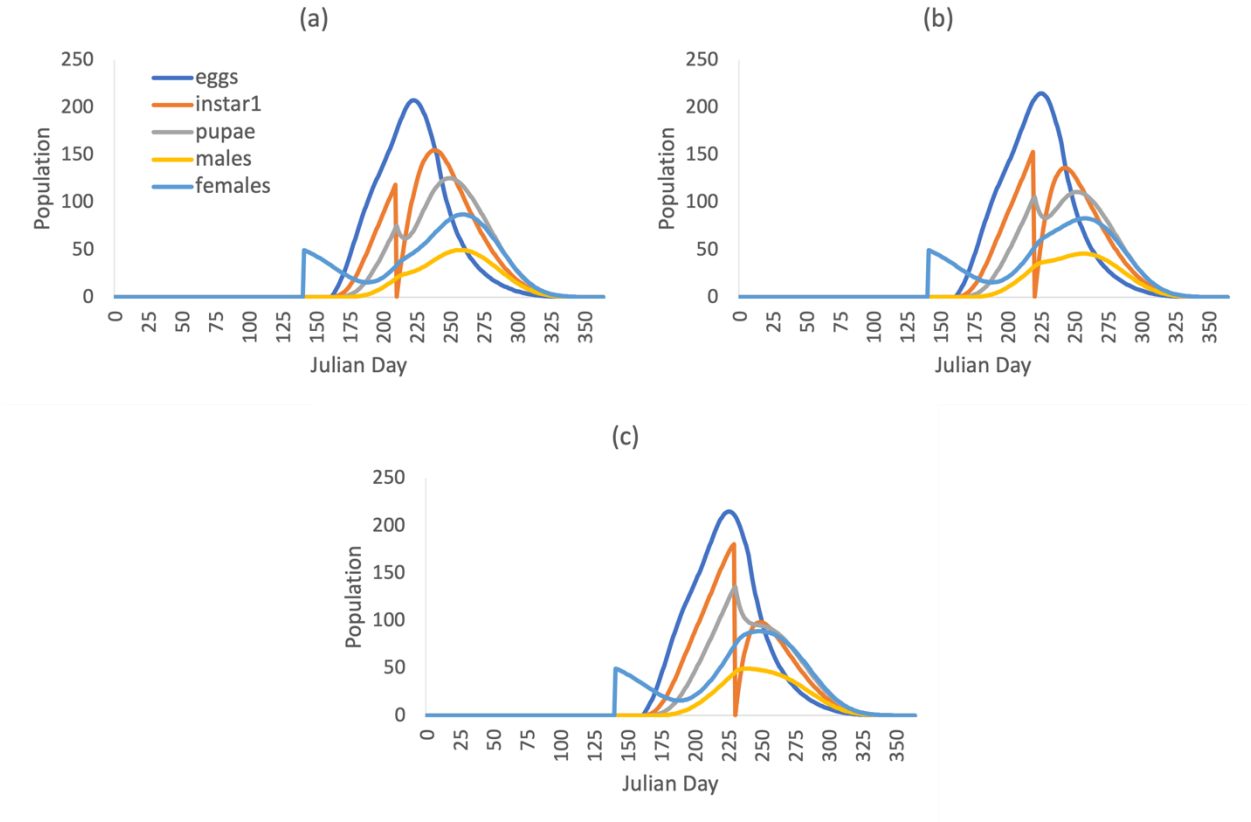

Figure 9.1 Supplementary Life stage toy species population curves for one year general model simulation with an initial population of 50 F1 adult females introduced on Julian day 140. A 100% mortality event was applied to the instar life stage on (a) Julian day 210, (b) Julian day 220, and (c) Julian day 230.

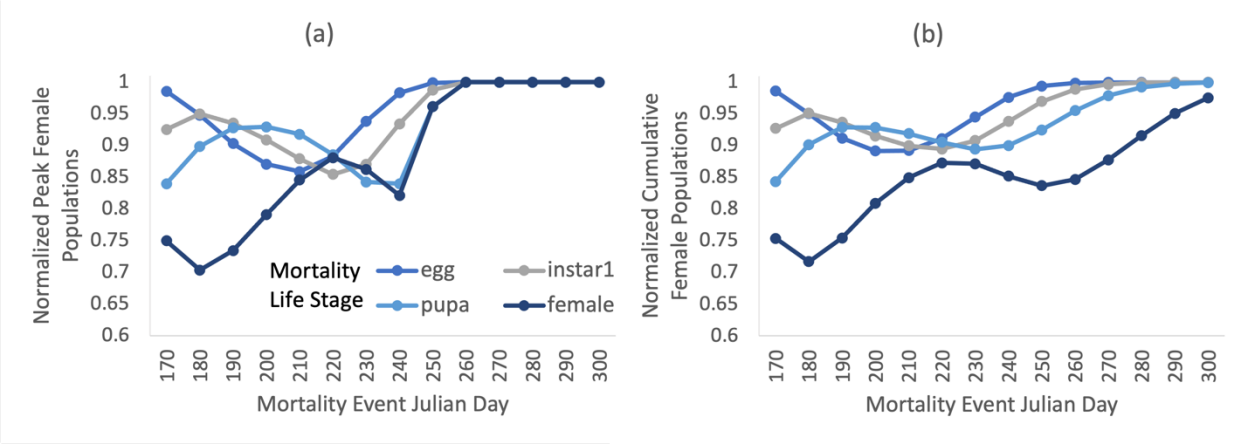

Figure 9.2 Supplementary (a) Peak and (b) cumulative adult female population produced by general model simulations where 50% mortality events were applied on various days (Julian day 170 to 300 with 10 day intervals) and to various life stages (egg, instar1, pupa, female). Each simulation is run for 365 days with the toy species parameters and under the temperature conditions of tempB. The model was initialized with an initial population of 50 instars on Julian day 140.

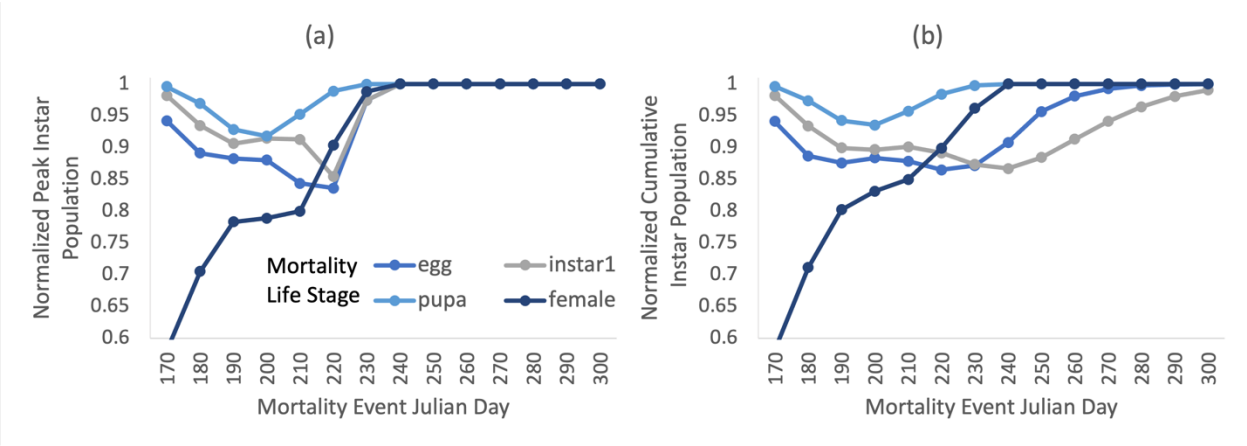

Figure 9.3 Supplementary (a) Peak and (b) cumulative instar population produced by general model simulations where mortality events were applied on various days (Julian day 170 to 300 with 10 day intervals) and to various life stages (egg, instar1, pupa, female). Each simulation is run for 365 days with the toy species parameters and under the temperature conditions of tempB. The model was initialized with an initial population of 50 F1 females on Julian day 140.

10. Appendix D: List of Sources Used to Parameterize the General Model for the Validation Tests

Insect Species	Sources Used to Parameterize the General Model
Drosophila suzukii	(Emiljanowicz et al. 2014; Ryan et al. 2016)
Halyomorpha halys	(Nielsen et al. 2016; Govindan and Hutchison 2020)
Dendroctonus ponderosae	(Safranyik 1998; Régnière et al. 2012a; Rosenberger et al. 2017; Bleiker and Smith 2019)
Contarinia nasturtii	(Stokes 1953; Readshaw 1961, 1966; Rogerson 1963; Corlay Herrera 2008; Hallett et al. 2009; Abram et al. 2012; Liu 2019 p. 20)
Aphis gossypii	(Aldyhim and Khalil 1993; Kocourek et al. 1993; Van Steenis 1995; Van Steenis and El-Khawass 1995; Kersting et al. 1999; Xia et al. 1999; Satar et al. 2005; Zamani et al. 2006; Singh and Singh 2015; Khan and Saljoki 2016)

11. Appendix E: Model User's Guide

Compiling the Model on the Command Line

A Makefile is provided with the source code to compile all general model C++ files (https://github.com/domdelay/GeneralizedInsectPopulationDynamicsModel) and produce the executable file execSingleCellRunner. The Makefile is simply run by typing "make" to the command line in the general model directory. Before the model is compiled, the user must first ensure that standard C++ libraries including vector, map, iostream, fstream, string, cmath and limits are present because the model's source code uses these libraries. These standard libraries are usually made available with most C++ distributions.

Executing the Model on the Command Line

When executing the general model's executable execSingleCellRunner file, the user must input three command line arguments. Arguments must appear in the correct order shown below.

Command: ./execSingleCellRunner parametersFileName temperatureFileName outputFileName

parametersFileName: Valid filename and optional path to the parameters text file (.txt).

temperatureFileName: Valid filename and optional path to the temperature text file (.txt).

outputFileName: Valid output filename and optional path for the results text file (.txt).

The name of each command line arguments file is left up to the user, but the content of these input files must follow a specified structure.

The configuration parameters file must follow the appropriate format to be read by the model. The model's configuration parameters file must contain all species parameters required by the general model (appendix A). In this file, parameters must be listed with one parameter per line

and written with the following format: parameter name, colon ":", parameter value. For example, numDaysToSim: 365.0. An example configuration parameters file for the "toy" species is available in appendix B.

The temperature file must also follow a certain format with a single temperature value per line. The file should be composed of 365 temperature values (integer or floating-point; °C) and no other information. The value on each line will be used as the temperature for one simulation day. If there are fewer temperature values in the file than the number of days that the model is run, the model will loop back and re-read through the temperatures.

Once the model is executed, the model output is printed in the user-defined output file. The file contains tab delimited columns of data for the life stages population (female life stages combined), temperature, and optionally the daylight hours. This format can easily be opened in software like excel and Matlab where the data can be graphed. A summary section is included at the end of the file, displaying each simulated life stage's total cumulative population and peak population, along with the date (time step) of the peak population's occurrence.

12. Appendix F: Model Vital Rate Fitting Algorithm

Since certain species parameters required by the model are not directly available through existing laboratory studies, a very simple curve fitting algorithm was created to provide an easy way to fit existing constant temperature data to the general model's vital rate curves (development, mortality, and fecundity) and obtain the general model's configuration parameters. The "built-in" curve fitting algorithm also improves the ease of use of the model, especially in the user interface since users can fit their species data to the model parameters, directly in the interface, without needing to find other fitting software.

The fitting algorithm requires a .csv file with vital rate values for each life stage at various constant temperatures. This file must be formatted with the life stage as columns and the constant temperature as rows (figure 12.1). The fitting algorithm produces an output file containing the resulting fitted configuration parameters that describe the vital rate equation's curve.

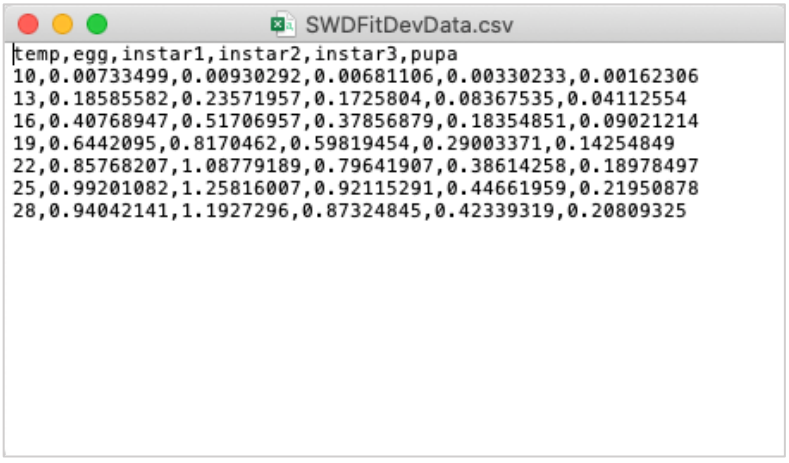

Figure 12.1 Example constant temperature vital rate file used as input in the curve fitting algorithm. The file contains values for the development rate of the life stages: egg, instar1, instar2, instar3, and pupa at various constant temperatures.

Vital rate curve fitting can be described as an optimization problem where the difference between real vital rate values at constant temperatures and the model's vital rate equation curves is minimized in a sum of square. For each vital rate, the optimization problem has 3 decision variables and no constraints (development: *a, TL, TU*; fecundity: *a, b, c*; mortality: *a, b, c*). The fecundity and mortality decision variables a, b and c describe the Gaussian (eqn. 2) and a parabola (eqn. 8) curve shapes respectively. The model parameters (mortality: *minMort, maxMort, TL, TU*; fecundity: *fmax, fTmin, fTmax*) are obtained (with: eqn. 3, eqn. 4, eqn. 5 & eqn. 9, eqn. 10, eqn. 11) based on the decision variables after the best fit has been found.

The objective functions (sum of square) for each of the model's vital rates, fecundity, development and mortality are defined below.

$$devF = \sum_{i=0}^{n} [dev(T_i) - (a * T_i * (T_i - TL) * (TU - T_i)^2)\ ]^2$$

where devF is the development objective function or sum of squares, T_i is the temperature at index i, dev(T_i) is the development rate point at temperature T_i, n is the number of points at different temperatures and a, TL & TU are the decision variables or development rate equation parameters.

$$mortF = \sum_{i=0}^{n} \left[mort(T_i) - (a * {T_i}^2 + b * T_i + c)\ \right]^2$$

where mortF is the mortality objective function or sum of squares, T_i is the temperature at index i, mort(T_i) is the mortality rate point at temperature T_i, n is the number of points at different temperatures and a, b & c are the decision variables or mortality rate equation parameters.

$$fecF = \sum_{i=0}^{n} \left[fec(T_i) - \left(a * e^{-\frac{1}{2}\left(\frac{T_i - b}{c}\right)^2} \right) \right]^2$$

where fecF is the fecundity objective function or sum of squares, T_i is the temperature at index i, $fec(T_i)$ is the fecundity rate point at temperature T_i, n is the number of points at different temperatures and a, b & c are the decision variables or fecundity rate equation parameters.

The algorithm uses a binary search to reach optimal parameter values that will produce the lowest sum of square value. This process is described below for the development rate equation's fitting; the same steps are also applied to the fecundity rate and mortality rate equations.

The algorithm starts with pre-set approximate values for each of the decision variables (parameters: a, TL, and TU). First, the algorithm tries to improve the curve's fit by changing the first variable a. It calculates the value of the objective function, increases the variable by a factor of itself and calculates the objective function again. The difference (residual) between the previous and the current objective functions is calculated. If the objective function got smaller (positive residual), the variable is increased again. If the objective function got bigger (negative residual), the variable is decreased by half of the previous increment's size. This process is repeated until the difference between the previous and the current objective value (residual) is less than 1xe^-6 (little change in the objective function). The objective function is then optimized by fitting the second variable TL, then the third TU. The fitting of the three variables is repeated 50 times to ensure that changes to one variable is accounted for by the other. Once this is complete, the objective function (sum of square) has been optimized, and the obtained parameters are output.

The fitting algorithms were written in C++ and were compiled using the GNU g++ compiler version 4.2.1 for Linux. The algorithms can be compile with the provided Makefile by

typing “make” to the command line in the algorithm’s directory. Compiling the algorithm will produce the executable file execFittingFec, execFittingDev, or execFittingMort, depending on the vital rate curve being fitted. The executable files take two inline arguments shown below.

Command: ./execFittingFec constantTemperatureFileName numberOfLifeStages

constantTemperatureFileName: Valid filename and optional path to the constant temperature vital rate (.csv) file (figure 12.1)

numberOfLifeStages: Positive integer value of the number of life stages contained in the constant temperature file

13. Appendix G: Model Graphical User Interface (GUI) Description and User's Guide

A user interface was created for the generalized insect population dynamics model to make the general model more accessible to a wider audience. A graphical user interface (GUI) can be less intimidating for users and doesn't require computer programming knowledge. The general model's GUI guides the user through insect species parameter input, model running, and result visualization. The general model GUI can be obtained at https://github.com/domdelay/GeneralizedInsectPopulationDynamicsModel

The model's user interface (UI) is used as a tool to build the insect species parameter file. The user interface goes step-by-step through each of the configuration parameters required to run the model, explains each parameter (and their use in the model) and ensures that input values are of the proper type (int, double, Boolean, ratio …). The parameters can be input manually into text fields or as .csv data tables. The UI also includes the optional built-in vital rate data fitting algorithm (appendix F) to obtain the model's parameters based on constant temperature vial rate values. This guided parameter input and data check, reduces the risk of users getting runtime errors on the command line related to improper parameter types, bad parameter file formatting, or missing data.

Once all species parameters have been input, the model can be run with the simple press of a button. The UI displays a graphical overview of the simulations results with three visualizations of the model's output data. On the UI's results screen, users also have the option to change the name, location and format of the model results file (save as), modify model parameters and rerun the model, or compare this simulation's results to other simulation results with a side-by-side visual comparison.

A storyboard of the GUI being run, including each of the parameter input windows and results window visualization options can be seen in figure 13.2.

After the model is run in the UI, a new folder is created, named based on the user input insect name, and the date and time that the model was run (e.g. Spotted_Wing_Fruit_Fly_2022-05-24_11.52.11). In this folder, users can find a configuration parameters file for the insect data input in the UI, along with .csv files for each of the vital rate data tables that were input. This folder is also where the model's output file can be found. Each of the files contained in this folder are named based on the insect species name input by the user and labeled with a number, starting at 1 with the first model run for the UI session and increasing for each run (e.g. Spotted_Wing_Fruit_Fly1JuvDev.csv). All output files can be examined by the user to better understand the model or used when rerunning the model for the same insect data, either on the command line or in the UI.

The general model and UI source code are kept separate, with the UI simply executing the model's executable file with the inline arguments that it collected from the user. By keeping the model's UI separate from the general model, either program could be modified without affecting the other, allowing for both changes to the model's source code and updates to the UI. Additionally, the separation of the model and the UI also allows the user to have direct access to the model's input and output files. Users have more freedom to modify and use these files to run the model independently or to examine the files to get a better understanding of how the model works. The connection between the model and the UI can be seen in figure 13.1.

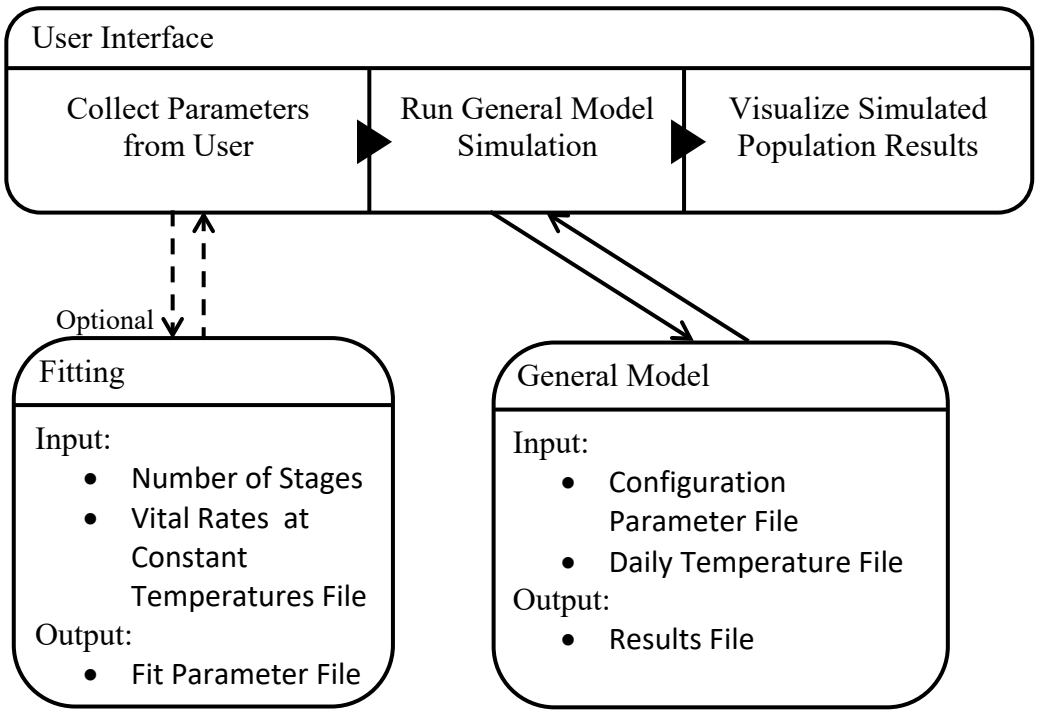

Figure 13.1 Flow diagram of the connection between the UI, the general model and the fitting algorithm. Arrows represent the user interface executing external programs. Dashed arrows are optional execution of a program and solid arrows are mandatory execution of a program.

The model's user interface was written in Java (Java SE 8) using the JavaFX GUI tools. The UI compiles both the model and fitting algorithm's C++ code using the GNU g++ compiler version 4.2.1 for Linux . The UI can be launched either by clicking on the UI's icon or by compiling and running the user interface's java file (GeneralModelIU.java).

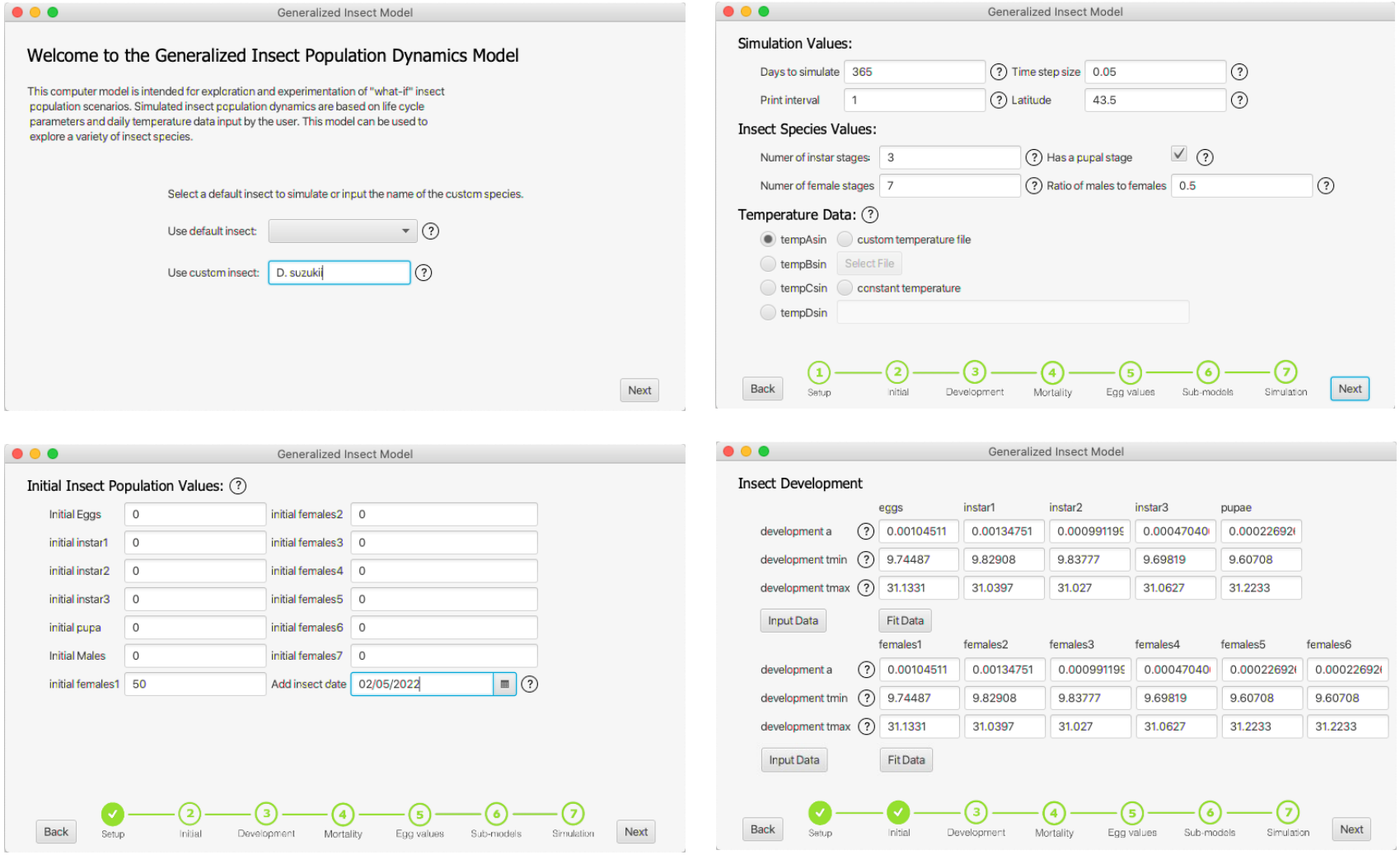

Figure 13.2 Storyboard of the general model graphical user interface being run for the spotted wing fruit fly.

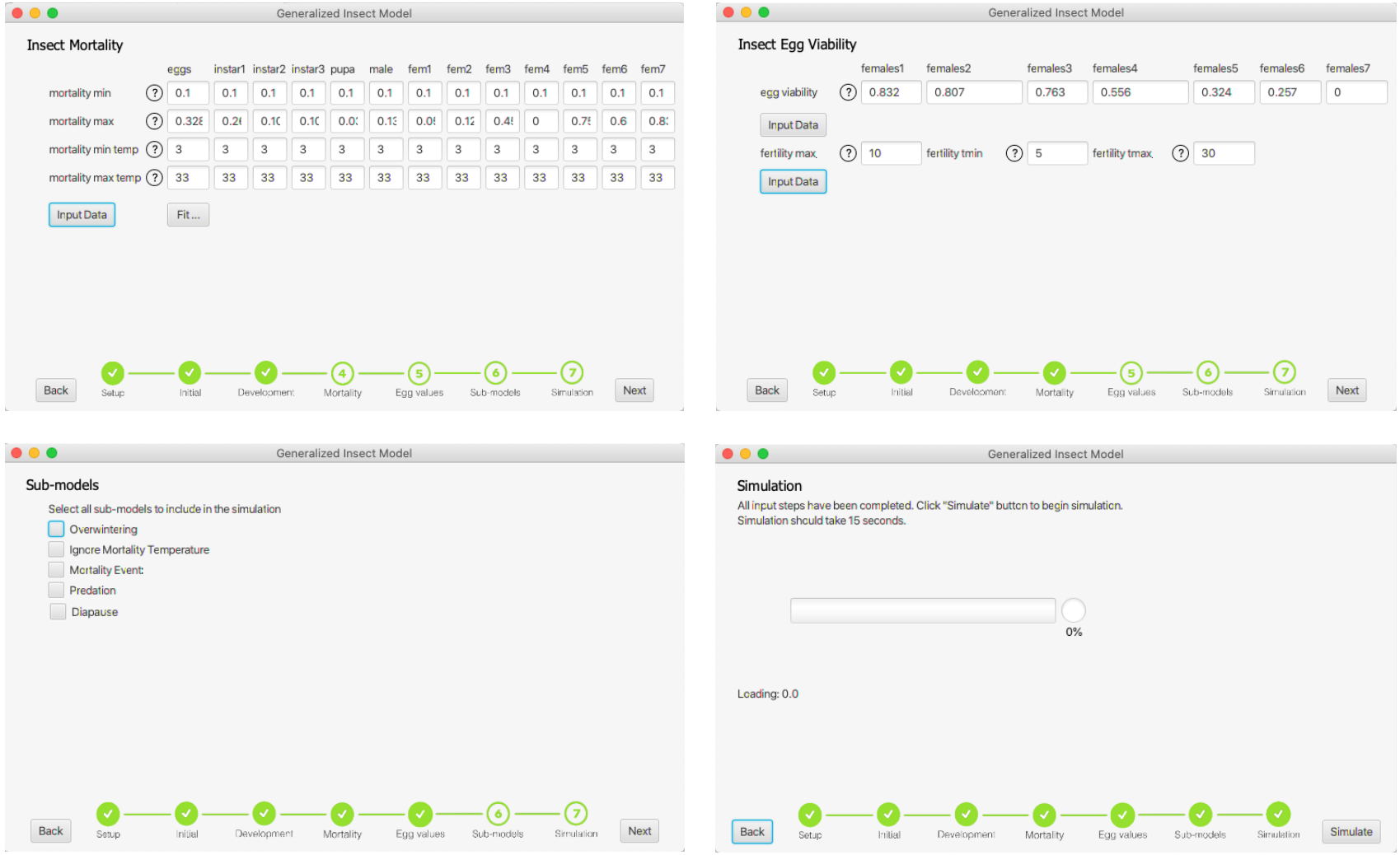

Figure 13.2 Storyboard of the general model graphical user interface being run for the spotted wing fruit fly. (continued)

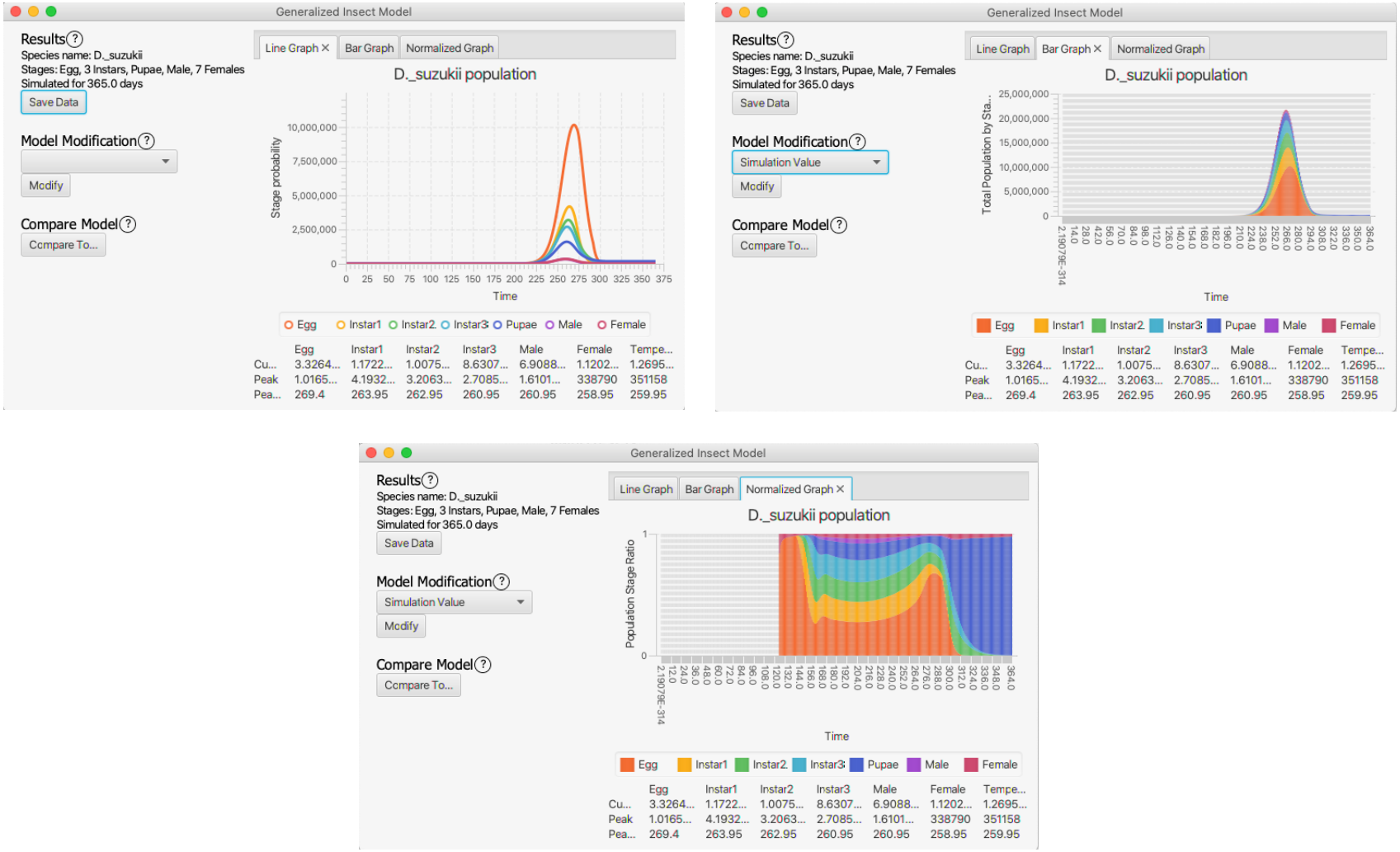

	Egg	Instar1	Instar2	Instar3	Male	Female	Tempe...
Cu...	3.3264...	1.1722...	1.0075...	8.6307...	6.9088...	1.1202...	1.2695...
Peak	1.0165...	4.1932...	3.2063...	2.7085...	1.6101...	338790	351158
Pea...	269.4	263.95	262.95	260.95	260.95	258.95	259.95

Figure 13.2 Storyboard of the general model graphical user interface being run for the spotted wing fruit fly. (continued)